Universidade de Aveiro Departamento de Química
Ano 2011

Ana Carolina Cardoso Alves de Barros

Matéria orgânica natural: estudo por cromatografia líquida bidimensional

Natural organic matter: study by two-dimensional liquid chromatography

Universidade de Aveiro
Ano 2011
Departamento de Química

Ana Carolina Cardoso Alves de Barros

Matéria orgânica natural: estudo por cromatografia líquida bidimensional

Natural organic matter: study by two-dimensional liquid chromatography

Dissertação apresentada à Universidade de Aveiro para cumprimento dos requisitos necessários à obtenção do grau de Mestre em Química, realizada sob a orientação científica do Doutor Armando da Costa Duarte, Professor Catedrático do Departamento de Química da Universidade de Aveiro, e da Doutora Regina Maria Brandão de Oliveira Duarte, Investigadora Auxiliar do Centro de Estudos do Ambiente e do Mar (CESAM) da Universidade de Aveiro.

o júri

presidente

Prof. Doutor Artur Manuel Soares da Silva
Professor Catedrático do Departamento de Química da Universidade de Aveiro

Prof. Doutora Teresa Alexandra Peixoto da Rocha Santos
Professora Associada do Instituto Piaget de Viseu

Prof. Doutor Armando da Costa Duarte
Professor Catedrático do Departamento de Química da Universidade de Aveiro

Doutora Regina Maria Brandão de Oliveira Duarte
Investigadora Auxiliar do Centro de Estudos do Ambiente e do Mar da Universidade de Aveiro

agradecimentos

Agradeço em primeiro lugar ao Professor Doutor Armando da Costa Duarte e à Professora Doutora Regina Duarte pela disponibilidade e orientação fundamental para a conclusão deste trabalho.

Agradeço aos meus colegas e amigos: Cristina, Joana, João, Paula e Sara pela amizade e apoio incondicional. Espero ter sido tão importante para vós como vocês foram para mim.

À minha mãe e ao Marco.

A todos aqueles que cruzaram o meu caminho durante este ano de trabalho. Foram todos fundamentais.

palavras-chave Cromatografia líquida compreensiva bidimensional; matéria orgânica natural; cromatografia de exclusão de tamanhos; cromatografia de fase reversa; cromatografia de interacção hidrofílica/fase reversa

resumo Com o objetivo de avaliar a heterogeneidade química da matéria orgânica natural (MON), foi aplicada pela primeira vez a técnica de cromatografia líquida compreensiva bidimensional (CL x CL) a três misturas orgânicas complexas: ácidos fúlvicos do Rio Suwannee (AF-RS) e do Lago Pony (AF-LP), ambos obtidos da Sociedade Internacional de Substâncias Húmicas, e matéria orgânica solúvel em água (MOSA) de aerossóis atmosféricos. Com esta nova técnica analítica, pretendeu-se efectuar a separação cromatográfica das amostras de MON tendo em conta a hidrofobicidade e polaridade *vs*. massa molar. Para o efeito, foram desenvolvidos dois métodos distintos, utilizando na primeira dimensão ou uma coluna de fase reversa convencional (C18) ou uma coluna de interação hidrofílica/fase reversa (HILIC, sigla inglesa), e na segunda dimensão uma coluna de exclusão por tamanhos (SEC, sigla inglesa). Os perfis cromatográficos das frações resultantes dos sistemas C18 x SEC e HILIC x SEC foram registados por três detetores: UV a 254 nm, fluorescência molecular a comprimentos de onda de excitação/emissão ($\lambda_{Exc}/\lambda_{Em}$) de 240/450 nm e detector evaporativo de dispersão de luz.

A distribuição da massa molar das amostras foi caracterizada pelas grandezas massa molar média em número (M_n), massa molar média em peso (M_w), e índice de polidispersão (M_n/M_w). Os resultados obtidos sugerem que a combinação de dois mecanismos de separação independentes constitui um método promissor na separação de amostras de MON. A distribuição de M_w obtida neste estudo foi de 745 a 2122 Da, 637 a 1950 Da e 157 a 891 Da para as amostras de AF-RS, AF-LP e MOSA de aerossóis atmosféricos, respectivamente. A gama de valores obtidos para a distribuição de M_w foram associados às diferentes origens e mecanismos de formação das amostras de MON, os quais podem influenciar a respectiva composição química e distribuição de tamanhos moleculares.

keywords Comprehensive two-dimensional liquid chromatography; natural organic matter; size-exclusion chromatography; reversed-phase liquid chromatography; mixed-mode reversed-phase/hydrophilic interaction

abstract For the purpose of resolving the chemical heterogeneity of natural organic matter (NOM), comprehensive two-dimensional liquid chromatography (LC x LC) was employed for the first time to map the hydrophobicity and polarity *vs.* molecular weight (MW) distribution of the following complex organic mixtures: Suwannee River (SR-FA) and Pony Lake (PL-FA) Fulvic Acids, both obtained from the International Humic Substances Society, and water-soluble organic matter (WSOM) from atmospheric aerosols. Two methods have been developed using either a conventional reversed-phase silica column (RP-C18) or a mixed-mode hydrophilic interaction column (mixed-mode HILIC) in the first dimension, and a size-exclusion column (SEC) in the second dimension. The RP-C18 x SEC and mixed-mode HILIC x SEC fractions were screened on-line by UV at 254 nm, molecular fluorescence at excitation/emission wavelengths ($\lambda_{Exc}/\lambda_{Em}$) of 240/450 nm, and by evaporative light scattering.

The MW distributions of these NOM samples were further characterized by number average molecular weight (M_n), weight average molecular weight (M_W), and polydispersity (M_n/M_w). Findings suggest that the combination of two independent separation mechanisms is promising in extend the range of NOM separation. The complete range of M_w values obtained in this study varied within 745-2122 Da, 637-1950 Da, and 157-891 Da for the SR-FA, PL-FA and WSOM, respectively. The obtained results were associated to the different origin and formation pathways of the three NOM samples, which strongly influence their chemical composition and MW distribution.

Table of contents

List of tables

List of figures

List of acronyms

DOC- dissolved organic carbon

ELSD- evaporative light scattering detector

FLD- fluorescence detector

HILIC- hydrophilic interaction liquid chromatography

HPLC- high performance liquid chromatography

HS- humic substances

IHSS- International Humic Substances Society

MW- molecular weight

M_w- weight average molecular weight

M_n – number average molecular weight

NOM-natural organic matter

NP- normal phase

PL-FA- Pony Lake fulvic acid

POM- particulate organic matter

RP- reversed phase

SEC- size exclusion chromatography

SR-FA- Suwannee River fulvic acid

UVD- Ultra-Violet detector

1^{st} D- first dimension

2^{nd} D- second dimension

1D-LC- one-dimensional liquid chromatography

2D-LC- two-dimensional liquid chromatography

3D-EEM- three-dimensional excitation-emission matrix

WSOM- water-soluble organic matter

Objectives of the current work

The chemical composition and physical properties of natural organic matter (NOM) are fundamental features that influence its behavior in the environment. So, it is crucial to understand and know their molecular structure. However, this understanding is limited by the complexity of the sample, which is impossible to be resolved by the traditional one-dimensional liquid chromatography (1D-LC) techniques, mostly due to the lack of resolving power. The 1D-LC has been widely applied and proved to be a fundamental tool in the separation of complex mixtures. However, the development of a multidimensional method could be a valid approach for accomplishing the characterization of NOM. Therefore, the main goal of this work is to apply a comprehensive two-dimensional liquid chromatography (2D-LC) methodology to three different NOM samples: Suwannee River fulvic acid standard material (SR-FA), Pony Lake fulvic acid reference material (PL-FA), both obtained from International Humic Substances Society (IHSS), and water-soluble organic matter (WSOM) from atmospheric aerosols collected during the Winter season in a rural site. Additional details on aerosol sampling, sample preparation, and structural characterization are described in the work of Duarte et al. (2007).

This work is organized in four chapters. In the first it is discussed the importance of NOM and the need for a deeply understanding of its structure, as well as some theoretical aspects of the aquatic and atmospheric NOM. The 2D-LC system and the need for applying this technique to NOM analysis is also discussed in this chapter. Chapter 2 encompasses the spectroscopic characterization of NOM by molecular fluorescence spectroscopy. It includes the description of the applied methodology and discussion of the obtained results. Chapter 3 consists in the optimization of the chromatographic conditions for the separation of NOM samples by 2D-LC. After the optimization of the chromatographic conditions of the first dimension (1^{st}D) and second dimension (2^{nd}D), chapter 4 describes the implementation of the comprehensive 2D-LC methodology for the analysis of the NOM samples and the results obtained. The discussion of the results is also presented in this chapter.Finally, some final remarks and conclusions are presented, as well as some perspectives for future work.

At the end of this work it is expected to demonstrate the applicability of the 2D-LC as a state-of-the-art analytical technique for the understanding of NOM compositional variability.

Chapter 1

Introduction

1.1. Natural organic matter: importance and composition

NOM is a complex heterogeneous mixture of organic compounds having a wide range of physico-chemical properties. Ubiquitous in terrestrial, aquatic and atmospheric environments, NOM is composed of different classes of compounds, that vary in terms of acidity, charge density, and molecular structure, and range from low molecular weight (MW), such as amino acids and urea, to high MW compounds, collectively called humic substances (HS) (humic and fulvic acids) (Swietlik *et al.*, 2004; Reemtsma, 2009a). Nowadays, there is still a lack of a consensual definition of NOM since its chemical composition and structural characteristics are not exactly known. Their composition depends not only on their sources (autochthonous and allochthonous), which are related to their geographical localization and seasonal variations (Kaiser *et al.*, 2002; Li *et al.*, 2006; Sharp *et al.*, 2006; Rosario-Ortiz *et al.*, 2007; Wei *et al.*, 2008; Kaiser and Benner, 2009; Tremblay and Gagné, 2009; Vancampenhout *et al.*, 2009; Micić; *et al.*, 2011; Selberg *et al.*, 2011), but also on the various complex biological and abiotic reactions.

NOM play a fundamental role in the environment. On soil it is responsible for the cation-exchange capacity (Oorts, 2003) and is extremely important in retaining cations against leaching (Caravaca *et al.*, 1999; Chen, 2003). It also form complexes with metal ions (Lu, 2002; Twardowska, 2003; Hur, 2011; Uchimiya, 2011) and reduces its oxidized forms. This lead to changes in their solubility, on their mobility, and make them less bioavailable (Xu, 1988). This capacity to form metal binding is probably the most important and the most study role of NOM not only in the soils, but also in water matrixes (Doig, 2006; Dessureault-Rompré *et al.*, 2010; Gheorghiu, 2010; Li, 2010). NOM also participate in mineral matter degradation (weathering of rocks and minerals) (Stevenson, 1985; Oliva, 1999; Lindroos, 2003) and adsorb organic chemical pollutants (e.g. pesticides and their derived residues), forming stable chemical linkages and thereby affect their bioactivity, persistence, biodegrability, leaching in soils, and volatility (Northcott, 2000; Mudhoo, 2011).

NOM also represent a major portion of the total organic carbon on earth's surface (water, soil and air) (Reemtsma, 2009b), thus having a very important influence

on the global carbon cycle (Mathur and Farnham, 1985; Lloret, 2011; Sepúlveda, 2011). It contributes to plant growth in soil due to its nutritional function as a source of nitrogen, phosphorous and sulfur (Stevenson, 1994c), and could as well participate in complexation of enzyme proteins that could inhibits their catalytic activities (Mathur and Farnham, 1985; Zech, 1997). The presence of certain functional groups influences their general properties and consequently influences their behavior in the natural environment (Yves Dudal and Frédéric Gérard, 2004; Uchimiya, 2011). So it is crucial to understand and know the chemical and molecular structure of NOM

All samples collected from different environmental matrices are constituted by an inorganic (e.g., metal and salt species) (Valsecchi and Polesello, 1999; Kazi *et al.*, 2009) and an biological component. The biological component, resulting from the decomposition of plants and animals by microbial, chemical, physical and enzymatic transformations, is the fundamental source of NOM (McKnight *et al.*, 1985; Stevenson, 1994c).

NOM is composed by a humic (humus or humified organic matter) and a non-humic fraction (Thurman, 1985). The non-humic fraction is composed by identifiable substances released directly from cells such as proteins, aminoacids, and sugars, and it appears to be less structured and complex than the humified fraction (Bot and Benites, 2005). This non-humic fraction can undergo transformation into humic compounds by means of aromatization and condensation reactions (Vergnoux *et al.*, 2011). The non-humic substances can also be associated to HS, such proteins and polysaccharides, through covalent bonding and electrostatic interactions, thus enabling a clear distinction between humic and non-humic fraction (Leenheer, 1985).

1.1.1. Humic fraction of NOM

Humic fraction is the part of organic matter that has been used and transformed by many different organisms (humification process) and that is formed by stable components that could be grouped in three sub-fractions: fulvic acids, humic acids and humin. This is an operational definition, developed by Odén in 1919 and

largely accepted by all the scientific community. It is based on the isolation procedure applied to solid-phase source materials, such as soils, and it relies on the differences in the solubility at different pH values and in the observed color (Stevenson, 1994b; Steinberg, 2003). Fulvic acids results from the association of small hydrophilic molecules with a certain number of acidic functional groups (particularly –COOH) which makes them soluble in water under all pH values. Humic acids results from the linkage of hydrophobic compounds by hydrophobic dispersive forces. Decreasing the pH to values lower than 2, the intermolecular hydrogen bonding increase and the humic acids flocculate (Piccolo, 2002). Humin is insoluble at any pH values and exhibit a black color (Bot and Benites, 2005). Despite of these differences, fulvic acids, humic acids and humin do not have three different types of organic molecules. In fact, these fractions correspond to different stages of a degradative or synthetic pathway in the humification process (Stevenson, 1985; 1994a; Bot and Benites, 2005).

According to the degradative theory, plants and microorganisms debris give rise to refractory high molecular mass organic compounds, i.e. humin, which are precursor material for humic and fulvic acids formation upon degradative oxidation. During these degradative processes, other organic compounds are formed exhibiting lower molecular weight, higher solubility, and constituted by more variable molecules with lower similarity compared to the source material (Stevenson, 1994a).This pathway are schematized in Figure 1.

Figure 1. Schematic illustration of the degradative pathway involved in the formation of HS.

Within the synthetic pathway, presented in Figure 2, plant and microorganisms synthesize and excrete small MW compounds (such as polyphenols), which together with the organic compounds released during the oxidative degradation of lignin,

undergo condensation reactions or polymerization and promote the formation of HS (Stevenson, 1994a).

Figure 2. Schematic illustration of the synthetic pathway involved in the formation of HS

The molecular structure of HS is still a matter of debate in the scientific community. The more traditional approach considers that HS are associated according to a macropolymeric model, constituted by high MW structures that can coil or expand under specific conditions of pH and ionic strength (Ghosh and Schnitzer, 1980; Relan *et al.*, 1984; Swift, 1999). A more recent concept considers that HS are formed by spontaneous aggregation of different and undefined small compounds (without macromolecular character). The aggregates are stabilized by weak forces (such as dispersive hydrophobic interactions and hydrogen bonds), are more or less well microscopic defined and they are viewed as supramolecular associations with different macroscopic organizations (Conte and Piccolo, 1999; Cozzolino *et al.*, 2001). This model is, however, just a theoretical approach, lacking of valid experimental verification. Recently, Baigorri *et al.* (2007) concluded that macromolecules, small molecules and supramolecular associations coexist in HS. With the evolution of the analytical methods, progressive refinements in the structural models of HS have been verified, and the determination of humic fraction components as specific molecular structures is beginning to be seen as an advantageous work. However, some authors are still skeptics and consider that the characterization of humic fraction at the molecular level is impossible to be achieved (Leenheer, 2007).

1.2. Extraction, fractionation, and characterization of NOM

1.2.1. NOM in lake and rivers waters

As previously mentioned, NOM is present in all compartments of the earth (water, soil and atmosphere) and interact with each other, thus constituting a dynamic and mutant system (McKnight *et al.*, 1985). In this work, a special attention will be devoted to aquatic (lake and river) and atmospheric environments, since the NOM from these matrices will be the focus of the current research work.

NOM is found in all aquatic environments in a typical concentration between 0.5 to 4 mg C L^{-1}, being present under the form of dissolved organic matter (DOM) and particulate organic matter (POM) (Haitzer *et al.*, 1998). These two fractions are also operational defined: the fraction that passes through a 0.45 μm pore size filter correspond to DOM, whereas the organic matter retained by the filter is designated as POM. In aquatic ecosystems, the largest pool of organic material in the water column is DOM (Hessen and Tranvik, 1998). When referring to the dissolved fraction of organic matter, the terms “DOM” and “dissolved organic carbon (DOC)” have been wrongly applied interchangeably along the literature. However, it is important to distinguish between these two terms. DOM corresponds to all organic matter dissolved in the aquatic sample, including the DOC. The DOC is determined by combustion techniques coupled to a carbon analyzer, and it corresponds only to the carbon dissolved in the water sample. Nevertheless, these two terms are associated and they can be interconvert, since the DOC accounts for approximately 45 to 50% of DOM (Kalbitz *et al.*, 2000; Allan and Castillo, 2007).

Since no standard protocol exists to characterize aquatic NOM, the comparison of the results obtained by different methods must be performed with caution. Nevertheless, the study of aquatic NOM entails four general steps, as depicted in Figure 3: (1) sampling, (2) extraction and isolation, (3) fractionation, and (4) structural characterization.

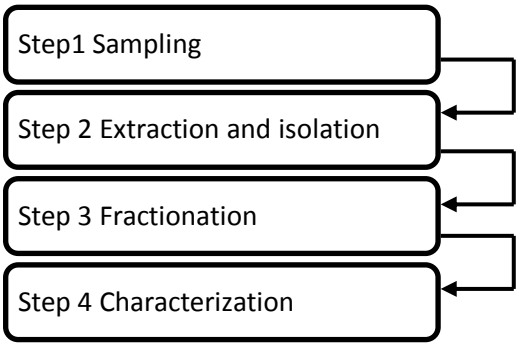

Figure 3. General procedure to study NOM

After the sampling procedure, it is crucial to proceed with the extraction and isolation of the organic compounds. The aim of this step is to remove possible interferences present at low concentration levels by employing an adequate analytical method that assures a representative fraction of the original sample (Varga *et al.*, 2001). Reverse osmosis (Koprivnjak *et al.*, 2009; Bagastyo *et al.*, 2011), XAD resins (Wang *et al.*, 2009; Pernet-Coudrier *et al.*, 2011), and ion exchange chromatography (Nagao *et al.*, 2003; Long Zhang *et al.*, 2009) have been the procedures most employed in this step. It is important to note that some of the analytical techniques used in the extraction and isolation procedure could also act as a fractionation technique. This suggest that steps 2 and 3 of Figure 3 can be performed in just one run. XAD- resins is a good example of such procedures (Wang *et al.*, 2009; Pernet-Coudrier *et al.*, 2011). The fractionation step can also be accomplished by electrophoresis (Peuravuori *et al.*, 2005; Tsukasaki and Tanoue, 2010), ultrafiltration (Kaiser and Benner, 2009; Bagastyo *et al.*, 2011), and by liquid chromatography (Minor and Stephens, 2008; Tercero Espinoza *et al.*, 2011).

Characterization has been mostly made by elemental analysis (Lankes *et al.*, 2008; Tremblay and Gagné, 2009), mass spectrometry (Minor and Stephens, 2008; Louchouarn *et al.*, 2010), fluorescence spectroscopy (Wang *et al.*, 2009; Bagastyo *et al.*, 2011), UV specific absorbance (Wang *et al.*, 2009; Selberg *et al.*, 2011), nuclear magnetic resonance (Koprivnjak *et al.*, 2009; Abdulla *et al.*, 2010), and Fourier

transform infrared spectroscopies (Minor and Stephens, 2008; Long Zhang *et al.*, 2009). It is important to note that NOM samples are very complex matrixes and any of these characterization techniques give clear results without a previous fractionation technique. This is especially evident when is employed a mass spectrometry technique.

1.2.2. NOM in atmospheric aerosols

Atmospheric aerosols are defined as liquid or solid suspended particles dispersed in the atmosphere (gas phase) with diameters ranging from 10^{-9} to 10^{-4} m (Ulrich Pöschl, 2005; Kimberly A. Prather *et al.*, 2008). Smoke, fog and smog are some examples of aerosols particles existing in the troposphere (Kimberly A. Prather *et al.*, 2008). They can originate from natural (e.g. volcanic eruptions, sea salt and soil emission particles, plant fragmentation, pollen, and microorganisms) and anthropogenic sources (e.g. biomass burning, combustion of fossil fuel, industry dust, and traffic-related dust) (Ulrich Pöschl, 2005). Atmospheric particles can also be classified as primary and secondary particles according to their formation mechanisms. Primary atmospheric aerosols are directly emitted as liquid or solid particles (from anthropogenic or/and natural sources) into the atmosphere, whereas secondary aerosols are formed *in situ* in the atmosphere by means of photo-oxidation reactions of primary organic volatile compounds with other species (namely, hydroxyl and nitrate radicals and ozone) emitted into the atmosphere. These photo-oxidation reactions originate a large number of compounds with different functional group composition, which are more reactive, highly oxidized, and less volatile than their precursors. This fact, together with the wide range of source contributions, explains the large variety of compounds that constitute the atmospheric aerosols (Ulrich Pöschl, 2005; Henry *et al.*, 2008; Kimberly A. Prather *et al.*, 2008).

Aerosol particles are constituted by an inorganic and organic component. The organic fraction, also referred as carbonaceous material, is composed by organic carbon and elemental carbon (sometimes also referred as black carbon) (Ulrich Pöschl, 2005). Previous works have shown that a highly variable fraction (from 20% to 77%) of

the aerosol carbonaceous material is soluble in water (Zappoli *et al.*, 1999; Decesari *et al.*, 2000; Duarte *et al.*, 2005). The WSOM has hygroscopic properties, thus influencing the effective density (Zelenyuk *et al.*, 2010), surface tension behavior (Facchini *et al.*, 2000; Tuckermann and Cammenga, 2004), and ability of the aerosol particles to act as cloud condensation nuclei (Saxena *et al.*, 1995; Shulman *et al.*, 1996; Cruz and Pandis, 2000; Peng *et al.*, 2001).

Studies on the chemical characterization of the WSOM have reported the presence of aliphatic structures (e.g. aliphatic alcohol, aliphatic mono-, di- and policarboxylic acids, hydroxylate acid compounds), amines (e.g. amino acids and hydroamines), alcohols, polyols, ketoacids, mono-, di-, and polycarbonyls, polyethers, sugars, and other oxygenated functional groups, as well as hydrocarbons and aromatic structures (Saxena and Hildemann, 1996; Facchini *et al.*, 1999; Facchini *et al.*, 2000; Krivácsy *et al.*, 2001; Kiss *et al.*, 2002; McFiggans *et al.*, 2005; Duarte *et al.*, 2007; Duarte *et al.*, 2008; Xia and Gao, 2010; Laitinen *et al.*, 2011). However, and despite this current knowledge on the main structural features of the aerosol WSOM, this fraction is still poorly characterized at the molecular level. The multitude of molecular forms, sources, and reactivity makes the complete characterization of this organic fraction extremely difficult.

In terms of standard methodology for the characterization of aerosol WSOM, no such method is current available in the literature. Extraction and isolation of WSOM have been made principally by solid-phase extraction (reversed phase (RP) (Varga *et al.*, 2001), Hydrophilic-lipophilic, anion exchange (Parshintsev *et al.*, 2010), and XAD-resins (Samy *et al.*, 2010)), and ion-exchange chromatography (Iinuma *et al.*, 2009). Seems that atmospheric aerosols are complex samples it is crucial to separate the components that constitute them. The techniques most frequently employed in the third step are liquid chromatography (Mancinelli *et al.*, 2007; Kitanovski *et al.*, 2011) and capillary electrophoresis (Krivácsy *et al.*, 2000; Dabek-Zlotorzynska *et al.*, 2005). It is important to note that step (2) and step (3) (isolation and fractionation procedures) could be done by just one analytical technique enclosing in one procedure those two steps. In what concerns the structural characterization of the aerosol WSOM,

techniques such as elemental analysis (Ma *et al.*, 2001; Duarte *et al.*, 2007), mass spectrometry (Stone *et al.*, 2009; Kitanovski *et al.*, 2011), UV-Vis spectroscopy (Duarte *et al.*, 2005; Krivácsy *et al.*, 2008) , Fourier transform infrared spectroscopy (Krivácsy *et al.*, 2001; Kiss *et al.*, 2002), fluorescence spectroscopy (Duarte *et al.*, 2005; Nakajima *et al.*, 2008),and nuclear magnetic resonance (Decesari *et al.*, 2005; Duarte *et al.*, 2008) are the most frequently employed.

An important portion of aerosols organic fraction that largely contribute to the mass of organic compounds is an macromolecular fraction that was firstly mentioned by Went and co-workers (1960). After that, Havers *et al.* (1998) concluded that these compounds have a certain degree of similarity with the naturally occurring humic acids and proposed the term humic-like substances to designate this organic fraction. After this, many researchers have been study this particularly fraction and confirm Havers discovery (Zappoli *et al.*, 1999; Kiss *et al.*, 2002; Duarte *et al.*, 2007; Stone *et al.*, 2009; Lin *et al.*, 2010). However, some of them found that water soluble organic macromolecular fraction is only qualitatively similar humic material (Sannigrahi *et al.*, 2005; Duarte *et al.*, 2007). The origin of these substances in aerosol particles has been also object of interest. They be from a primary source (directly emitted from the source to the atmosphere) (Cavalli *et al.*, 2004; Mayol-Bracero *et al.*, 2002) or secondary origins resulting from different pathways like condensation, polymerization and/or oligomerization of the polar low MW particles directly emitted to the atmosphere (Gelencsér *et al.*, 2002; Hung *et al.*, 2005).

1.2.3. Limitations of the studies developed so far

Due to the huge complexity of NOM samples, the analytical techniques applied so far were unable to provide detailed information on the molecular structure of these samples. In fact, some authors believe that full molecular characterization could be impossible to achieve in spite of the recent evolution in the field of advanced analytical techniques (Gašparović *et al.*, 1997; MacCarthy, 2001; Leenheer, 2007). The solution to this current situation could pass through the application of fractionation methods in

order to reduce the heterogeneity of the NOM samples. The 1D-LC is the technique most employed for NOM separation (Parlanti *et al.*, 2002; Dittmar and Kattner, 2003; Alberts and Takács, 2004a; Kennedy *et al.*, 2005; Persson *et al.*, 2006; Allpike *et al.*, 2007; Koch *et al.*, 2008; Tercero Espinoza *et al.*, 2009; Duarte and Duarte, 2010; Huber *et al.*, 2011).

In spite of the improvements verified in the recent years in the liquid chromatography system (specially on the evolution of the new stationary phases (de Villiers *et al.*, 2006), in coupling columns in series (Lestremau *et al.*, 2006), and in operating at elevated temperatures (Wang *et al.*, 2006)) 1D-LC does not meet the expectations of researchers due to its limitations in resolving power. According to Guiochon *et al. (2008)*, there is the need for shorter separation times in complex systems, and the actual methods applied in 1D-LC will not be able to provide a significant progress on this issue. If the number of sample components exceeds the chromatographic peak capacity in 37%, then the separation resolution is compromised, and even in simple mixtures the separation by 1D-LC can not provide an adequate response (Davis and Giddings, 1983). A possible way for innovation in this field is the development of multidimensional separations, using different separation mechanisms at the various dimensions.

1.3. Comprehensive 2D-LC

A 2D-LC system consists of two 1D-LC systems connected through an interface or flow modulator. In order to take full advantage of the two dimensionalities, the sample is subjected to two different separation mechanisms, which must be completely independent from each other and show distinct retention profiles, that is, the separations must be orthogonal (Dugo *et al.*, 2008).

One of the main problems associated to the 2D-LC is the need for designing the separation for maximum orthogonality and, simultaneously, avoiding any potential incompatibility and immiscibility between the mobile phases of the first and second column (Dugo *et al.*, 2008). The most recent developments in multidimensional LC,

especially in 2D-LC, have been associated to the needs for increasing resolution and peak capacity in proteomic research, as well as for an independent relationship between size and chemical structure selectivity in the industry of polymers (Cohen and R.Schure, 2008). The 2D-LC provides a higher peak capacity (twice as much when compared to the peak capacity of the 1D-LC), higher resolving power, higher selectivity, and it takes less analytical time (Shellie and Haddad, 2006; Guiochon *et al.*, 2008; Dugo *et al.*, 2008). Consequently, all of the above mentioned aspects led to an improvement in the analytical performance of 2D-LC when compared to 1D-LC.

As demonstrate in Figure 4, the 2D-LC systems can be classified in on-line and off-line, depending on the way how the sample is transferred from the first to the second column. In an off-line approach, fractions of the eluent from the first column are collected, concentrated, and subsequently injected into the second column. In the on-line approach, the two dimensions are linked by an interface or flow modulator capable of collecting fractions from the first column and simultaneously inject them into the second column (François *et al.*, 2009). The off-line 2D-LC has the advantage of being easy to manipulate, but it is prone to sample losses and contaminations. Furthermore, it usually has longer times of analysis than the on-line systems. The on-line approach is faster and more reproducible; however, it needs specific interfaces, and it is more sophisticated regarding the operational procedures (François *et al.*, 2009).

On-line systems can be further divided into heart-cutting (usually abbreviated as LC-LC) and comprehensive (usually abbreviated as LC × LC), and the main difference between these two modes of operation is related to the quantity of sample that is transferred from the 1^{st}D to the 2^{nd}D (Shellie and Haddad, 2006). In heart-cutting 2D-LC, only the fractions identified in the 1^{st}D as relevant and containing the components of interest are subjected to separation in the 2^{nd}D.

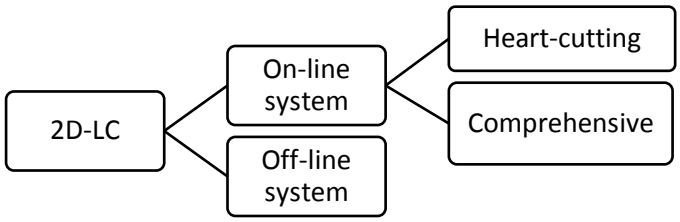

Figure 4. 2D-LC systems classification according to the transferred mode of the sample from the 1stD to the 2ndD column

In comprehensive 2D-LC, successive fractions of the entire sample separated in the first column are sequentially sent to the second column. Therefore, in comprehensive 2D-LC, the entire sample is subjected to both separation processes associated to each column (François *et al.*, 2009). The scheme of this system is above describe in Figure 5. The great advantage of this technique is that the whole sample is fractionated by two completely independent separation mechanisms, and the separation accomplished in the 1stD is preserved along the 2ndD analysis. The final comprehensive 2D-LC profile is the end result of the combination of the two separation mechanisms (François *et al.*, 2009; Dugo *et al.*, 2008).

While the sample fractions are being separated in the 2ndD, the loop of the interface collects one more fraction of the effluent from the 1stD. Therefore, the adequate flow rates must be chosen in such a way that the analysis time of the 2ndD corresponds to the necessary time to fill the loop with the effluent from the 1stD. Furthermore, this time must be sufficient to accomplish the analysis of the entire sample without interrupting the flow (Shellie and Haddad, 2006).

To maintain the separation obtained along the 1stD it is crucial to chose an adequate modulation period. If the sampling period is too longer (modulation period larger than the 1st D peak widths), the separation obtained in the 1stD is lost and the compounds co-elute. If the sampling period is too short (several sampling collections by each peak), a huge analysis time is spent. In order to avoid the loss of information

and unnecessary analysis time, the collection of the effluent from the 1stD must correspond to three or four modulations periods by each 1D peak (Dugo *et al.*, 2008).

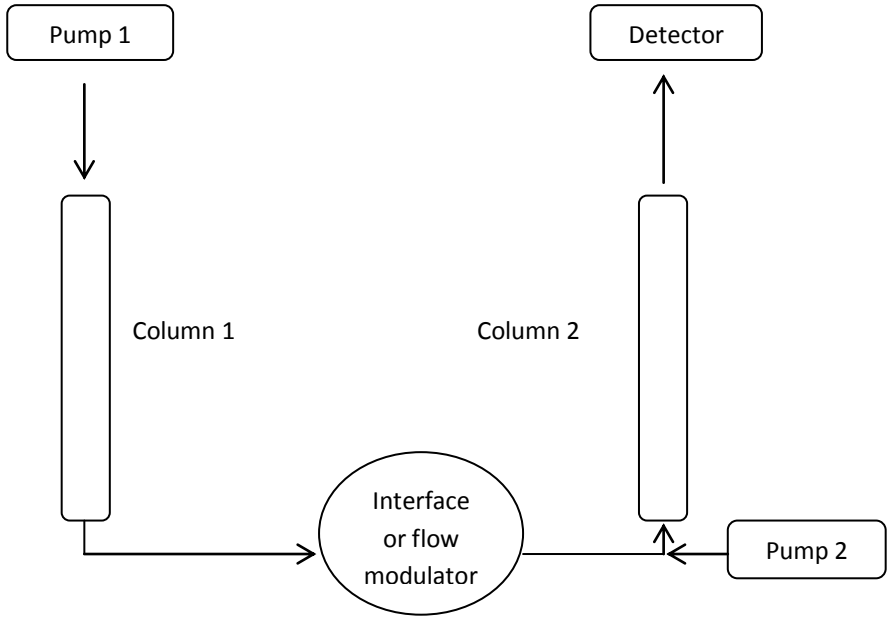

Figure 5. Schematic representation of a comprehensive 2D-LC system components

A 2D-LC system, as in the case of 1D-LC, allows the use of more than one detector connected in series, which are usually coupled at the end of the 2ndD column for maximum analytical information. Mass spectrometry (Kivilompolo *et al.*, 2008; Pól *et al.*, 2006) and ultra-violet spectroscopy (Hu *et al.*, 2005; Brudin *et al.*, 2010) are the most frequently detectors employed in 2D-LC systems. The main issue here lies in the fact that the 2ndD analysis should be very fast, and the detector must be able to detect a large number of peaks in a short period of time (Stoll *et al*., 2007). Mass spectrometry detection don´t support fast acquisition rate and the flow need to be split before the detector (Guiochon *et al.*, 2008).

1.3.1. Comprehensive 2D-LC applied to complex organic mixtures

2D-LC is the most develop method in the field of the multidimensional separation and has been largely employed in the analysis of complex organic mixtures such as proteins (Opiteck *et al.*, 1998; Stoll and Carr, 2005; Rao and Shinde, 2009; Boyan Zhang *et al.*, 2009; Wang *et al.*, 2010; Turtoi *et al.*, 2010), plant and herb extracts (Chen *et al.*, 2004; Hu *et al.*, 2005; Wang *et al.*, 2007a; Pól *et al.*, 2007; Kivilompolo and Hyötyläinen, 2007; Jeong *et al.*, 2010), food and beverages samples (Blahov *et al.*, 2006; Cacciola *et al.*, 2006; F. Cacciola *et al.*, 2007; Francesco Cacciola *et al.*, 2007; Kivilompolo *et al.*, 2008; Brudin *et al.*, 2010), and polymers(Floyd, 1988; Horst and Schoenmakers, 2003; Coulier *et al.*, 2005; Popovici *et al.*, 2005; Jandera *et al.*, 2006; Vivó-Truyols and Schoenmakers, 2006; Im *et al.*, 2009; Raust *et al.*, 2010). However, this technique has not been used in the separation of NOM from environmental samples and until now, just one work has been reported in the literature addressing the application of comprehensive 2D-LC for the quantitative determination of acidic compounds in rural and urban atmospheric aerosols (Pól *et al.*, 2006).

Chapter 2

Spectroscopic characterization of NOM by three-dimensional excitation-emission matrix fluorescence spectroscopy

2.1. Introduction

Since one of the detectors employed in the 2D-LC chromatographic system is a fluorescence detector (FLD), it is fundamental to study each sample and to identify the specific excitation/emission ($\lambda_{Exc}/\lambda_{Em}$) wavelengths to be employed in the subsequent 2D-LC analyses. With this as an objective, three-dimensional excitation-emission matrix (3D-EEM) fluorescence spectroscopy was performed, and the general spectroscopic characteristics of each sample were described.

When a molecule absorbs electromagnetic radiation with a certain wavelength, electrons are excited to a higher state level. The return to the fundamental state could occur by non-radiative relaxation processes or by radiative process with the emission of a photon of radiation in the UV-Vis region. Non-radiative processes compete with the radiative emission and the rate at each occur give quantitative and qualitative information about the sample. The fluorescence phenomenon is typically associated to $\pi \rightarrow \pi^*$ transitions. The most intense fluorescence occurs in compounds with conjugated π bond systems like aromatic functional groups and their quantum efficiency increase with the increasing number of aromatic rings and condensation degree (Lakowicz, 2010).

Fluorescence spectra has been one of the most employed techniques in the characterization of water soluble organic fraction (Santos *et al.*, 2001; Duarte *et al.*, 2003; Guéguen *et al.*, 2005; Mancinelli *et al.*, 2007). However, due to the lack of resolving power, this technique give little and featureless information when compared to the high complexity of NOM samples composed by a multi-chromophoric system (Hautala *et al.*, 2000).

More recently, 3D-EEM florescence spectroscopy has been successfully employed in the study of DOM (Her *et al.*, 2003; Duarte *et al.*, 2004; Yamashita *et al.*, 2010; Gonsior *et al.*, 2011). This technique consists in scanning and recording a emission spectra at different excitation wavelengths, in sequential increments. It is obtained a sample matrix fluorescence map that consists in a 3D fluorescence spectra of fluorescence excitation wavelength, emission wavelength and intensity (Matthews *et al.*, 1996; Duarte *et al.*, 2004; Hudson *et al.*, 2007).

2.2. Experimental procedure

Each NOM sample was studied at different pH values: 4.0, 5.0, 7.0, and 8.5. For the pH values of 5.0, 7.0, and 8.5, each sample was dissolved in a phosphate buffer in the rage of 0.018-0.0036 mg mL^{-1}, 0.0027-0.0094 mg mL^{-1}, 0.0037-0.0125 $mg.mL^{-1}$, and 0.0034-0.021 $mg.mL^{-1}$ for the SR-FA, in the range of 0.0050-0.0051 mg mL^{-1}, 0.0050-0.0080 mg mL^{-1}, 0.0040-0.0090 $mg.mL^{-1}$, and 0.0050-0.0080 $mg.mL^{-1}$ for the PL-FA sample, and in the range of 0.0012-0.0015 mg mL^{-1}, 0.0082-0.0089 mg mL^{-1}, 0.0024-0.0068 $mg.mL^{-1}$, and 0.0057-0.0060 $mg.mL^{-1}$ for the WSOM sample at pH 4, 5, 7, and 8.5, respectively. The fluorescence spectra were recorded on a spectrophotometer JASCO, model FP-6500. The 3D-EEM fluorescence spectroscopy involved scanning and recording of 18 individual emission spectra (230-500 nm) at sequential increments of 10 nm of excitation wavelength between 220 and 400 nm. The spectra were recorded at a scan speed of 100 nm min^{-1} using excitation and emission slit bandwidths of 10 nm. Phosphate and acetate buffer solutions were used as blank, and the peaks due to water Raman scatter were eliminated from all spectra by subtracting the blank spectra.

2.3. Results and discussion

The 3D-EEM contour and surface profiles of SR-FA, PL-FA, and WSOM samples are shown in Figure 6, 7, and 8. For the sake of easier comparison between different samples, the 3D-EEM data was normalized to the DOC content of each sample and to the maximum fluorescence intensity. The carbon content of the WSOM sample was previously estimated by Duarte *et al.* (2007) who reported an average percentage of 57.5%. The carbon content of the SR-FA and PL-FA samples was provided by the IHSS supplier: 52.4 % and 52.5%, respectively. This normalization is only possible since the aim of this study was to obtain qualitative information on the fluorescence characteristics of the selected NOM samples.

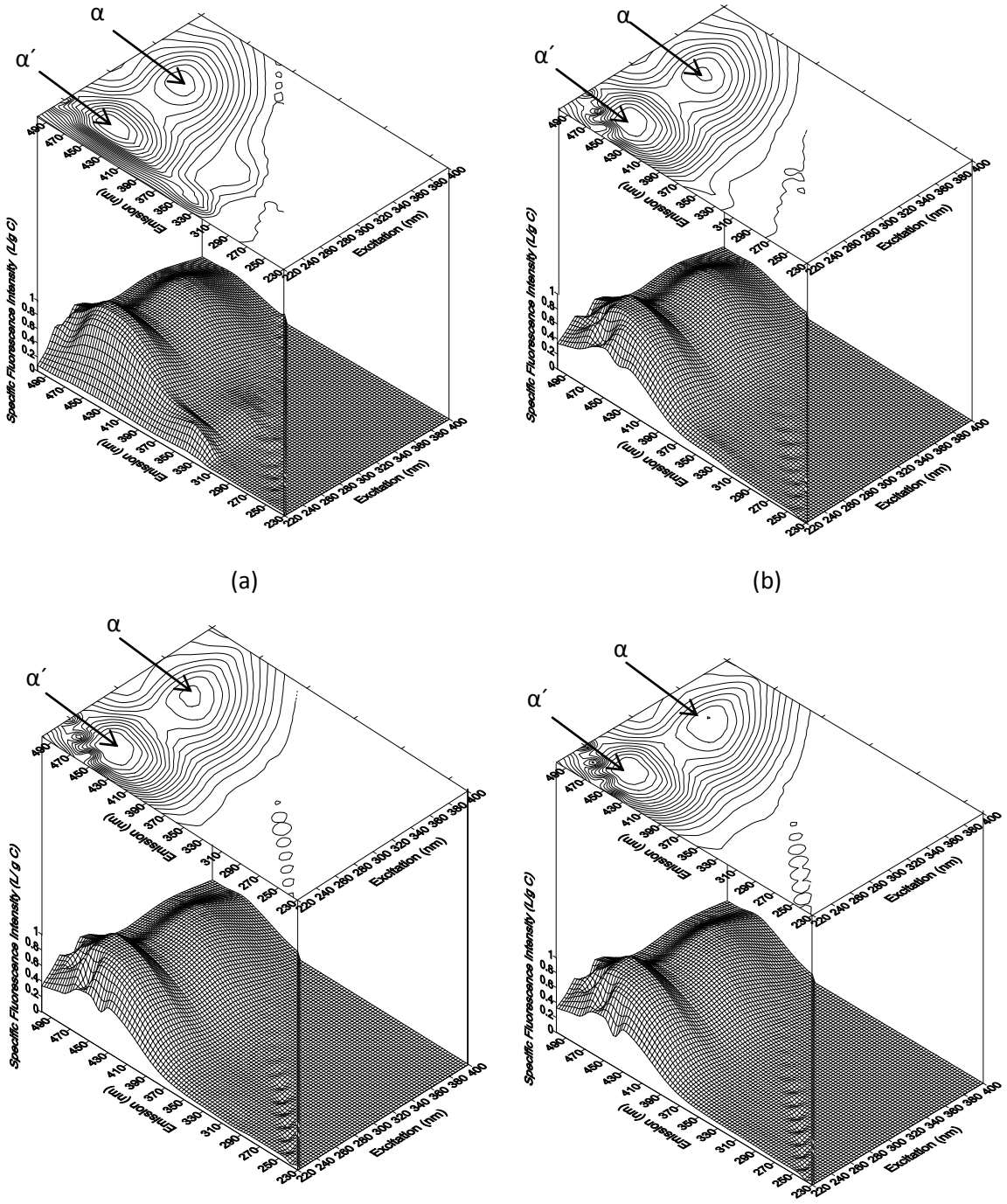

Figure 6. 3D-EEM fluorescence spectra of SR-FA at pH 4.0 (a), 5.0 (b), 7.0 (c), and 8.5 (d)

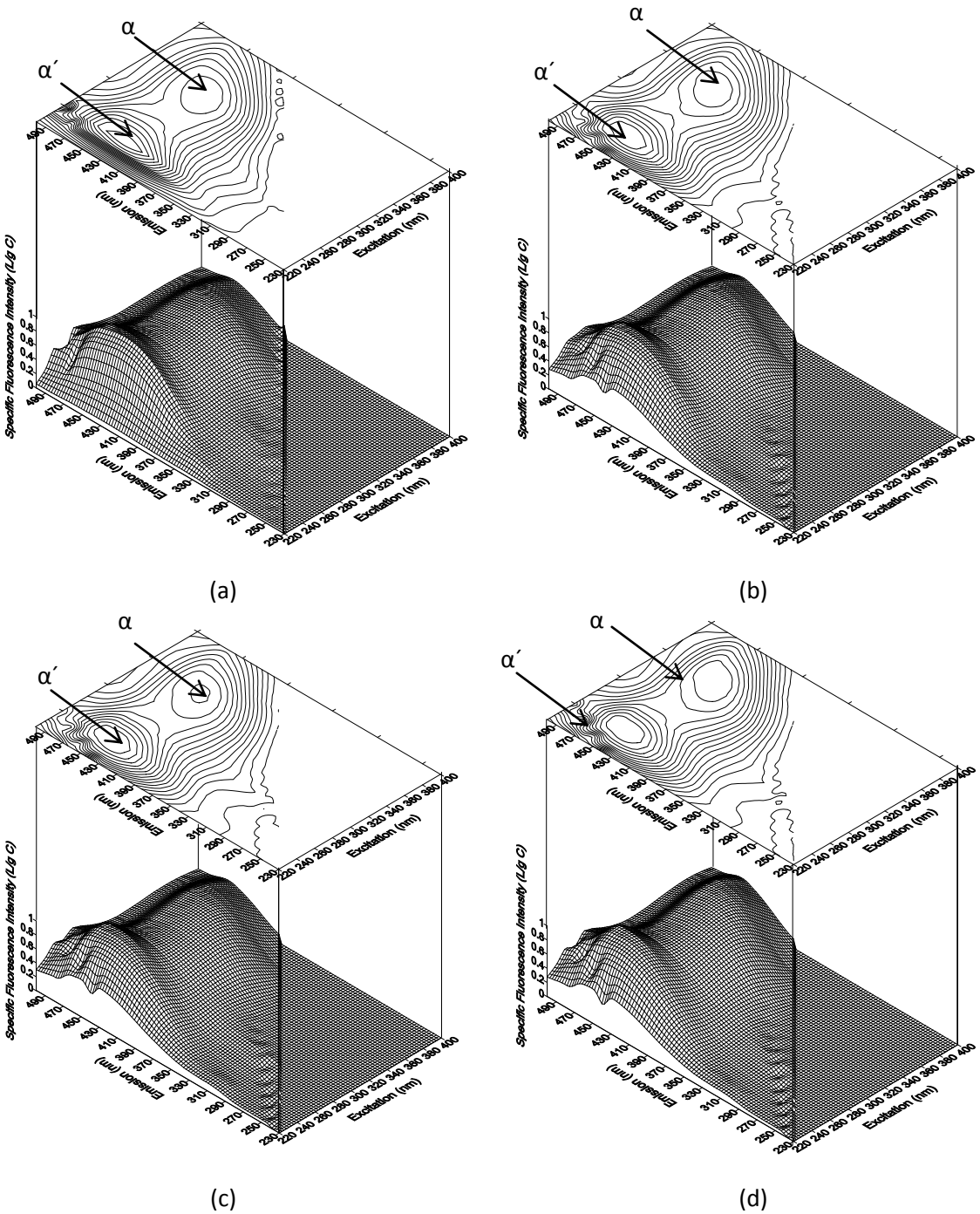

Figure 7. 3D-EEM fluorescence spectra of PL-FA at pH4.0 (a), 5.0 (b), 7.0 (c), and 8.5 (d)

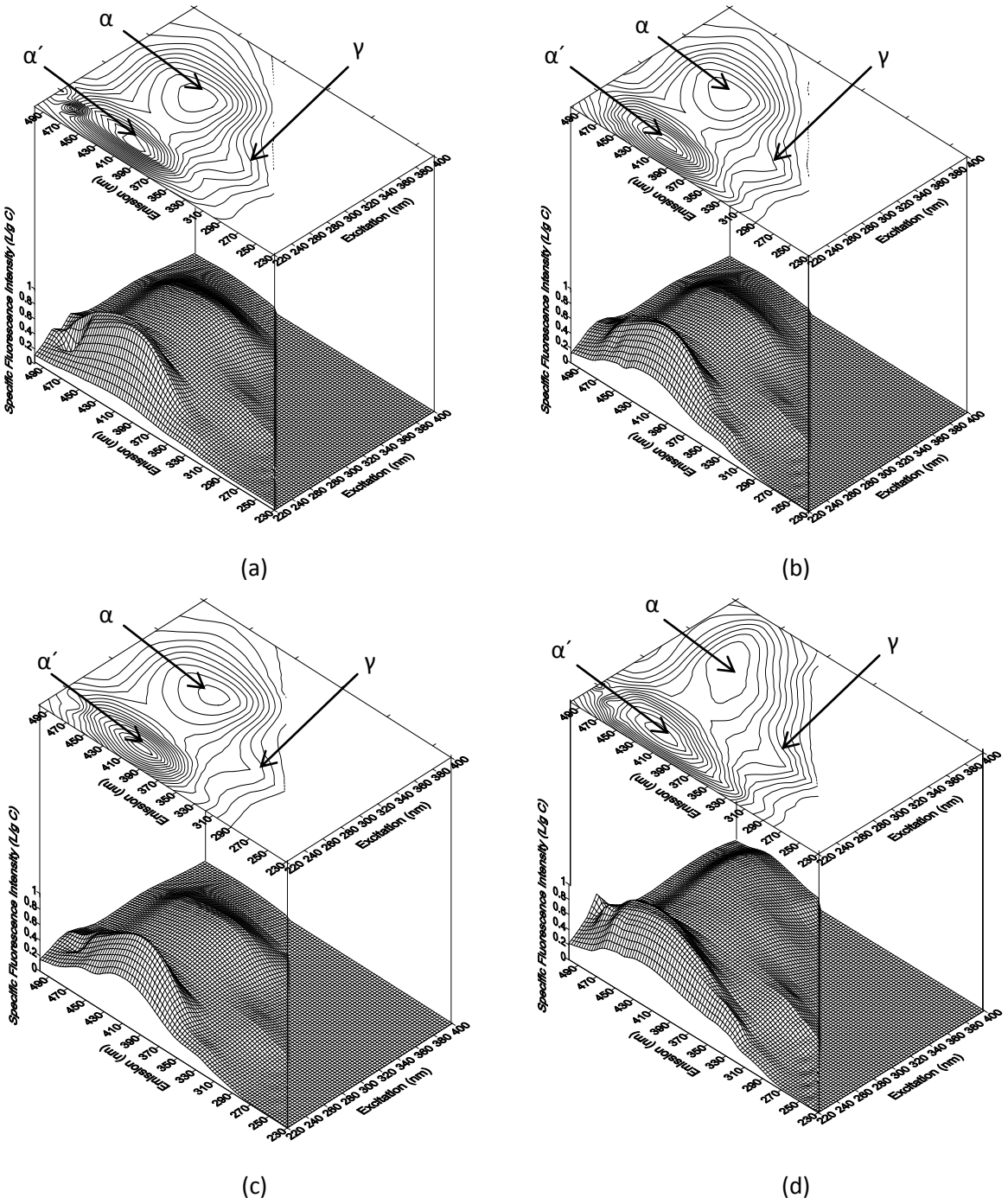

Figure 8. 3D-EEM fluorescence spectra of aerosol WSOM at pH 4.0 (a), 5.0 (b), 7.0 (c), and 8.5 (d)

The identification of each fluorophore was made in agreement to Parlanti *et al.* (2000) work that according to the λ_{Exc} and λ_{Em} name five types of fluorophores (or groups of fluorophores) as α´(237-260/400-500 nm), α (300-370/400-500 nm), β (312/380-420 nm), γ (225-237/309-321 nm and 275/310 nm), and δ (225-237/340-381 nm and 275/340 nm).

For the aquatic fulvic acid samples (SR-FA and PL-FA), and independently of the pH value, two different groups of fluorophores can be distinguished (α´ and α). The λ_{Exc} and λ_{Em} of each one are described in Tables 1 and 2, to SR-FA and PL-FA samples respectively. The obtained results are in agreement with those published in the literature for aquatic fulvic acids, whose fluorescence spectra also exhibit two peaks within the same $\lambda_{Exc}/\lambda_{Em}$ regions (Paula G, 1996; Diane M. McKnight *et al.*, 2001; Her *et al.*, 2003; Alberts and Takács, 2004b; Sierra *et al.*, 2005). Furthermore, the small differences detected between SR-FA and PL-FA on the exact location of the λ_{Exc} and λ_{Em} of each fluorophore can be associated to the different origin of each sample (Sierra *et al.*, 2005). The PL-FA have a microbial source and result from the degradation of algal biomass in the lake sediments or in the water column, whereas SR-FA originate from terrestrial plant and soil-derived organic matter inputs (McKnight *et al.*, 1985).

pH	$\lambda_{Exc}/\lambda_{Em}$ (nm) (α´ peak)	$\lambda_{Exc}/\lambda_{Em}$ (nm) (α peak)
4.0	250/454	329/437-454
5.0	242/445-448	329/454-459
7.0	250/451-453	330/457-458
8.5	250/459	340/460

Table 1. Excitation and emission wavelengths of the peaks identified in the 3D-EEM fluorescence spectrum of the SR-FA sample at different pH values (4.0, 5.0, 7.0, and 8.5)

pH	$\lambda_{Exc}/\lambda_{Em}$ (nm) (α´ peak)	$\lambda_{Exc}/\lambda_{Em}$ (nm) (α peak)
4.0	250/432	332-340/429-435
5.0	250/441-442	340/437
7.0	250/443	340/440
8.5	250/444	350/444

Table 2. Excitation and emission wavelengths of the peaks identified in the 3D-EEM fluorescence spectrum of the PL-FA sample at different pH values (4.0, 5.0, 7.0, and 8.5)

In the 3D-EEM fluorescence spectra of the aerosol WSOM sample, two different groups of fluorophores (α´ and α) and one shoulder (γ) can be distinguished. The λ_{Exc} and λ_{Em} of fluorophores α´ and α at different pH values are described in Table 3. These fluorophores were recognized as microbial and terrestrial derived aquatic fulvic acids structures (Diane M. McKnight *et al.*, 2001). However in the 3D-EEM spectra of WSOM sample there is a shift to shorter wavelengths when compared to SR-FA and PL-FA results suggesting a smaller content of condensed and unsatured structures in the aerosol sample. This conclusion is supported by Duarte *et al.* work (2006) where it was show that WSOM from atmospheric aerosol present a higher content of aliphatic structures when compared with aquatic humic substances. Furthermore some authors have proved that the MW of organic compounds present in the water soluble fraction of atmospheric aerosols are lower than those find in the aquatic humic material (Kiss *et al.*, 2003; Stone *et al.*, 2009; Duarte and Duarte, 2011). The presence of lower MW compounds may also be responsible for the shift towards lower wavelengths in the aerosol WSOM sample (Chin *et al.*, 1994; Chen *et al.*, 2003; Duarte *et al.*, 2004).

pH	$\lambda_{Exc}/\lambda_{Em}$ (nm) (α´ peak)	$\lambda_{Exc}/\lambda_{Em}$ (nm) (α peak)
4	240-242/407-410	320-321/410-413
5	239/410	320/415-418
7	239/407	321-329/413
8.5	239-241/412-420	340/445-448

Table 3. Excitation and emission wavelengths of the peaks identified in the 3D-EEM fluorescence spectrum of the WSOM sample at different pH values (4.0, 5.0, 7.0, and 8.5)

In order to clearly identify the $\lambda_{Exc}/\lambda_{Em}$ values of fluorophore γ, the 3D-EEM data were analyzed as a synchronous spectra obtained by fitting the mathematical equation $\lambda_{Em} = \lambda_{Ex} + \Delta\lambda$ to the 3D-EEM profiles with a Δλ of 40 nm. The synchronous spectrum obtained is presented in Figure 9 and exhibit two main peaks: the first located at $\lambda_{Exc} \approx 280$ nm (λ_{Em} =320 nm) and identified as γ in the 3D-EEM spectra of Figure 8, whereas the second peak is due to the influence of fluorophore α.

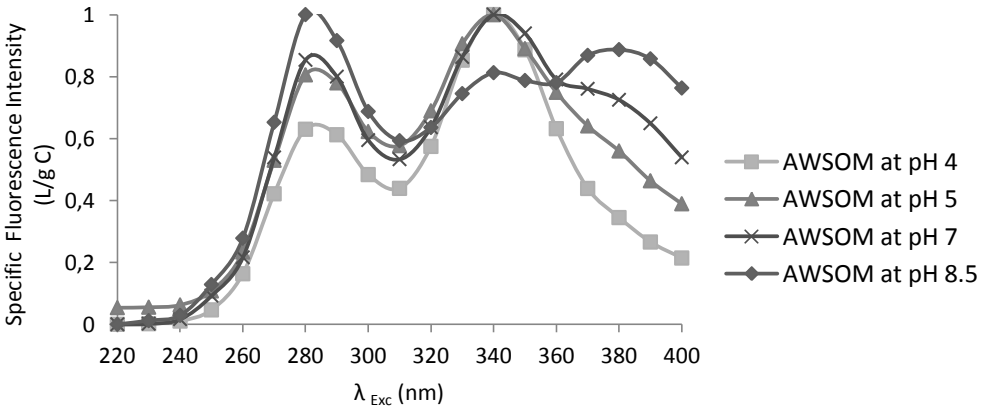

Figure 9. Synchronous fluorescence spectra with Δλ = 40 nm of the aerosol WSOM sample, at different pH values

Duarte *et al.* (2004, 2005), based on the works of Ahmad *et al.* (1995), Parlanti *et al.* (2000), Peuravuori *et al.* (2002), and Yamashita and Tanoue. (2003), suggested that fluorophore γ can be attributed to aromatic amino acids, proteinaceous material, and phenolic compounds.

In what concerns the influence of pH in the 3D-EEM fluorescence features of the NOM samples, it was possible to conclude that different pH environments affect the wavelength localization of the maximum fluorescence intensity. With increasing pH from 4.0 to 8.5 there is shift of the $\lambda_{Exc}/\lambda_{Em}$ of fluorophore α towards higher values. For the SR-FA sample, the $\lambda_{Exc}/\lambda_{Em}$ pair 329/437-454 nm at pH 4, shifts to 340/460 nm at pH 8.5. In the case of the PL-FA sample, from a $\lambda_{Exc}/\lambda_{Em}$ of 332-340/429-435 at pH 4.0 to 350/444 nm at pH 8.5, whereas the WSOM sample from atmospheric aerosol from 320-321/410-413 nm at pH 4 to 340/445-448 nm at pH 8.5. These changes can be attributed to conformational changes in the humic molecules. According to the supramolecular theory, the humic molecule tends to coil and hide their fluorescent components at low pH values as a consequence of increasing the electron-withdrawing groups as a result of the protonation of the organic molecules. At alkaline pH, the molecule tends to extend and expose the fluorescent constituent due to the disruption of the intermolecular hydrogen bindings (Hudson *et al.*, 2007; Carletti *et al.*, 2010).

2.4. Conclusions

The application of the 3D-EMM fluorescence spectroscopy to the SR-FA, PL-FA, and WSOM samples allow concluding that:

- SR-FA and PL-FA samples exhibit two groups of fluorophores (α´and α);
- independently of their different origin, the 3D-EEM spectra of the SR-FA and PL-FA are very similar, thus suggesting that these NOM could exhibit similar functional groups;
- a shoulder at λ_{Exc} /λ_{Em} = 280/320 nm (γ) was found in the aerosol WSOM sample;

- as a consequence of the pH environment change it was verified a shift of the $\lambda_{Exc}/\lambda_{Em}$ towards higher values of fluorophore α as a result of the conformational changes in the fulvic acid molecules;
- seems that the FLD is one of the three detectors that will be then used in the 2D-LC system it was important to available the fluorescence spectroscopic profile of each sample and chose one pair of λ_{Exc} /λ_{Em}.;
- fluorophore α is more susceptible to changes in their λ_{Exc} /λ_{Em}. position as a consequence of the pH environment. Therefore, the pair that will be lately used in the FLD of the 2D-LC system is the one that correspond to fluorophore α´ (240 nm/450 nm).

Chapter 3

Optimization of the experimental conditions for the comprehensive 2D-LC analysis of NOM samples

3.1. Introduction

Before proceeding with the comprehensive 2D-LC analyses of the NOM samples, it is important to optimize the chromatographic conditions in both dimensions, in regard to mobile phase composition, flow rate, and modulation period. Besides mobile phase compatibility, important for avoiding adsorption phenomena of the analytes into the 2^{nd}D column under the injection plug (i.e. transfer volume) conditions, the flow rate used in the 2^{nd}D will determine the sampling rate of the 1^{st}D effluent (i.e. the switching-valve modulation period) and, ultimately, the time needed for accomplishing a high resolved comprehensive 2D-LC map of the NOM samples. In practical terms, the flow rate in the 2^{nd}D must be about 100 times higher than in the 1^{st}D, which usually operates under sufficiently slow flow rate to produce broad peaks. Furthermore, the fast separation in the 2^{nd}D is mandatory to make the modulation period small enough for obtaining a high resolution for the whole comprehensive 2D-LC procedure (Murphy *et al.*, 1998; Pól *et al.*, 2006).

This third chapter presents the results of the optimization of the separation of the NOM samples in both 1^{st}D and 2^{nd}D columns. This optimization procedure was performed independently in each dimension. In the 1^{st}D, either a reversed-phase or a mixed-mode hydrophilic interaction column were used in an attempt to pull apart the NOM samples into more chemically distinct fractions. In the 2^{nd}D, a size exclusion chromatography (SEC) column was used to further fractionate each NOM fraction according to its size and, therefore, obtain a MW distribution. The composition of the mobile phases was selected according to what has been reported in the literature for the chromatographic analysis of NOM from various environments (Wu *et al.*, 2003; Stenson, 2008; Koch *et al.*, 2008; Duarte and Duarte, 2010; 2011; Woods *et al.*, 2011).

3.2. Experimental procedure

3.2.1 Preparation of NOM samples

SR-FA standard material and PL-FA reference material were obtained from IHSS, whereas the WSOM sample was obtained within the framework of a research

project. Additional details on aerosol sampling, WSOM preparation, and structural characterization are described in the work of Duarte *et al.* (2007). NOM solutions were prepared by dissolving an appropriate amount of each sample in the mobile phase of the 1^{st}D or 2^{nd}D, according to the optimization process under study (see the eluent composition for each column in Section 3.2.2). The concentration of each sample was in the range of 0.23-0.42 mg mL^{-1}, 0.23-0.78 mg mL^{-1}, and 0.22-0.57 mg mL^{-1} for the SR-FA, PL-FA, and aerosol WSOM, respectively. Before injection, all NOM solutions were filtered through high performance liquid chromatography (HPLC) Certified Syringe Filters (SPARTAN, Whatman GmbH, Germany) of 0.20 μm pore size.

3.2.2 Instrumentation and chromatographic conditions

The 1^{st}D consisted of a JASCO semi-micro HPLC pump (model PU-2085 Plus), a Rheodyne injection valve (model 7725i) equipped with a 20 μL loop. Two columns were applied in the 1^{st}D: i) RP Kromasil 100-5C18 (Akzo Nobel; diameter 4.6 mm; length 150 cm; particle size 5 μm); and ii) Acclaim Mixed-Mode HILIC-1 column (Dionex, Sunnyvale, CA, USA; diameter 4.6 mm; length 150 mm; comprised of 5 μm high-purity, porous, spherical silica particles with 120 Å diameter pores bonded with alkyl diol functional groups). The 1^{st}D was operated in isocratic mode using a mobile phase composition comprising different amounts of acetonitrile (0, 10, 15, 20, 25, and 30% (v/v)) in the RP-C18 Kromasil column, and 20 mM ammonium acetate, 10% acetonitrile, and acetic acid at concentration of 11 mM and 1.1 mM for two different pH values (5 and 6, respectively) in the mixed-mode HILIC column. The flow rate was 0.1 mL min^{-1} and the temperature of the analytical columns was maintained at 30°C in a JASCO column oven (model CO-2065 Plus). It should be mentioned that for avoiding long elution times (almost three hours) in this optimization procedure, the flow rate used in both RP-C18 and mixed-mode HILIC separations is five times higher than the flow rate that actually will be applied in the comprehensive 2D-LC separations. It was assumed that the flow rate had negligible effects on the chromatographic profile of the NOM samples in the 1^{st}D.

In the 2ndD, a JASCO quaternary low pressure gradient pump (model PU-2089 Plus) and a PSS SEC Suprema 30 Å analytical column (Polymer Standards service GmbH, Mainz, Germany; diameter 8 mm; length 300 mm; particle size 10 µm; separation range 100-30.000 Da; stationary phase polydroxymethacrylate copolymer) were applied. The 2ndD was also operated in isocratic mode with a mobile phase composition consisting of 11% acetonitrile and 20 mM ammonium carbonate. The flow rate was 2.0 mL min^{-1} and the temperature of the analytical column was also maintained at 30°C in a JASCO column oven. All the mobile phases employed in this part of the work were previously filtered by a Millipore 0.22 µm filter and degasified in an ultrasound bath.

The outlet of the 2ndD was connected to three detectors in series: a diode array detector (DAD) (JASCO, model MD-2010) operating at 254, 280, and 365 nm, a fluorescence detector (FLD) (JASCO, model FP-2020 Plus) operating at emission/excitation wavelengths of 240/450 nm, and a evaporative light scattering detector (ELSD) (SEDEX model 80-LT-ELSD) operating at 60°C and 3.5 bar.

The software used to control the chromatographic systems and acquire the chromatograms was the *ChromNav* Chromatography Data System (JASCO corporation, Tokyo, Japan).

3.3. Results and Discussion

3.3.1. Optimization of the chromatographic conditions using the RP-C18 column

The RP chromatography includes any chromatographic method that uses a non-polar stationary phase and a polar eluent. In this work, a C18 column has been employed, which retains the compounds according to their hydrophobic character and it relies on a partitioning mechanism between the mobile phase and the surface of the stationary phase (Snyder *et al.*, 2010). In order to understand which mobile phase composition provides the best results, in terms of separation within the short analysis time, different amounts of acetonitrile were tested: 0%, 10%, 15%, 20%, 25%, and 30% %(v/v). It should be mentioned that the selection of the optimum mobile phase

composition must also take into account the characteristics of the column used in the 2ndD. As previously mentioned, it is important to avoid adsorption phenomena of the analytes into the 2ndD column under the injection plug conditions (i.e. when the fractions of NOM from the 1stD are separated in the 2ndD). Previous works, employing a size-exclusion column similar to that used in this study, suggested that concentrations of acetonitrile much higher than 20% (v/v) may yield a decrease in peak resolution and longer elution times as a result of the occurrence of non-size exclusion interactions (e.g., weak hydrophobic interactions) between the NOM structures and the stationary phase of the size-exclusion column (Duarte and Duarte, 2010; 2011). Therefore, in this first optimization study in the RP-C18 column, only concentrations of acetonitrile lower than 30% were tested due to the possibility of occurrence of adsorption phenomena of NOM moieties onto the stationary phase of the size-exclusion column.

For the sake of easier comparison all the chromatograms were normalized to the maximum and minimum of intensity.

As depicted in Figure 10 for the SR-FA sample, a mobile phase containing 20% (v/v) of acetonitrile provided the best separation results in the RP-C18 column, with two distinguishable peaks in all chromatograms acquired by the different detectors. In this section, only the 1stD chromatograms obtained using the mobile phase composition selected for the subsequent comprehensive 2D-LC experiments are shown. The chromatograms obtained for the other mobile phase compositions are compiled in Annex.

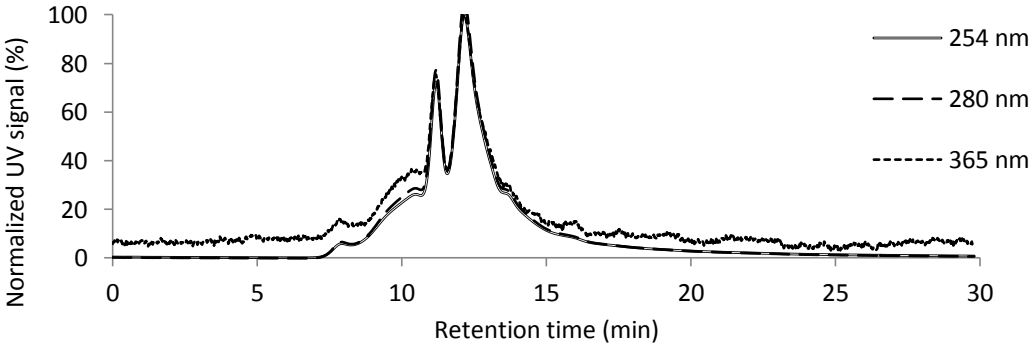

(a)

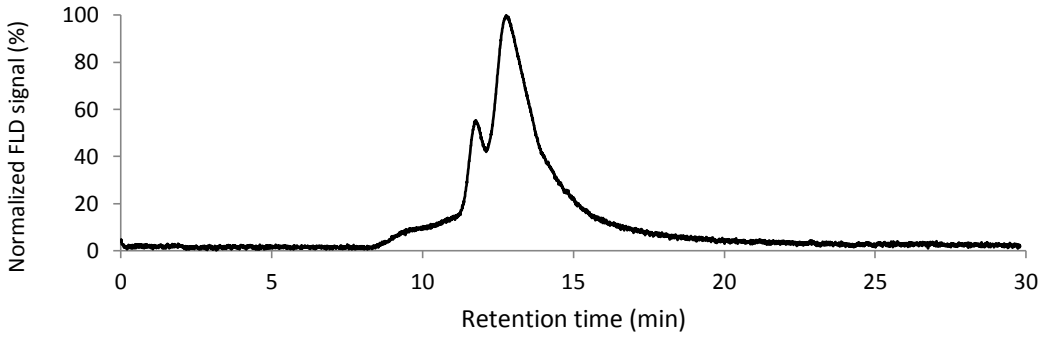

(b)

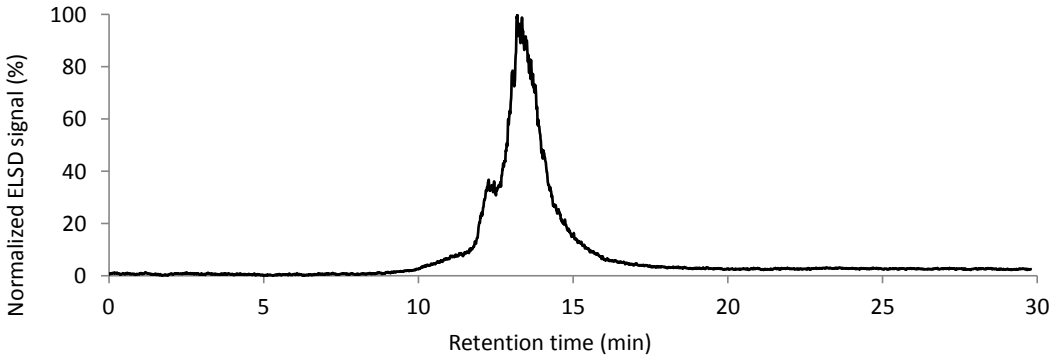

(c)

Figure 10. Chromatograms of the SR-FA sample obtained in the RP-C18 column, with a mobile phase composition consisting of 20% (v/v) of acetonitrile, and recorded by different detection methods: UV absorption at 254 nm, 280 nm, and 365 nm (a), FLD at λ_{Exc} /λ_{Em} = 240/450 nm (b), and ELSD (c)

In the case of the PL-FA sample, a mobile phase composition consisting of 25% acetonitrile provided the best separation results in the RP-C18 column, also yielding two distinguishable peaks in all chromatograms (please, see Figures 39, 40, and 41 in Annex). Unexpectedly, a serie of comprehensive 2D-LC experiments conducted under these chromatographic conditions were not successful in resolving the PL-FA sample into more chemically distinct fractions. In fact, no separation of the PL-FA sample was achieved using these analytical conditions in the comprehensive 2D-LC system (RP-C18 x SEC). Furthermore, the time required to complete a comprehensive 2D-LC protocol with a mobile phase composition of 25% (v/v) acetonitrile in the 1^{st}D is of 135 minutes, which is almost twice of that required for a comprehensive 2D-LC protocol using a lower content of acetonitrile. Therefore, and for the sake of easier comparison, it was

decided to proceed with the comprehensive 2D-LC analysis of the PL-FA sample using a mobile phase composition of 20% (v/v) acetonitrile in the 1stD column. The RP-C18 chromatograms of this sample, recorded by the different detectors, are shown in Figure 11.

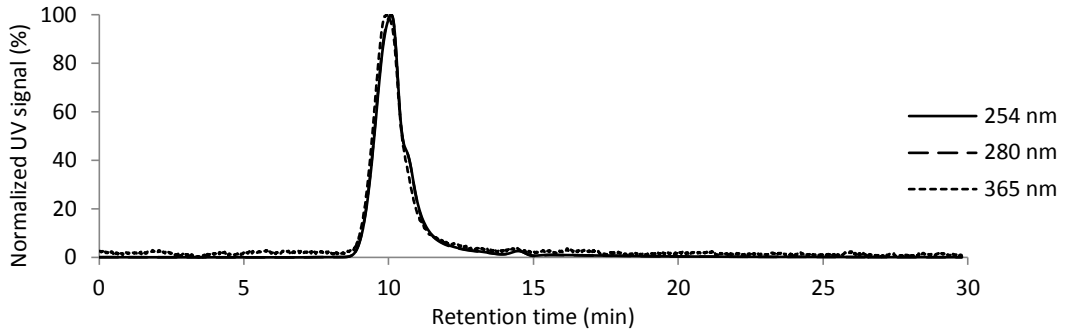

(a)

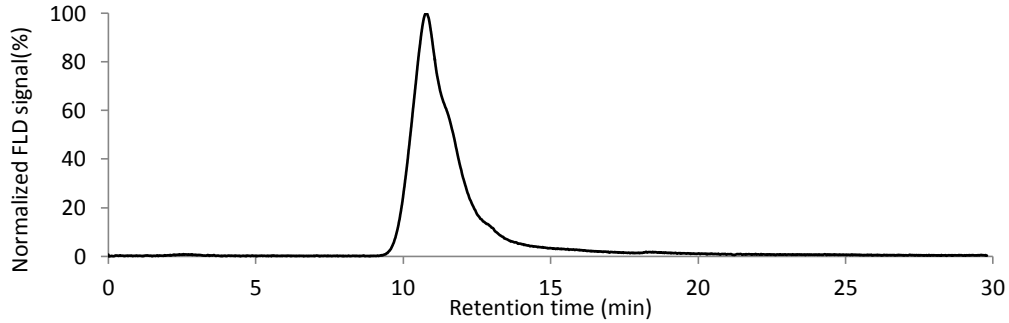

(b)

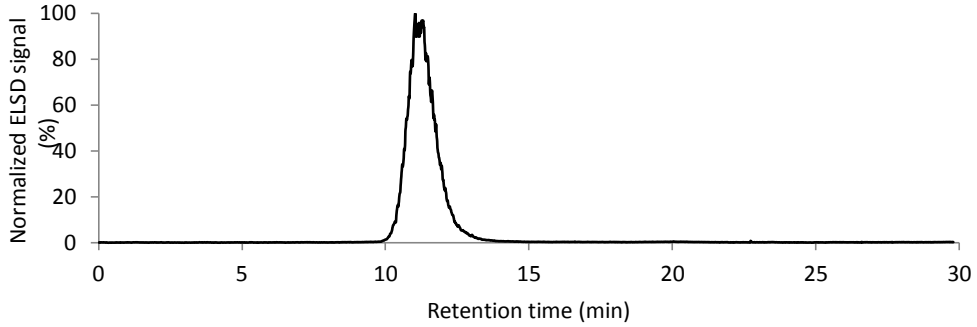

(c)

Figure 11. Chromatograms of the PL-FA sample obtaioned in the RP-C18 column, with a mobile phase composition consisting of 20% (v/v) of acetonitrile, and recorded by different detection methods: UV absorption at 254 nm, 280 nm, and 365 nm (a), FLD at λ_{Exc} /λ_{Em} = 240/450 nm (b), and ELSD (c)

Regarding the RP-C18 separation of the aerosol WSOM, and due to the low amount of sample available to proceed with further structural characterization studies, just two mobile phase compositions (20% and 25% (v/v) acetonitrile) were tested. Apparently, better separation results were achieved using a mobile phase composition of 20% (v/v) acetonitrile, as shown by the UV and FLD chromatograms in Figure 12.

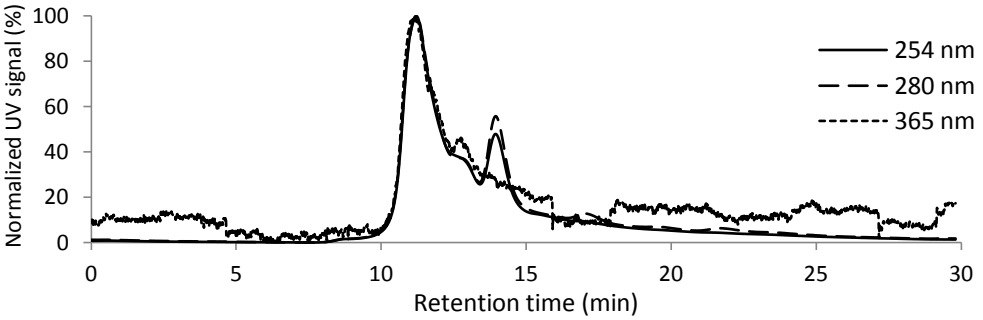

(a)

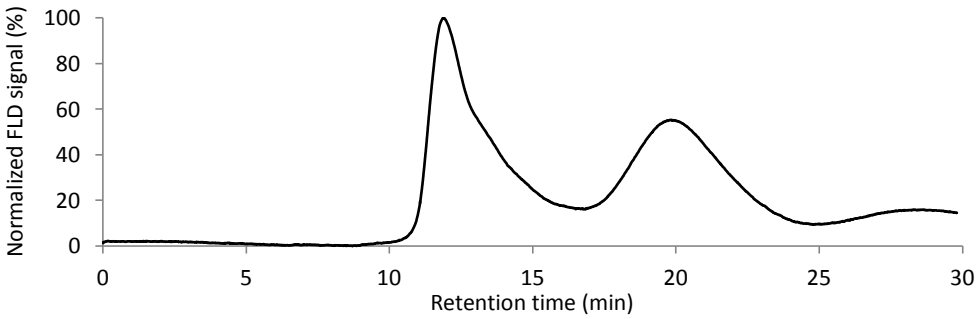

(b)

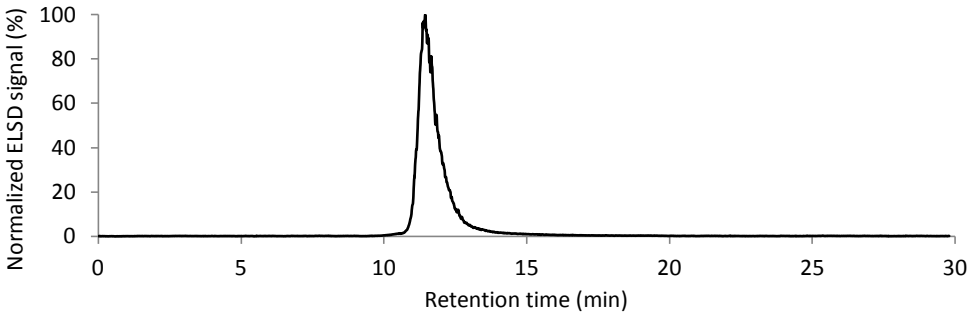

(c)

Figure 12. Chromatograms of the aerosol WSOM sample obtained in the RP-C18 column, with a mobile phase composition consisting of 20% (v/v) of acetonitrile, and recorded by different detection methods: UV absorption at 254 nm, 280 nm, and 365 nm (a), FLD at λ_{Exc} /λ_{Em} = 240/450 nm (b), and ELSD (c)

3.3.2. Optimization of the chromatographic conditions using the mixed-mode HILIC column

Hydrophilic interaction liquid chromatography (HILIC) combines the normal phase (NP) and the RP chromatography, and it employs a polar stationary phase with an aqueous mobile phase (Bernal *et al.*, 2011). Consequently, it allows the retention and separation of polar compounds with different selectivity when compared to the traditional RP chromatography. According to Bernal *et al.* (2011) the most common theory states that HILIC retention results from the portioning of the analytes between the mobile phase and a water-enriched layer in the surface of the stationary phase. Several works have already been published employing an HILIC column to the separation of NOM (Woods *et al.*, 2011), as well as for the analysis of specific organic compounds in environmental matrices (Barbaro *et al.*, 2011; Kitanovski *et al.*, 2011; Woods *et al.*, 2011). It should be mentioned, however, that these works were exclusively based on the conventional 1D-LC approach.

HILIC can be performed on a variety of stationary phases (e.g, amino-, amido-, cyano, carbamate, and polyol groups). The column employed in this work is an Acclaim Mixed-Mode HILIC-1, whose stationary phase consists in a silica-based material with alkyl diol bonding. It combines RP and traditional HILIC properties due to the hydrophobic alkyl chain and hydrophilic diol functionalities of the terminal groups that can interact by means of hydrogen bonding with analytes that contain hydroxyl and carboxyl groups (Jandera, 2008; 2011). When using a low content of organic solvent in the mobile phase, this column will operate in the RP mode, whereas in an organic-rich mobile phase this column will operate in the traditional HILIC mode (Jandera, 2011). Buffered mobile phases were employed in this work, following closely the conditions used by Woods et al (2011) for the HILIC separation of NOM, although the authors used gradient elution instead of isocratic elution, which was applied in present study. The mobile phases consisted of 20 mM ammonium acetate (pH 5 and 6) and 10% (v/v) acetonitrile. The pH of the mobile phases were adjusted to the appropriate values with acetic acid.

In this part of the work all the chromatograms obtained with the mobile phase composition that will be used in the 2D-LC experiments are shown. For the SR-FA

sample, whose results are depicted in Figure 13 and 14, the elution time at pH 6 is lower than that at pH 5. In terms of 2D-LC analysis, these results suggest that the use of a mobile phase at pH 5 originates an increase in the analysis time of more than 20 minutes as compared to that at pH 6. Therefore, and due to the lower time needed to complete the analysis, it was decided to use the mobile phase at pH 6 for the subsequent 2D-LC experiments. It is also important to note that the ELSD chromatogram presents very sharp peaks superimposed to the broad peak. This is likely to be a consequence of the concentration of both salt buffer and acetic acid in the mobile phase. According to Vervoort *et al.* (2008), a buffer concentration of 20 mM and acetic acid at 0.1% (v/v) yields a higher detector baseline noise when compared to that obtained at lower concentrations. More recently, Eom *et al.* (2010) also concluded that concentrations of salt buffer of 0.05 mM and acetic acid of 0.01% (v/v) increased the sensitivity of the detector, being in line with the results of Vervoort *et al.* (2008). It should be mentioned, however, that the apparent loss in detector sensitivity for SR-FA in the mixed-mode HILIC chromatography, was not verified in the ELSD chromatogram of the NOM sample in comprehensive 2D-LC analysis (section 4.3). It is suggested that the transferred fraction from the 1stD experiences some mixing and dilution with the mobile phase of the 2ndD, thus arriving with a somewhat dispersed concentration at the SEC column and subsequent detection systems.

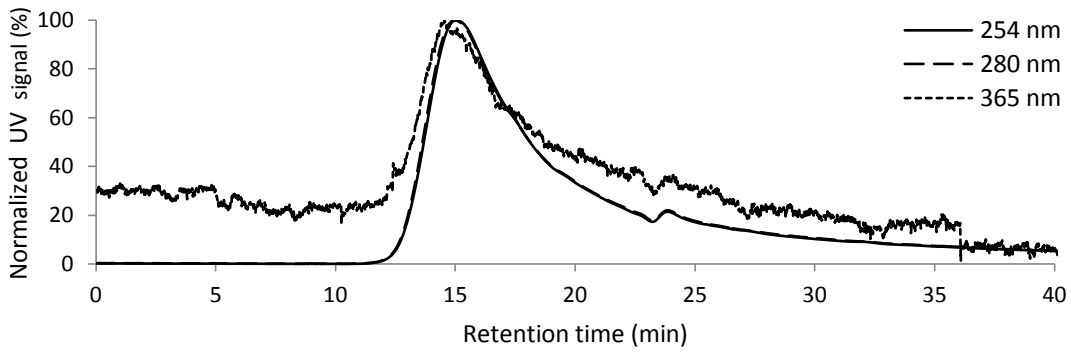

(a)

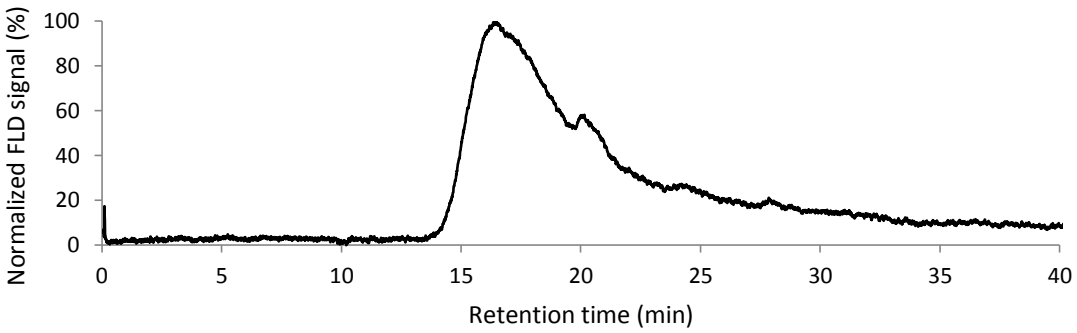

(b)

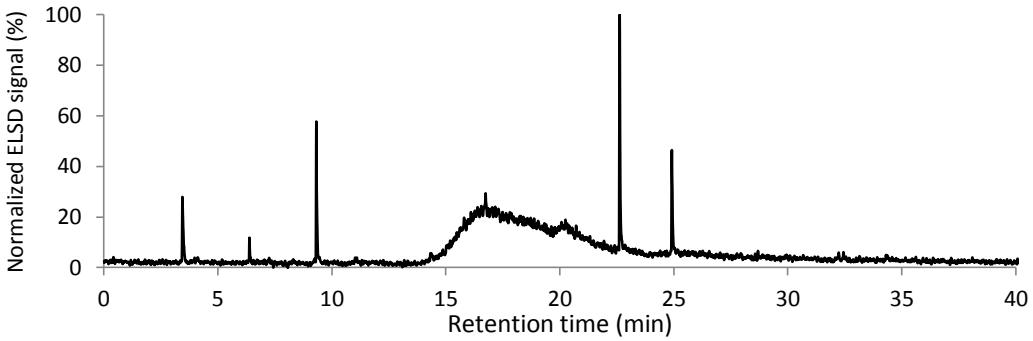

(c)

Figure 13. Chromatograms of the SR-FA sample obtained in the mixed-mode HILIC column, with a mobile phase composition consisting of 20 mM ammonium acetate, 11 mM acetic acid, and 10% (v/v) acetonitrile, at pH 5, and recorded by different detection methods: UV absorption at 254 nm and 280 nm, (a), FLD at λ_{Exc} /λ_{Em} = 240/450 nm (b), and ELSD (c)

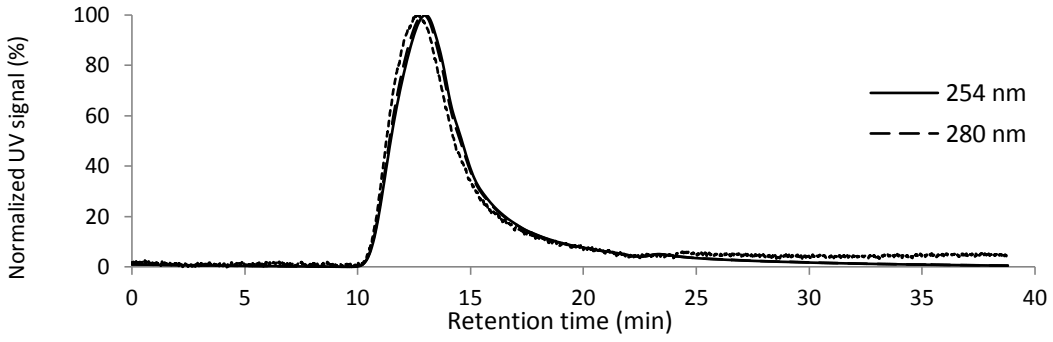

(a)

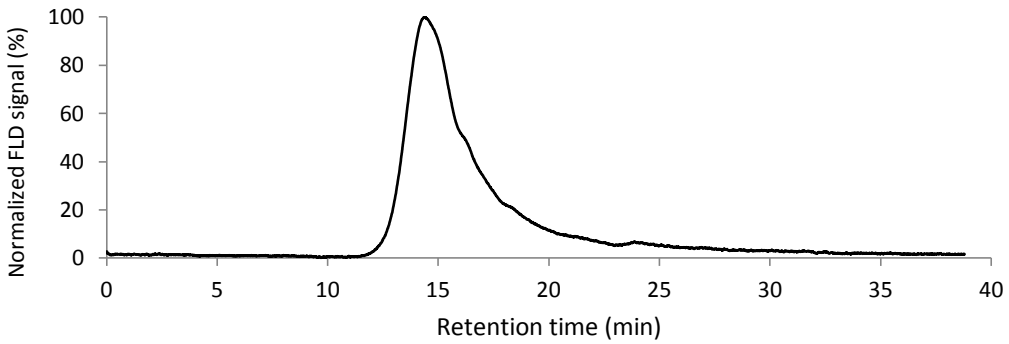

(b)

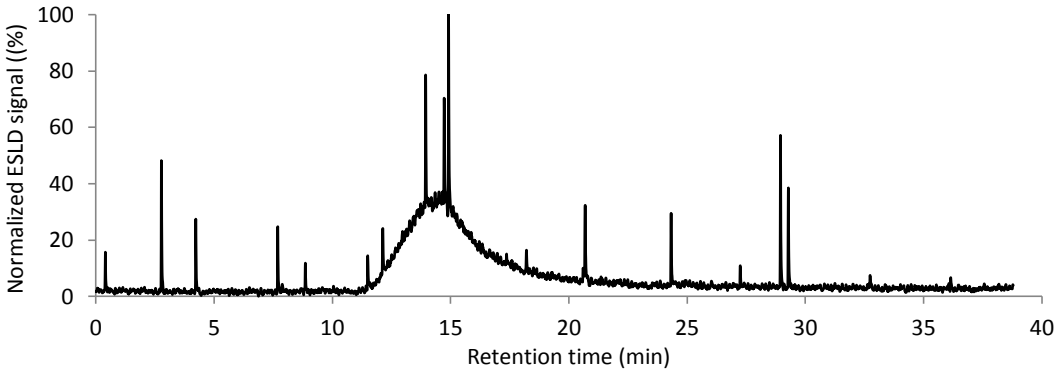

(c)

Figure 14. Chromatograms of the SR-FA sample obtained in the mixed-mode HILIC column, with a mobile phase composition consisting of 20 mM ammonium acetate, 11 mM acetic acid, and 10% (v/v) acetonitrile, at pH 6, and recorded by different detection methods: UV absorption at 254 nm and 280 nm, (a), FLD at λ_{Exc} /λ_{Em} = 240/450 nm (b), and ELSD (c)

In what concerns the separation of the PL-FA sample, shown in Figure 15 and 16, the use of a mobile phase at pH 6 allowed not only a lower elution time to complete the analysis, but also the organic material seems to undergo some kind of fractionation, as demonstrated by the presence of subpeaks and shoulders in both UV and FLD chromatograms. The ESLD chromatogram also exhibit very sharp peaks and a high baseline noise, being these features also explained by the concentration of the additives in the mobile phase. Furthermore any compound was detectable in UVD at 365 nm at pH5. This fact is explained by the difference on pH that reduce considerably the absorbance values of the sample due to the formation of intra- and intermolecular hydrogen bonds between the protonate acidic groups and the oxygen-containing groups in the humic molecule. This change will lead to conformational alterations that enable the molecule to absorb radiation at this wavelength (Cozzolino *et al.*, 2001).

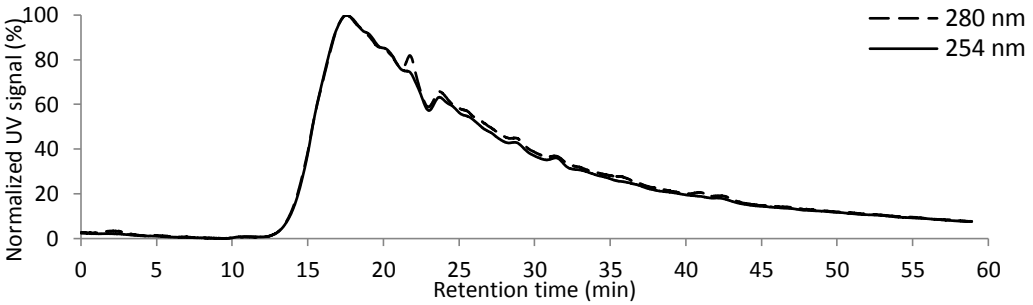

(a)

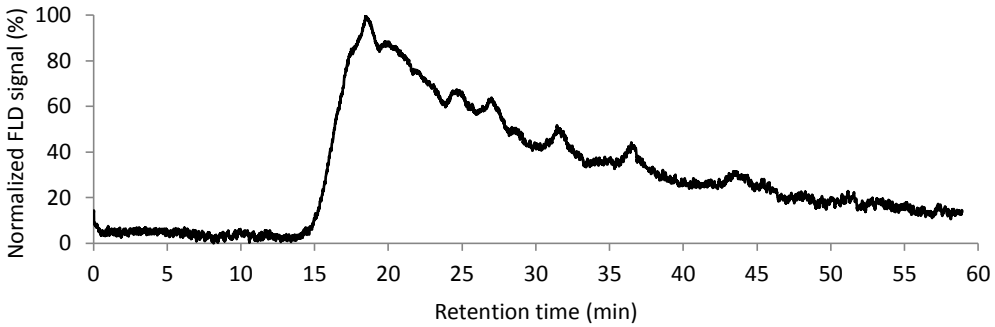

(b)

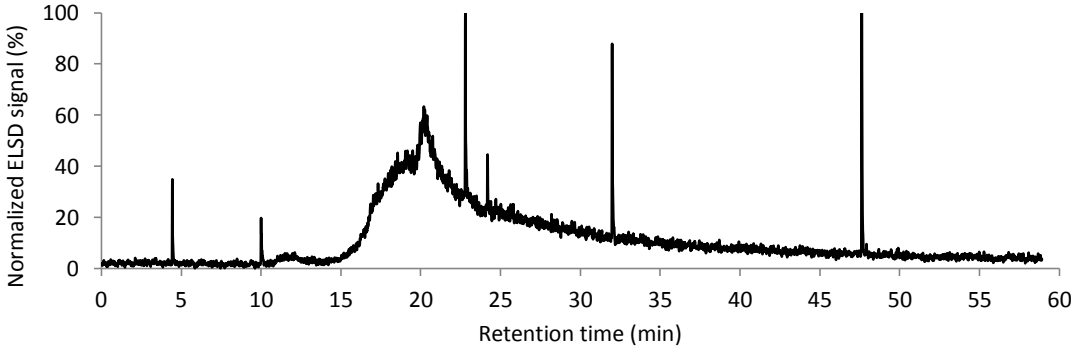

(c)

Figure 15. Chromatograms of PL-FA obtained in the mixed-mode HILIC column with a mobile phase composition consisting of 20 mM ammonium acetate, 11 mM acetic acid, and 10% (v/v) acetonitrile, at pH 5, and recorded by different detection methods: UV absorption at 254 nm, 280 nm, and 365 nm (a), FLD at λ_{Exc} 240 nm/λ_{Em} 450 nm (b), and ELSD (c)

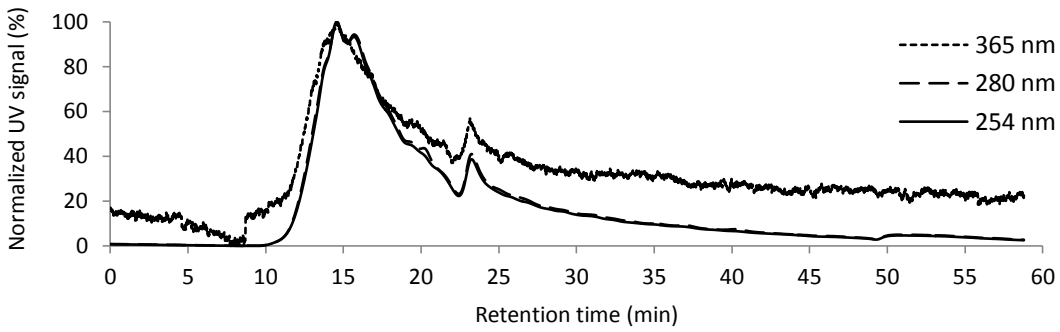

(a)

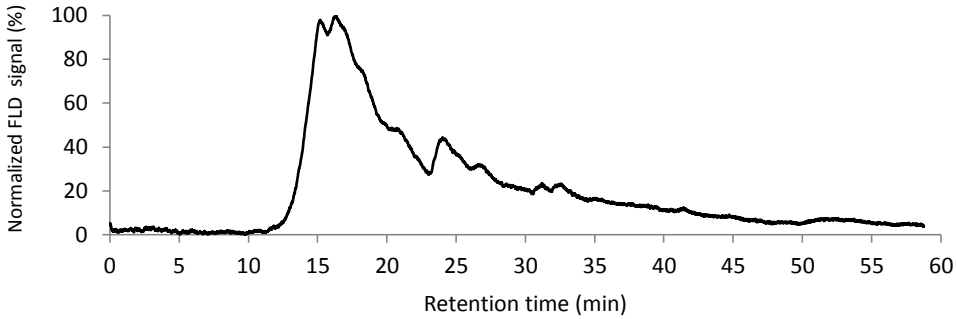

(b)

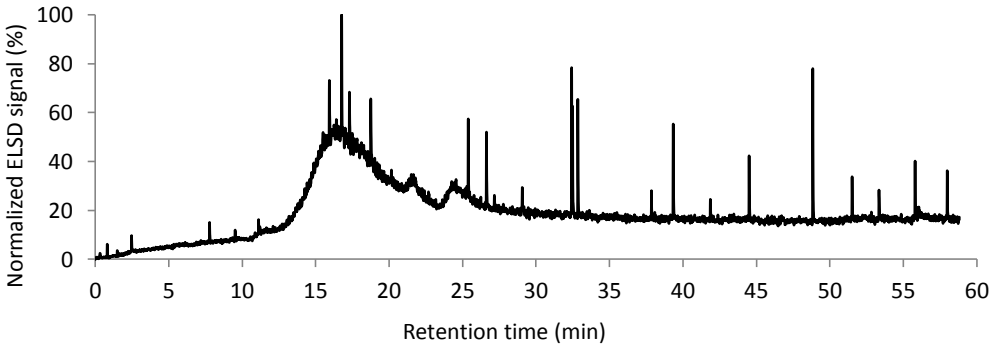

(c)

Figure 16. Chromatograms of PL-FA obtained in the mixed-mode HILIC column with a mobile phase composition consisting of 20 mM ammonium acetate, 11 mM acetic acid, and 10% (v/v) acetonitrile, at pH 6, and recorded by different detection methods: UV absorption at 254 nm, 280 nm, and 365 nm (a), FLD at λ_{Exc} 240 nm/λ_{Em} 450 nm (b), and ELSD (c)

Regarding the chromatographic analysis of the aerosol WSOM sample, the use of different pH values in the mobile phase (Figures 17 and 18) induced different fractionation patterns, particularly evident in the UV and ELSD chromatograms. Therefore, these two mobile phase compositions were used for the subsequent comprehensive 2D-LC analysis of the aerosol WSOM sample. It should also be mentioned that no signal was recorded in the UV detector at 365 nm. According to Duarte *et al.* (2005) work, this sample doesn't present higher specific absorptivity at this wavelength value.

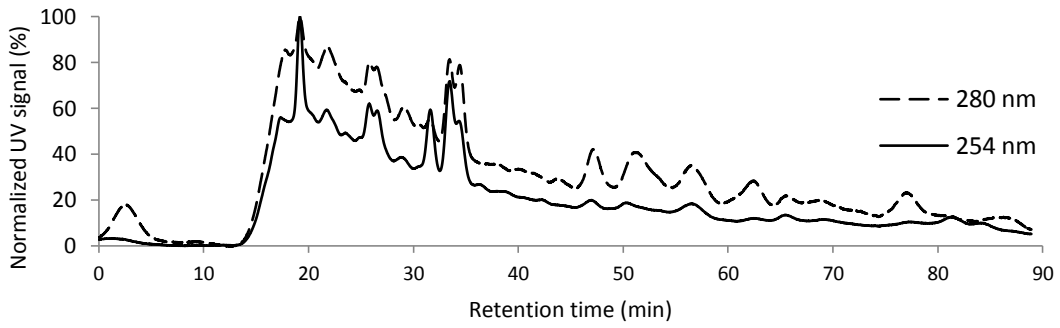

(a)

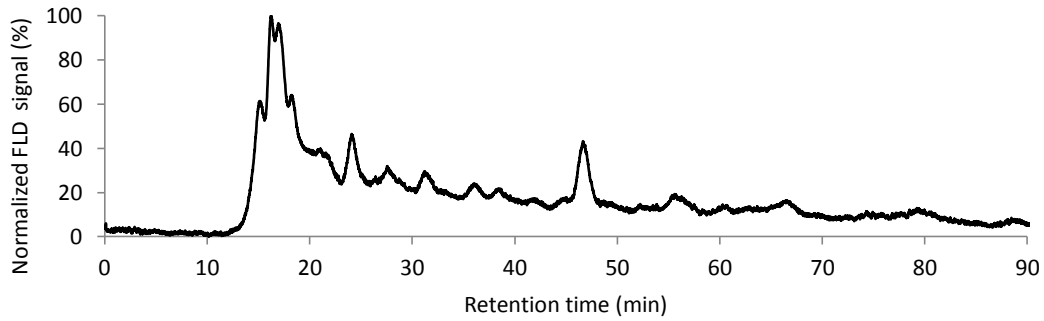

(b)

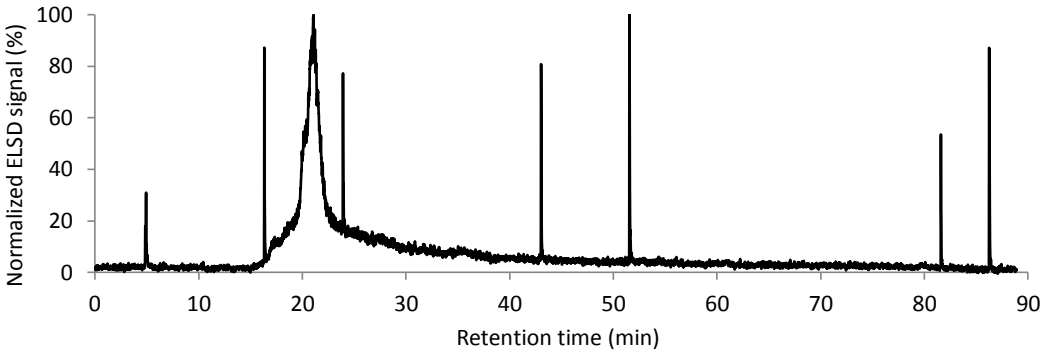

(c)

Figure 17. Chromatograms of aerosol WSOM sample obtained in the mixed-mode HILIC column with a mobile phase composition consisting of 20 mM ammonium acetate, 11 mM acetic acid, and 10% (v/v) acetonitrile at pH 5, and recorded by different detection methods: UV absorption at 254 nm and 280 nm (a), FLD at λ_{Exc} 240 nm/λ_{Em} 450 nm (b), and ELSD (c)

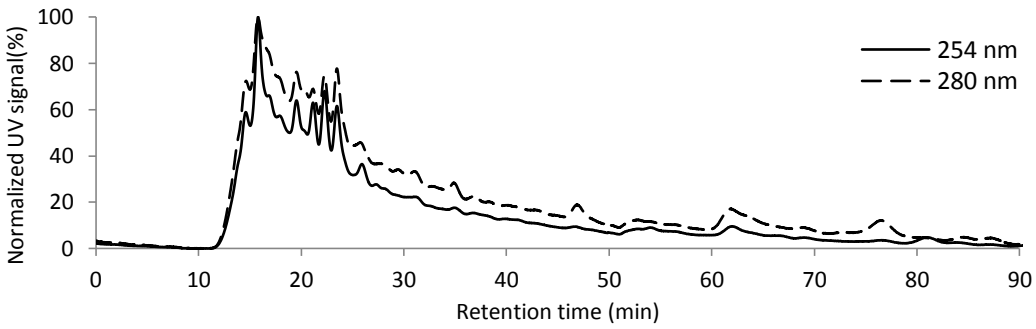

(a)

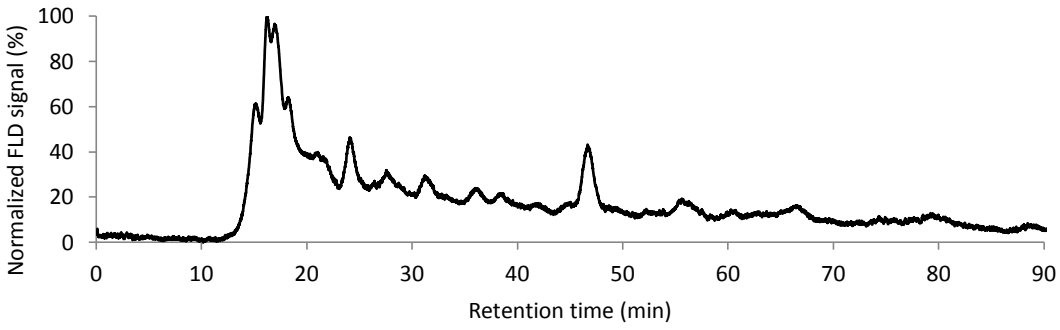

(b)

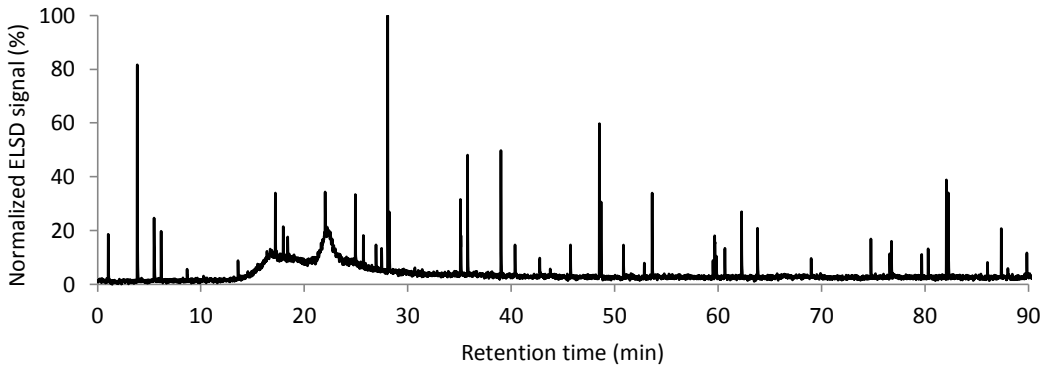

(c)

Figure 18. Chromatograms of aerosol WSOM obtained in the mixed-mode HILIC column with a mobile phase composition of 20 mM ammonium acetate, 11 mM acetic acid, and 10% (v/v) acetonitrile at pH 6, and recorded by different detection methods detection: UV absorption at 254 nm and 280 nm (a), FLD at λ_{Exc} 240 nm/λ_{Em} 450 nm (b), and ELSD (c)

3.3.3. Optimization of the chromatographic conditions using the SEC column

The SEC column used is this work consists in a polydroxymethacrylate copolymer stationary phase that fractionate the NOM sample according to the molecular hydrodynamic volume of the NOM structures. Molecules that are smaller than the pore size of the stationary phase can enter into these pores and be retained for a longer time than larger molecules, which cannot penetrate into the pores of the packing material.

For the SEC separation, the mobile phase composition was set according to the results obtained in a previous study by Duarte and Duarte (2011). Using an identical SEC column, these authors concluded that the best mobile phase composition that allows achieving a size fractionation of NOM consists of phosphate buffer and 11% (v/v) acetonitrile. It should be mentioned, however, that the non-volatile phosphate buffer used in this previous work has been replaced by the volatile ammonium carbonate buffer, which is compatible with the ELSD method. Therefore, the mobile

phase composition used in this work consists of 20 mM ammonium carbonate and 11% acetonitrile (v/v).

The results obtained for the SR-FA, PL-FA, and aerosol WSOM samples are shown in Figures 19, 20, and 21, respectively. The NOM samples elute from the SEC column in about 150 s, which was set as the modulation time to avoid wrap around in the 2ndD when performing comprehensive 2D-LC analysis. All SEC profiles show a unimodal distribution under the selected chromatographic conditions.

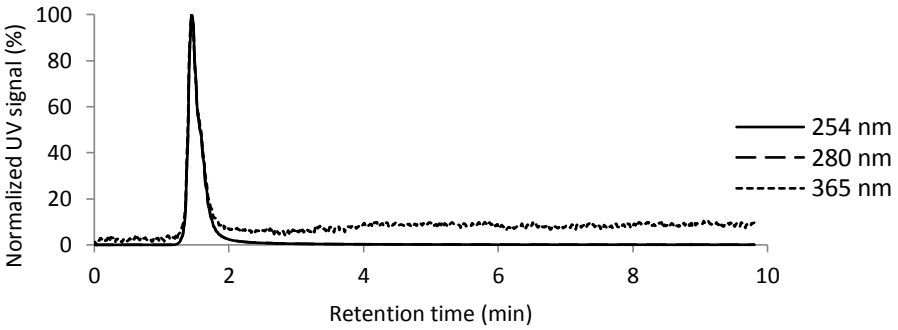

(a)

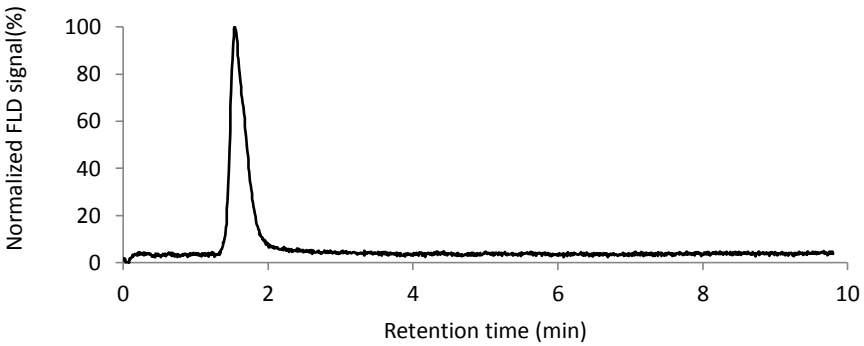

(b)

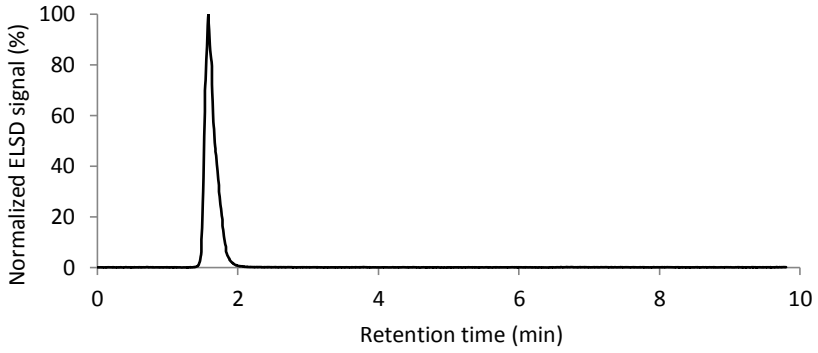

(c)

Figure 19. Chromatograms of the SR-FA sample obtained in the Suprema 30 Å SEC column, with a mobile phase composition consisting of 20 mM ammonium carbonate and 11% (v/v) acetonitrile, and recorded by different detection methods: UV absorption at 254 nm and 280 nm (a), FLD at λ_{Exc} /λ_{Em} = 240/450 nm (b), and ELSD (c)

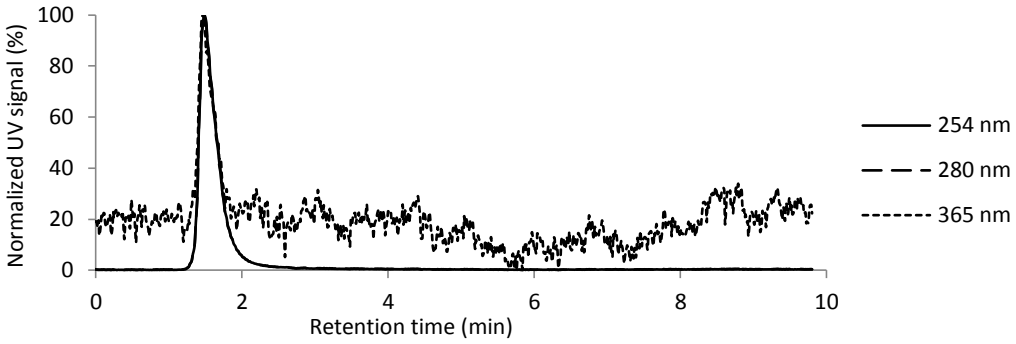

(a)

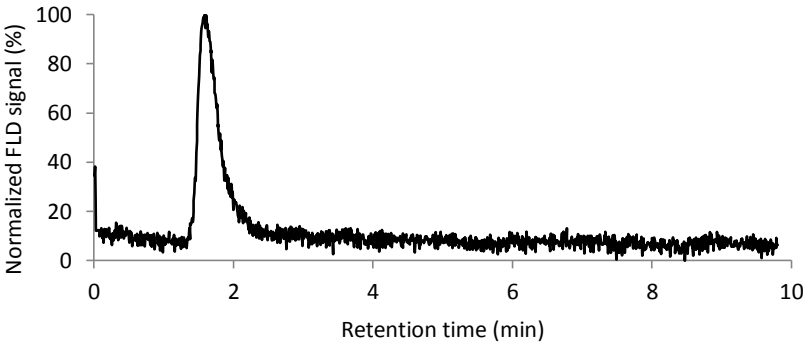

(b)

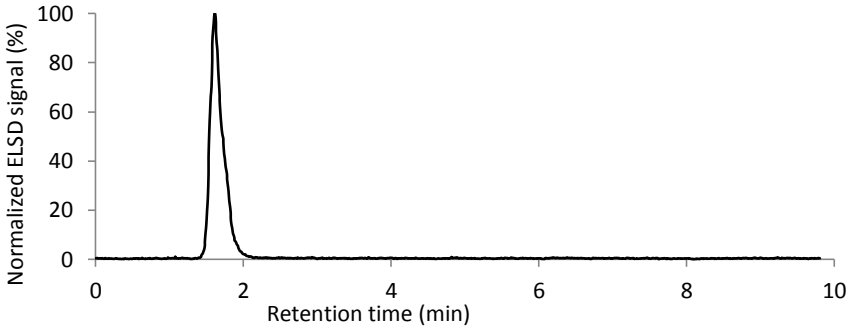

(c)

Figure 20. Chromatograms of the PL-FA sample obtained in the Suprema 30 Å SEC column, with a mobile phase composition consisting of 20 mM ammonium carbonate and 11% (v/v) acetonitrile, and recorded by different detection methods: UV absorption at 254 nm, 280 nm, and 365 nm (a), FLD at λ_{Exc} /λ_{Em} = 240/450 nm (b), and ELSD (c)

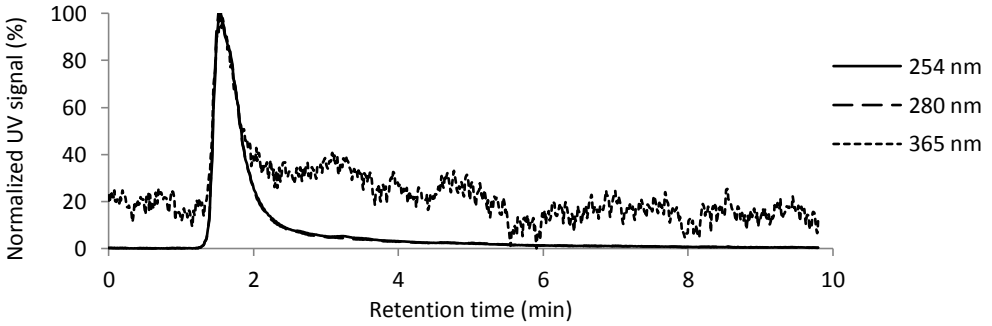

(a)

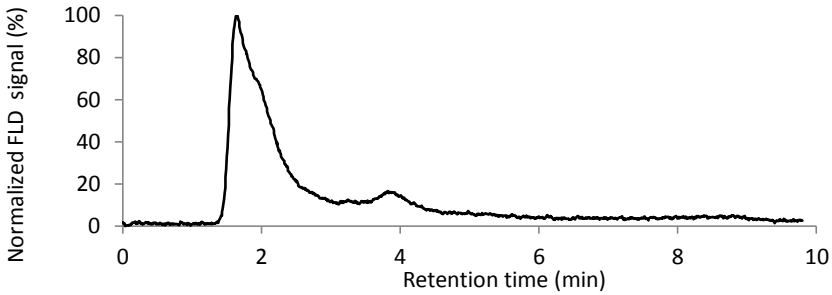

(b)

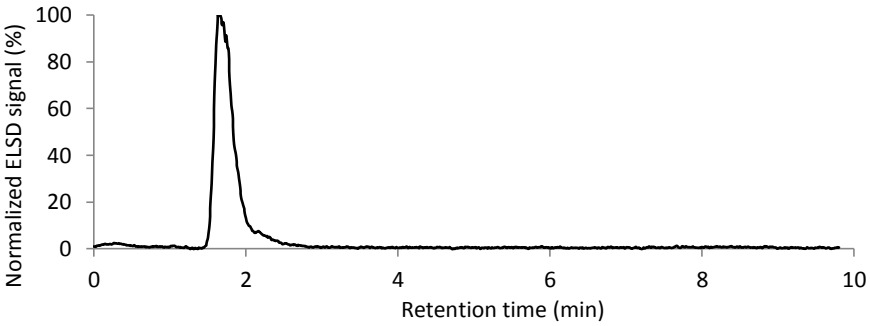

(c)

Figure 21. Chromatograms of the atmospheric WSOM sample obtained in the Suprema 30 Å SEC column, with a mobile phase composition consisting of 20 mM ammonium carbonate and 11% (v/v) acetonitrile, and recorded by different detection methods: UV absorption at 254 nm, 280 nm, and 365 nm (a), FLD at λ_{Exc} /λ_{Em} = 240/450 nm (b), and ELSD (c)

3.4. Conclusions

The objective of the work described in this third chapter was to optimize the chromatographic conditions for the subsequent the 2D-LC analyses. Two columns with different stationary phases were tested for the 1stD separation (RP-C18 and mixed-mode HILIC columns), whereas a SEC column was selected for the 2ndD fractionation. The following mobile phase compositions have been tested and will be employed in the RP-C18 x SEC and mixed-mode HILIC x SEC chromatographic systems:

- 20% (v/v) acetonitrile for the RP-C18 separation of the selected NOM samples;
- 20 mM ammonium acetate, 11 mM acetic acid and 10% (v/v) acetonitrile, at pH 5, for the fractionation of the SR-FA, PL-FA, and aerosol WSOM samples in the mixed-mode HILIC column. This mobile phase, but at pH 6, will also be used for the separation of the aerosol WSOM sample in the mixed-mode HILIC column;
- 20 mM ammonium carbonate and 11% acetonitrile (v/v) for the SEC fractionation of the three NOM samples.

After optimizing the mobile phase compositions and estimate the elution time of each sample in the 2ndD, it was possible to set the following parameters: the flow rate

of the 1^{st}D, the modulation period, the number of fractions that will be transferred from the 1^{st}D to the 2^{nd}D, and the total run time of the entire analysis. These parameters are important for ensuring efficient comprehensive RP-C18 x SEC and mixed-mode HILIC x SEC separations of the NOM samples.

Chapter 4

Separation of NOM by comprehensive 2D-LC

4.1. Introduction

A 2D-LC system combines two different separation mechanisms by means of an interfacing valve. By combining those two mechanisms it is possible to obtain a more complete survey of a given sample than just by employing each separation protocol separately. Aiming at resolving the chemical heterogeneity of the selected NOM samples, comprehensive 2D-LC is employed for the first time to map the hydrophobicity and polarity *versus* MW distribution of NOM samples. For accomplishing this objective, two comprehensive 2D-LC methods have been applied: RP-C18 x SEC and mixed-mode HILIC x SEC. The obtained results are described in this fourth chapter.

It should also be mentioned that for characterizing the MW distribution of the NOM samples, the SEC column must be calibrated with a set of standards with well-defined MWs. The results are usually described in terms of number-average MW (M_n), weight-average MW (M_w), and polydispersity index (M_w/M_n). According to Chin *et al.* work (1994) the M_n parameter (Equation 1) is calculated taking into account the average of the MW values and it expresses the average properties of the sample related to the total weight fraction of the detected molecules. The M_w parameter (Equation 2) is calculated taking into account that the structures with higher MW contains more of the total mass. M_n and M_w were determined using the Equation 1 and 2 where *Mi* is the MW of the analyte and *hi* is the weight of the sample eluted at volume *i* (Chin et al., 1994).

$$M_n = \frac{\sum_{i=1}^{N} h\,i}{\sum_{i=1}^{N} h\,i/Mi} \qquad \text{Equation 1}$$

$$M_w = \frac{\sum_{i=1}^{N} h\,i.Mi}{\sum_{i=1}^{N} h\,i} \qquad \text{Equation 2}$$

In the current work, the values of M_n and M_w where estimated using the PSS WinGPC Unity software package, after calibration of the SEC column.

Two 2D-LC systems were applied (C18 x SEC and HILIC x SEC), at three different samples (SR-FA, PL-FA and AWSOM).

4.2. Experimental procedure

4.2.1 Preparation of NOM samples

NOM solutions were prepared by dissolving an appropriate amount of each sample in the mobile phase of the 1stD (see the eluent composition for each column in section 4.2.2). The concentration of each sample was in the range of 0.23-0.39 mg mL^{-1}, 0.31-0.78 mg mL^{-1}, and 0.26-0.48 mg mL^{-1} for the SR-FA, PL-FA, and aerosol WSOM, respectively. Before injection, all NOM solutions were filtered through HPLC Certified Syringe Filters (SPARTAN, Whatman GmbH, Germany) of 0.20 µm pore size.

4.2.2 Instrumentation and chromatographic conditions

The instrumentation used in these experimental procedure is the same used in section 3.2.2 (Chapter 3). Two columns were applied in the 1stD: i) RP Kromasil 100-5C18; and ii) Acclaim Mixed-Mode HILIC-1 column. The 1stD was operated in isocratic mode using a mobile phase composition comprising 20% (v/v) of acetonitrile in the RP-C18 Kromasil column, ,and 20 mM ammonium acetate, 10% acetonitrile, and 11 mM and 1.1 mM acetic acid at two different pH values (5 and 6, respectively) in the mixed-mode HILIC column. According to the conclusions obtained in the third chapter, SR-FA and PL-FA sample were study at pH 5 and atmospheric WSOM at pH 5 and 6. The flow rate was 0.020 mL min^{-1} for all samples excepted in the WSOM sample in the mixed-mode columns (at pH 5 and 6) where was 0,04 mL min^{-1}. The temperature of the analytical columns was maintained at 30°C in a JASCO column oven. In the 2ndD, a PSS SEC Suprema 30 Å analytical column was operated in isocratic mode at 2.0 mL min^{-1} with a mobile phase composition consisting of 11% (v/v) acetonitrile and 20 mM ammonium carbonate. All the mobile phases were previously filtered by a Millipore 0.22 µm filter and degasified in an ultrasound bath. The outlet of the 2ndD column was

connected to three detectors in series: a diode array detector operating at 254 nm, a FLD operating at λ_{Exc} /λ_{Em} = 240/450 nm, and an ELSD operating at 60°C and 3.5 bar.

The 1stD and 2ndD were interfaced with an eight-port high pressure two-position interfacing valve (VICI® AG International) equipped with two identical of 50 μL sampling loops. A sampling loop of 100 μL was used in WSOM sample in the mixed-mode HILIC column. Modulation time was 150 s. The valve was controlled by the PSS WinGPC Unity software (Polymer Standards Service GmbH) by receiving a start-up signal from a PSS Universal Data Center (model UDC 810). This software was also used for the acquisition and handling of all data set.

The SEC column in the 2ndD was calibrated using HPLC grade acetone 5% (v/v) and sodium polystyrenesulfonate standards of various MWs, Mp (MW at peak maximum): 186, 891, 2240, 3420, and 8390 Da (obtained from Sigma Aldrich). These standards were prepared by dissolving an appropriate amount of each compound in the mobile phase of the 2ndD.

4.3. Results and Discussion

Two replicas of the RP-C18 x SEC and mixed-mode HILIC x SEC analyses were conducted for each NOM sample. In this chapter, only the two-dimensional chromatograms of one of the replica are shown. The results obtained for the SR-FA sample are illustrated in Figures 22, 23, and 24, each recorded by a different detector, and in Table 4. The comprehensive RP-C18 x SEC system allowed the separation of the SR-FA sample into two fractions, with apparently different hydrophobicity. According to the mechanisms of retention in the RP-C18 stationary phase, signals 1, 3 and 5 (Figures 22(a), 23(a), and 24(a), respectively) are likely to encompass organic structures with little affinity to the stationary phase and, therefore, more hydrophilic, than the structures present in signals 2, 4 and 6. On the other hand, and under the selected chromatographic conditions, the mixed-mode HILIC column in the 1stD was unable to pull apart the SR-FA sample into chemically distinct fractions and just one signal was detected in all chromatograms (signals 7, 8, and 9 in Figures 22(b), 23(b), and 24(b), respectively). It should be further mentioned the good agreement between

the two replica in terms of retention time of the peaks along the 1stD, in both RP-C18 and mixed-mode HILIC columns (in Table 4). Furthermore, in both RP-C18 x SEC and mixed-mode HILIC x SEC systems, there seems to be a unimodal MW distribution of the organic structures along the 2ndD, ranging M_w from 745 to 1224 Da and 1050 to 2122 Da (Table 4), respectively, being these estimates influenced by both the detection method and separation mechanism in the 1stD. Regarding the M_w/M_n values, they varied within the range of 1.02-1.76, with the maximum values of polydispersity being recorded through the FLD method. Furthermore, the lowest M_w/M_n values (close to 1.0) were consistently found in the results of the ELSD method.

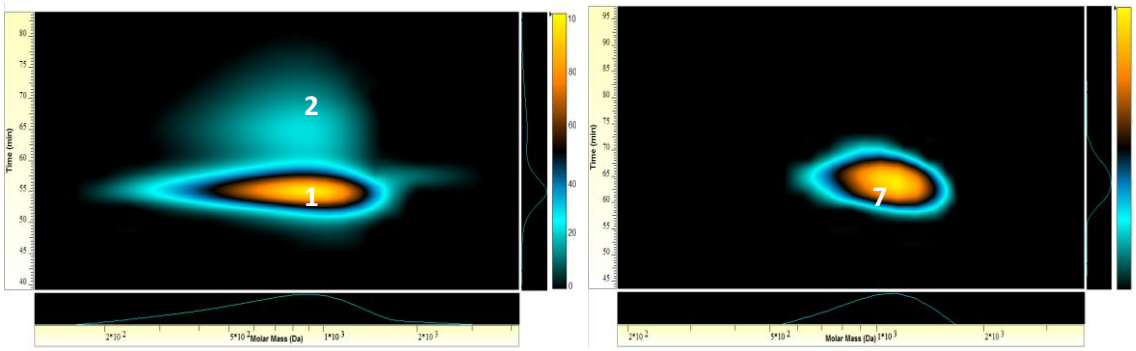

(a) (b)

Figure 22. Comprehensive RP-C18 x SEC (a) and mixed-mode HILIC x SEC (b) contour plots of the SR-FA sample recorded by UV absorption at 254 nm. Colours are used to represent the intensity of the signal at a given 1stD retention time versus molar mass (Da)

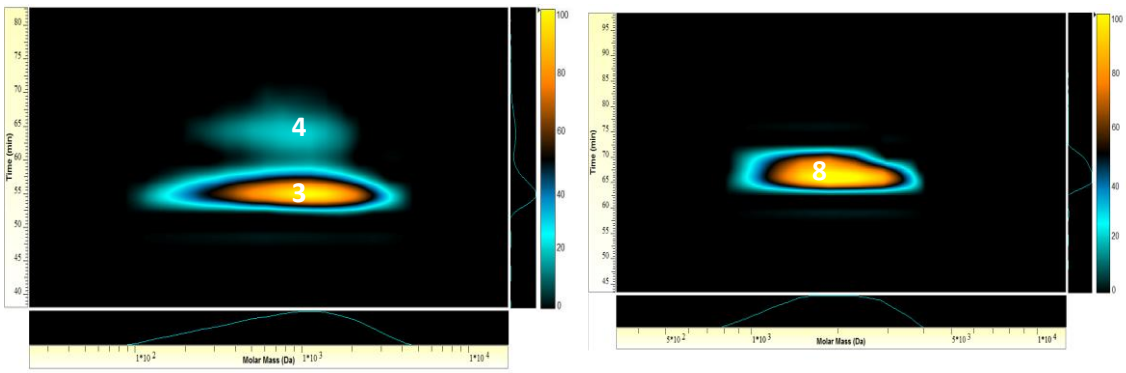

(a) (b)

Figure 23. Comprehensive RP-C18 x SEC (a) and mixed-mode HILIC x SEC (b) contour plots of the SR-FA sample recorded by FLD at λ_{Exc} /λ_{Em} = 240/450 nm. Colours are used to represent the intensity of the signal at a given 1stD retention time versus molar mass (Da)

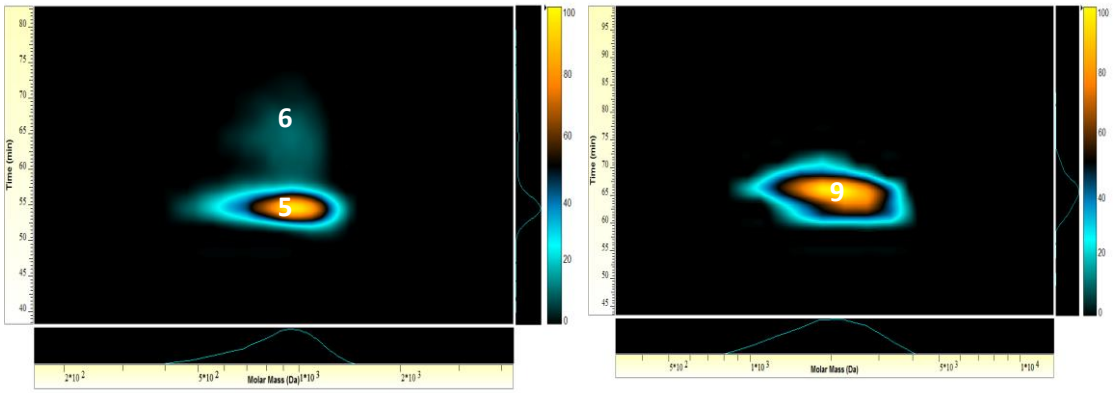

(a) (b)

Figure 24. Comprehensive RP-C18 x SEC (a) and mixed-mode HILIC x SEC (b) contour plots of the SR-FA sample recorded by ELSD (60°C and 3.5 bar). Colours are used to represent the intensity of the signal at a given 1st D retention time versus molar mass (Da)

Mechanisms of separation	Detector	Elution Time 1st D (min)	M_w (Da)	M_n (Da)	M_w/M_n
C18 x SEC	UV 254 nm	(1) : 55; 55	(1) : 807; 790	(1) : 634; 645	(1) : 1.27; 1.22
		(2) : 59; 60	(2) : 745; 786	(2) : 691; 711	(2) : 1.08; 1.11
	FLD- 240/450 nm	(3) : 55; 55	(3) : 1038; 1224	(3) : 590; 696	(3) : 1.76; 1.76
		(4) : 64; 64	(4) : 870; 1055	(4) : 698; 914	(4) : 1.25; 1.15
	ELSD	(5) : 55; 55	(5) : 904; 924	(5) : 854; 865	(5) : 1.06; 1.07
		(6) : 59; 60	(6) : 940; 911	(6) : 926; 884	(6) : 1.02; 1.03
HILIC x SEC	UV 254 nm	(7) : 63; 64	(7) : 1050; 1056	(7) : 998; 1008	(7) : 1.05; 1.05
	FLD- 240/450 nm	(8) : 66; 66	(8) : 1926; 1936	(8) : 1728; 1758	(8) : 1.11; 1.10
	ELSD	(9) : 65; 66	(9) : 2058; 2122	(9) : 1902; 1946	(9) : 1.08; 1.09

Table 4. MW characteristics of the SR-FA sample estimated through comprehensive RP-C18 x SEC and mixed-mode HILIC x SEC (the results of each replica are separated by a semicolon and the peak number is presented in parenthesis)

The results obtained for the PL-FA sample are shown in Figures 25, 26, and 27, and in Table 5. Once again, it is clear the good agreement between the two replica in terms of retention time of the signals along the 1^{st}D. Nevertheless, in the comprehensive RP-C18 x SEC system, no separation was achieved and just one signal appear in all chromatograms (Fig. 25(a), 26(a), and 27(a)). On the other hand, an despite the continuous signal overlap, it seems that the comprehensive mixed-mode HILIC x SEC system was more successful in fractionating the PL-FA sample than the comprehensive RP-C18 x SEC system. Accordingly, two factions were detected by means of UV absorption at 254 nm (signals 13 and 14) and ESLD (signals 18 and 19), whereas three fractions (signals 15, 16, and 17) were clearly visible in the chromatogram recorded by FLD. In the particular case of the comprehensive mixed-mode HILIC x SEC contour plots screened by UV absorption and ELSD, those two fractions can be more clearly distinguished in the three-dimensional surface plots of Figure 28. In mixed-mode HILIC, the retention of constituents is based on very complex mechanisms, consisting of partitioning, adsorption, ionic interactions and sometimes even hydrophobic interactions (Guo and Gaiki, 2011). Recently, (McCalley, 2010) conducted a survey on the retention mechanism of a mixture of neutral, strongly acidic and strongly basic compounds in HILIC using five different stationary phases, including the mixed-mode phase. Basic compounds seem to be more retained on all the phases, whereas the strong acids are poorly retained in the mixed-mode phase, which presumably has a significant concentration of acidic silanol groups. These results suggest that the organic structures of the PL-FA sample eluting first in the comprehensive mixed-mode HILIC x SEC method are likely to be more acidic than those of the latest-eluting material. However, definite structural assignments on the organic moieties present in each fraction are not possible, which means that these assumptions must be further substantiated by other screening techniques (e.g. NMR spectroscopy). Apparently, no separation was achieved along the 2^{nd}D in the comprehensive RP-C18 x SEC system, and the chromatograms exhibit a unimodal distribution in terms of M_W, ranging from 637 to 838 Da (Table 5), being these estimates also influenced by the detection method. In what concerns the fractionation

in the comprehensive mixed-mode HILIC x SEC system, the complete range of MW variability was of 792-1026 Da, 921-1912 Da, and 1366-1950 Da for the UV absorption, FLD and ELSD methods, respectively. The M_w/M_n values varied within the range of 1.03-2.10, with the maximum values of polydispersity being also recorded through the FLD method. The lowest M_w/M_n values (close to 1.0) were also consistently found in the results of the ELSD method.

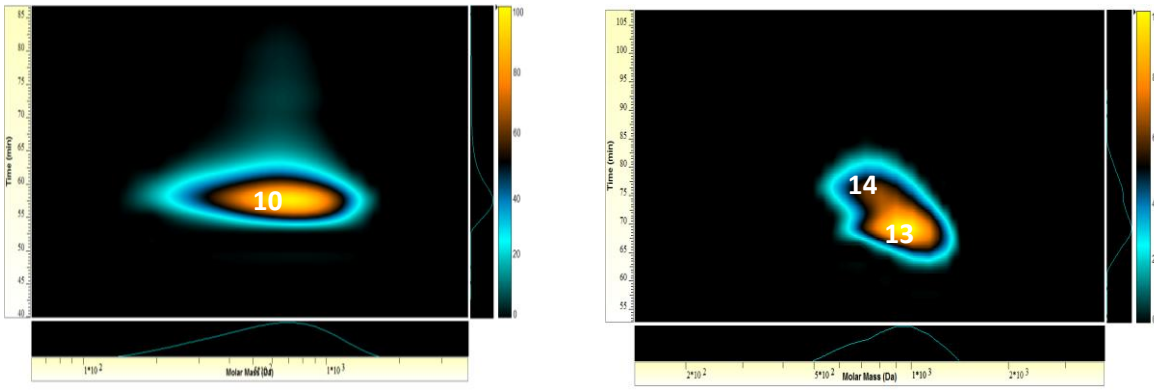

(a) (b)

Figure 25. Comprehensive RP-C18 x SEC (a) and mixed-mode HILIC x SEC (b) contour plots of the PL-FA sample recorded by UV absorption at 254 nm. Colours are used to represent the intensity of the signal at a given 1stD retention time versus molar mass (Da)

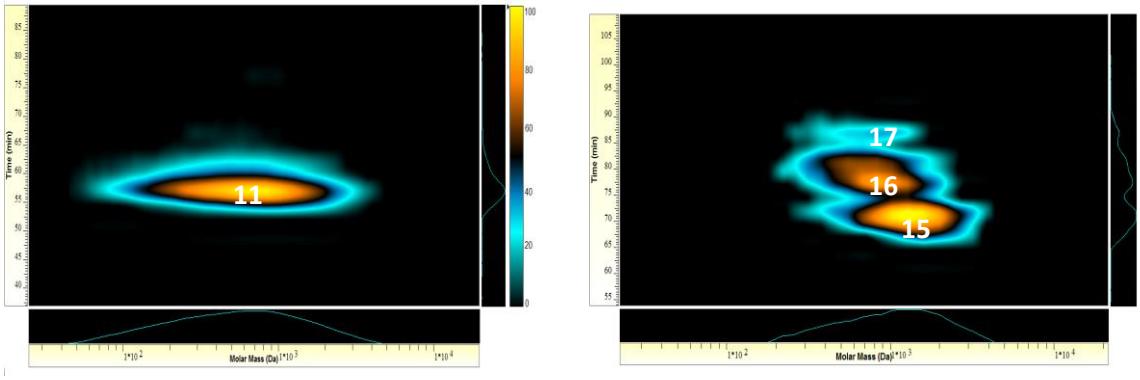

(a) (b)

Figure 26. Comprehensive RP-C18 x SEC (a) and mixed-mode HILIC x SEC (b) contour plots of the PL-FA sample recorded by FLD at λ_{Exc} /λ_{Em} = 240/450 nm. Colours are used to represent the intensity of the signal at a given 1stD retention time versus molar mass (Da)

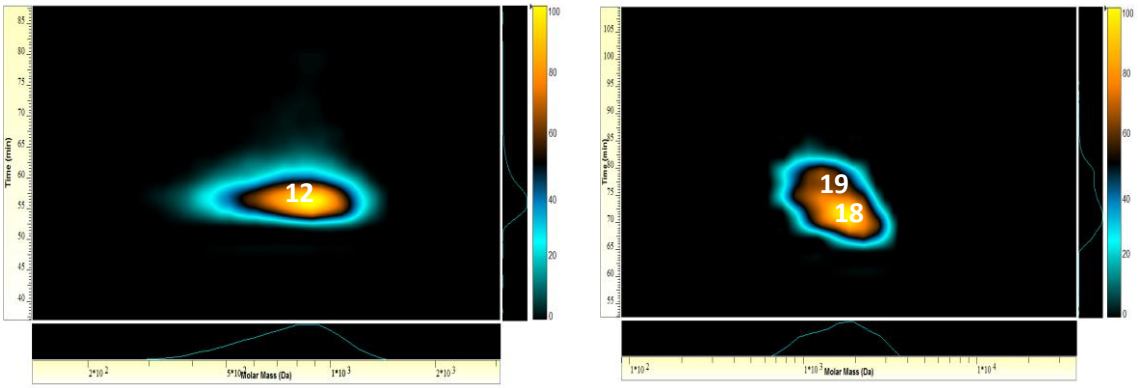

(a) (b)

Figure 27. Comprehensive RP-C18 x SEC (a) and mixed-mode HILIC x SEC (b) contour plots of the PL-FA sample recorded by ELSD (60°C and 3.5 bar). Colours are used to represent the intensity of the signal at a given 1st D retention time versus molar mass (Da)

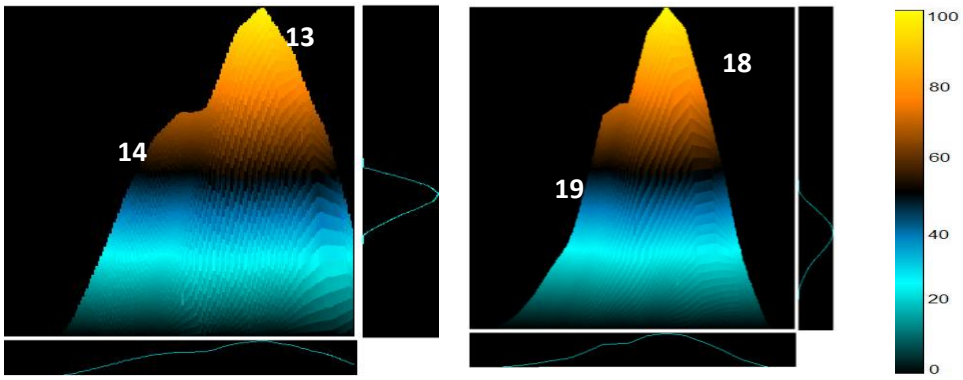

(a) (b)

Figure 28. Comprehensive mixed-mode HILIC x SEC three-dimensional surface plots of the PL-FA sample recorded by UV absorption at 254 nm (a) and ELSD (b)

Mechanisms of separation	Detector	Elution Time 1st D (min)	M_w (Da)	M_n (Da)	M_w/M_n
C18 x SEC	UV 254 nm	(10) : 56; 58	(10) : 638; 637	(10) : 486; 515	(10) : 1.31; 1.24
	FLD- 240/450 nm	(11) : 56; 57	(11) : 714; 753	(11) : 340; 375	(11) : 2.10, 2.01
	ELSD	(12) : 56; 57	(12) : 795; 838	(12) : 734; 794	(12) : 1.08; 1.06
HILIC x SEC	UV 254 nm	(13) : 70; 71	(13) : 964; 1026	(13) : 933; 985	(13) : 1.03; 1.04
		(14) : 73; 75	(14) : 792; 823	(14) : 769; 792	(14) : 1.03; 1.04
	FLD- 240/450 nm	(15) : 71; 71	(15) : 1488; 1912	(15) : 1193; 1466	(15) : 1.25; 1.30
		(16) : 77; 78	(16) : 921; 1235	(16) : 754; 980	(16) : 1.22; 1.26
		(17) : 87; 88	(17) : 931; 861	(17) : 864; 742	(17) : 1.08; 1.16
	ELSD	(18) : 72; 71	(18) : 1688 ; 1950	(18) : 1536; 1785	(18) : 1.10; 1.09
		(19) : 79; 75	(19) : 1366; 1457	(19) : 1293; 1368	(19) : 1.06; 1.06

Table 5. MW characteristics of the PL-FA sample estimated through comprehensive RP-C18 x SEC and mixed-mode HILIC x SEC (the results of each replica are separated by a semicolon and the peak number is presented in parenthesis)

The results obtained for the aerosol WSOM sample in the comprehensive RP-C18 x SEC system are shown in Figures 29, 30, and 31. No separation was achieved and just one signal is detected, showing a unimodal MW distribution ranging M_w from 299 to 719 Da. The M_w/M_n values varied within the range of 1.04-1.45. These results are described in the Table 6. However, the comprehensive mixed-mode HILIC x SEC system, whose chromatograms are illustrated in Figures 32, 33, and 34, provided a different fractionation pattern. In terms of UV absorption, and with a mobile phase at pH 5, the aerosol WSOM sample was separated into six fractions with different polarity and MW distribution, as described in Table 6. The ELSD chromatogram exhibited much less resolution as compared to that of absorbance, and just one signal is observed. Surprisingly, no signal was detected in the FLD under the selected mobile phase composition (pH 5). At this point, however, no plausible reason was found to explain

such a result. Opposite to the results obtained for the SR-FA and PL-FA samples (Tables 4 and 5, respectively), no agreement was found between the two replica in terms of retention time of the signals along the 1stD (Table 7). Such a shift in the elution time was not verified at pH 6, thus suggesting that uncontrolled mechanisms such as adsorption, charge interactions and even hydrophobic effects might be affecting WSOM selectivity and fractionation at pH 5. In what concerns the MW distribution of the aerosol WSOM sample, the values varied within the M_w range of 157-649 Da and 680-714 Da for the UV absorption and ELSD methods, respectively. Overall, the M_w/M_n values were found to be close to 1.0, except for signals 24 and 25, which exhibit higher values of polydispersity (1.16/1.21 and 1.12/1.13, respectively).

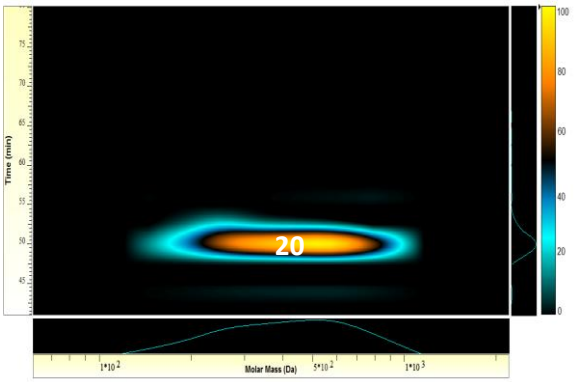

Figure 29. Comprehensive RP-C18 x SEC contour plots of the aerosol WSOM sample recorded by UV absorption at 254 nm. Colours are used to represent the intensity of the signal at a given 1stD retention time versus molar mass (Da)

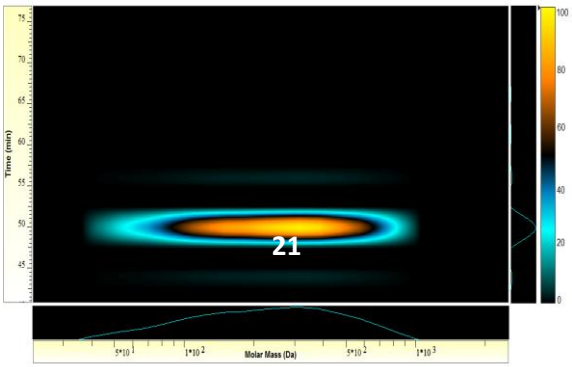

Figure 30. Comprehensive RP-C18 x SEC contour plots of the aerosol WSOM sample recorded by FLD at λ_{Exc} /λ_{Em} = 240/450 nm. Colours are used to represent the intensity of the signal at a given 1stD retention time versus molar mass (Da)

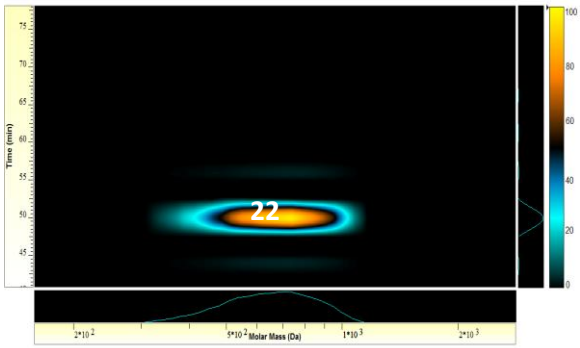

Figure 31. Comprehensive RP-C18 x SEC contour plots of the aerosol WSOM sample recorded by ELSD (60°C and 3.5 bar). Colours are used to represent the intensity of the signal at a given 1st D retention time versus molar mass (Da)

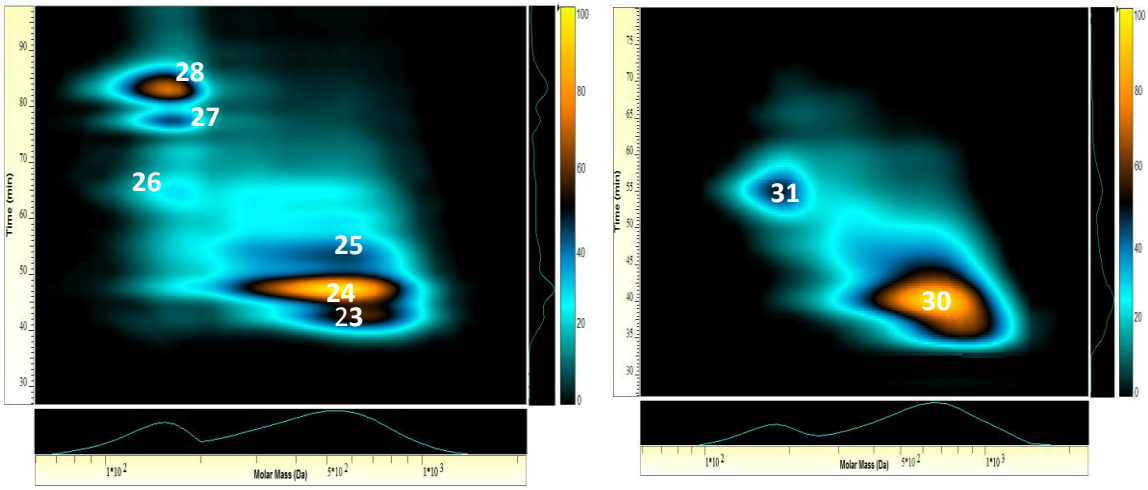

(a) (b)

Figure 32. Comprehensive mixed-mode HILIC x SEC contour plots of the aerosol WSOM sample at pH5 (a) and pH 6 (b) of the mobile phase, and recorded by UV absorption at 254 nm. Colours are used to represent the intensity of the signal at a given 1st D retention time versus molar mass (Da)

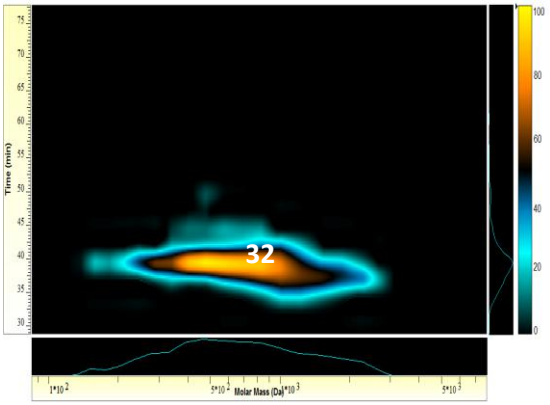

Figure 33. Comprehensive mixed-mode HILIC x SEC contour plots of the aerosol WSOM sample at pH 6 of the mobile phase, and recorded by FLD at λ_{Exc} /λ_{Em} = 240/450 nm. Colours are used to represent the intensity of the signal at a given 1stD retention time versus molar mass (Da)

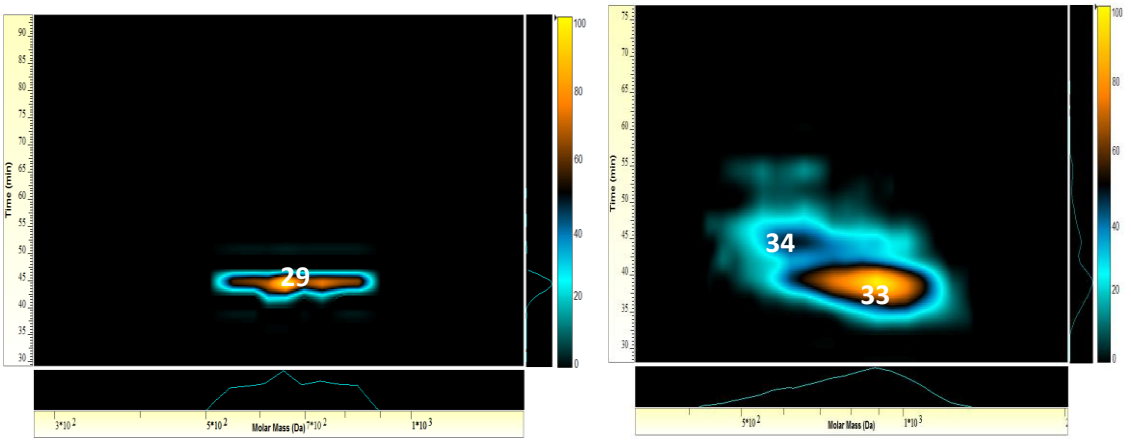

(a) (b)

Figure 34. Comprehensive mixed-mode HILIC x SEC contour plots of the aerosol WSOM sample at pH5 (a) and pH 6 (b) of the mobile phase, and recorded by ELSD (60°C and 3.5 bar). Colours are used to represent the intensity of the signal at a given 1stD retention time versus molar mass (Da)

When employing a mobile phase at pH 6, the UV absorption chromatogram (Figure 32(b)) of the aerosol WSOM sample exhibit only two signals (30 and 31) with different MWs: 593-639 Da and 175-185, respectively (Table 7). In the FLD chromatogram, just one signal is detected (peak 32 in Figure 33 (b)) with a M_W between 771 and 891 Da. The ELSD chromatogram (Figure 34 (b)) also has two signals with different polarity and M_W distribution: 845-861 Da and 664-665 Da. The M_w/M_n values varied within the range of 1.02-1.47, with the

maximum values of polydispersity being also recorded through the FLD method. The lowest M_w/M_n values were registered through the UV absorption and ELSD methods.

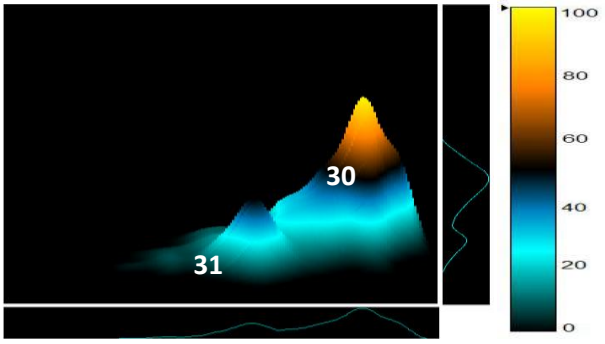

Figure 35. Comprehensive mixed-mode HILIC x SEC three-dimensional surface plot of the aerosol WSOM sample at pH 6 of the mobile phase, and recorded by UV absorption at 254 nm

Comparing the results of the MW distribution here obtained for the SR-FA and PL-FA samples with those described in the literature, it is possible to concluded that higher values have been reported in the literature (Chin *et al.*, 1994; Perminova *et al.*, 1998; Zhou *et al.*, 2000; O'Loughlin and Chin, 2001; Duarte and Duarte, 2011). These differences are likely be explained by the application of a fractionation scheme previous to the size-exclusion in the 2D-LC system. It is recognized that the amount of organic material within the fractions sampled from the 1^{st}D effluent and re-injected into the 2^{nd}D (i.e. the SEC column) is lower than when injecting the original NOM sample without a pre-fractionation procedure. This previous separation step leads to a decrease in the interaction between NOM constituents, which in turns can affect NOM aggregate formation and, consequently, their molecular size. These results also questions all the results reported in the literature, and opposite to what has been reported, it also suggests the lack of a preferential range of MW distribution for the studied NOM samples.

Another important conclusion drawn from these results is that the constituents of the PL-FA sample have smaller molecular size than those of the SR-FA sample. These differences are likely to be explained by their different origin. As already mentioned in

Chapter 2, the PL-FA have a microbial source and result from the degradation of algal biomass, whereas SR-FA originate from terrestrial plant and soil-derived organic matter inputs. Groups of compounds such as cellulose, lignines and other organics with high MWs are known to be present in the SR-FA sample (McKnight *et al.*, 1985). When comparing the results obtained for the aerosol WSOM sample with those of the aquatic fulvic samples, it is also evident that the WSOM present the lowest molecular size range. These results are supported by previous works where it is shown that atmospheric organic compounds have MWs much lower than those of the terrestrial fulvic and humic acids (Kiss *et al.*, 2003; Graber and Rudich, 2006; Stone *et al.*, 2009). According to the work of Duarte and Duarte (2011), the occurrence of organic compounds with such a low molecular size range in this particular atmospheric aerosol sample may be explained by the higher abundance of freshly emitted organic particles.

Mechanisms of separation	**Detector**	**Mobile phase at pH5**			
		Elution Time 1st D (min)	**M_w (Da)**	**M_n (Da)**	**M_w/M_n**
C18 x SEC	**UV 254 nm**	(20) : 50; 55	(20) : 457; 521	(20) : 391; 462	(20) : 1.17; 1.13
	FLD- 240/450 nm	(21) : 50; 54	(21) : 299; 493	(21) : 206;390	(21) : 1.45; 1.26
	ELSD	(22) : 50; 55	(22) : 681; 719	(22) : 651; 693	(22) : 1.05; 1.04

Table 6. MW characteristics of the aerosol WSOM sample estimated through comprehensive RP-C18 x SEC (the results of each replica are separated by a semicolon and the peak number is presented in parenthesis)

Mechanisms of Separation	Detector	Mobile phase at pH5				Mobile phase at pH6			
		Elution Time 1st D (min)	M_w (Da)	M_n (Da)	M_w/M_n	Elution Time 1st D (min)	M_w (Da)	M_n (Da)	M_w/M_n
HILIC x SEC	UV 254 nm	(23) : 40; 43	(23) : 523; 649	(23) : 507; 610	(23) : 1.03; 1.06				
		(24) : 45; 48	(24) : 552; 524	(24) : 455; 543	(24) : 1.21; 1.16				
		(25) : 51; 53	(25) : 406; 468	(25) : 363; 414	(25) : 1.12; 1.13	(30) : 40; 40	(30) : 593; 639	(30) : 529; 566	(30) : 1.12; 1.13
		(26) : 62; 65	(26) : 176; 181	(26) : 175; 180	(26) : 1.01; 1.01	(31) : 55; 55	(31) : 175; 185	(31) : 172; 182	(31) : 1.02; 1.02
		(27) : 75; 78	(27) : 164; 168	(27) : 161; 165	(27) : 1.02; 1.01				
		(28) : 81; 83	(28) : 157; 159	(28) : 151; 155	(28) : 1.04; 1.02				
	FLD- 240/450 nm					(32) : 41; 40	(32) : 771; 891	(32) : 525; 642	(32) : 1.47; 1.39
	ELSD	(29) : 45; 47	(29) : 680; 714	(29) : 668; 700	(29) : 1.02; 1.02	(33) : 40 ; 39	(33) : 845; 861	(33) : 824; 838	(33) : 1.03; 1.03
						(34) : 45; 45	(34) : 664; 665	(34) : 647; 652	(34) 1.03; 1.02

Table 7. MW characteristics of the aerosol WSOM sample estimated through comprehensive mixed-mode HILIC x SEC (the results of each replica are separated by a semicolon and the peak number is presented in parenthesis)

It is also important to note that for the SR-FA and PL-FA samples, the MW distribution obtained through the comprehensive mixed-mode HILIC x SEC system is systematically higher than those estimated through the comprehensive RP-C18 x SEC system. Possible explanations for these results can include not only the effect of the different separation protocols in the 1^{st}D, but also the occurrence of adsorption phenomena of NOM constituents into the 2^{nd}D column under the injection plug conditions of the mixed-mode HILIC separation procedure. Either way, these results also reinforce the idea that the estimative of the MW distribution is strongly dependent on the chromatographic conditions and, consequently, the comparison of the results obtained upon different conditions is not straightforward. Furthermore, within the same comprehensive 2D-LC mechanism, the estimative of MW distribution for all NOM samples obtained by UV absorption, FLD or ESLD detection differ strongly. An important effect may have contributed to these differences between the three detectors: spectroscopic methods are dependent of the optical properties of the NOM samples (such as the number and type of chromophores) and not all organic components show the same molar absorptivity. The ELSD, on the other hand, is a universal detection method that depends only on the concentration of the analyte. This feature is likely to be the reason why values of polydispersity close to 1.0 were registered by the ESLD detection method. In contrast, the FLD method provided the highest polydispersity values, being this a consequence of the significant differences in the fluorescence pattern of the NOM constituents (e.g. aliphatic and aromatic compounds). It is also important to highlight the differences between the two replicas in both 2D-LC systems and for all NOM samples. These differences put into evidence the need to perform additional experiments to estimate the MW distribution of these samples with a greater confidence level.

4.4. Conclusions

In this fourth chapter, two 2D-LC separation systems (comprehensive RP-C18 x SEC and comprehensive mixed-mode HILIC x SEC) were applied to map the

hydrophobicity and polarity *versus* MW distribution of three different NOM samples: SR-FA, PL-FA, and aerosol WSOM. The obtained results allowed concluding that:

- no fractionation of the SR-FA sample has occurred when a mixed-mode HILIC column was employed as 1^{st}D separation mechanism, but with the conventional RP-C18 column two fractions were obtained along the 1^{st}D. On the other hand, for both PL-FA and aerosol WSOM samples, no separation was observed when using a RP-C18 column in the 1^{st}D, although the mixed-mode HILIC column was able the separate these samples into chemically distinct fractions;
- the complete range of M_W distribution obtained in this study varied within the range of 745-2122 Da, 637-1950 Da, and 157-891 Da for the SR-FA, PL-FA, and aerosol WSOM sample, respectively;
- based on the obtained MW values, the NOM samples can be arranged in the following order: aerosol WSOM < PL-FA < SR-FA. The obtained trends are due to the different origin and formation pathways of the these NOM samples, which strongly influence their chemical composition and MW distribution;
- higher MW values are reported in the literature for these NOM samples, thus suggesting the important role played by the additional separation mechanism in the 1^{st}D for an accurate estimative of the MWs through an 2D-LC system.

Final remarks and perspectives for future work

Most of the studies reported to date on the application of 2D-LC are focused on method development employing standard mixtures of compounds whose structure and elution pattern is well known (Tanaka *et al.*, 2004; Im *et al.*, 2009; Ginzburg *et al.*, 2011). Furthermore, the analysis of real samples (e.g. food and beverages, plant extracts, and environmental samples) is still limited to the identification of specific classes of well-known compounds (Pól *et al.*, 2006; Wang *et al.*, 2007b; Brudin *et al.*, 2010). When dealing with complex organic mixtures with unknown structures, such as those of NOM, the characterization of the sample should start from a holistic point of view rather than searching for specific compounds. The solution to this problem passes through the development of fractionation protocols for multidimensional systems.

Following a optimization procedure, two different 2D-LC systems were developed and implemented into the analysis of three different NOM samples. The 2D-LC proved to be a valid technique and a useful tool for the fractionation of such complex organic mixtures. Although from a qualitative point of view the obtained results can be considered to be reliable, their reproducibly still needs to be improved. Furthermore, the obtained results were also found to be dependent on the chromatographic conditions, which suggests the need for improving both mobile and stationary phases choices for NOM separation.

With future developments in multidimensional systems, NOM fractionation can be further improved in order to achieve the homogeneity necessary for full understand of their structure via other screening techniques (e.g. NMR spectroscopy). In fact, understanding on how structural information is linked to size fractions should be a major goal for future research works.

Annexes

Annexes

Optimization of the chromatographic conditions using the RP-C18 column

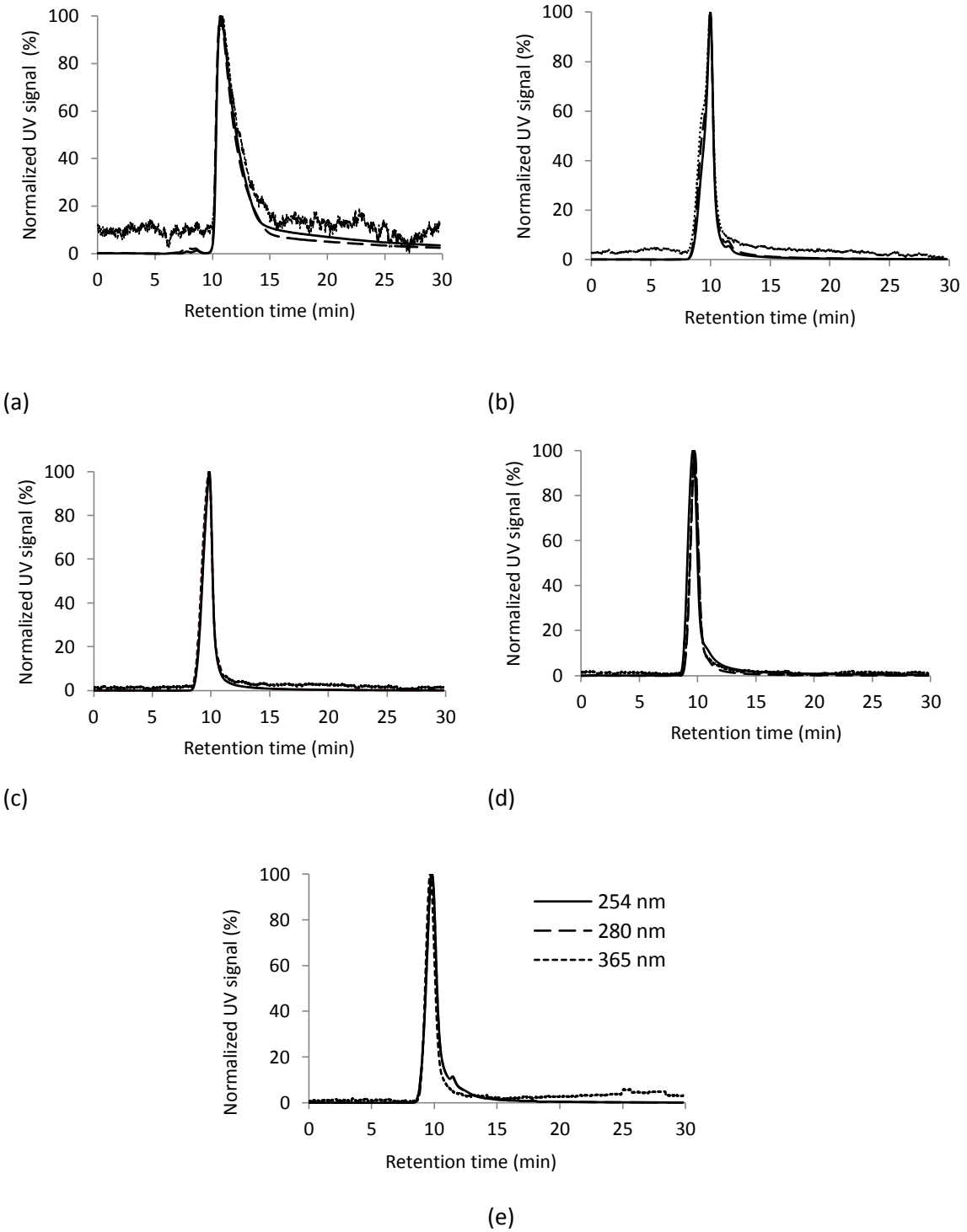

Figure 36. Chromatograms of the SR-FA sample obtained in the RP-C18 column and recorded by UV absorption at 254 nm, 280 nm, and 365 nm, using a mobile phase composition consisting of 0% (a), 10% (b), 15% (c), 25% (d), and 30% (e) (v/v) of acetonitrile

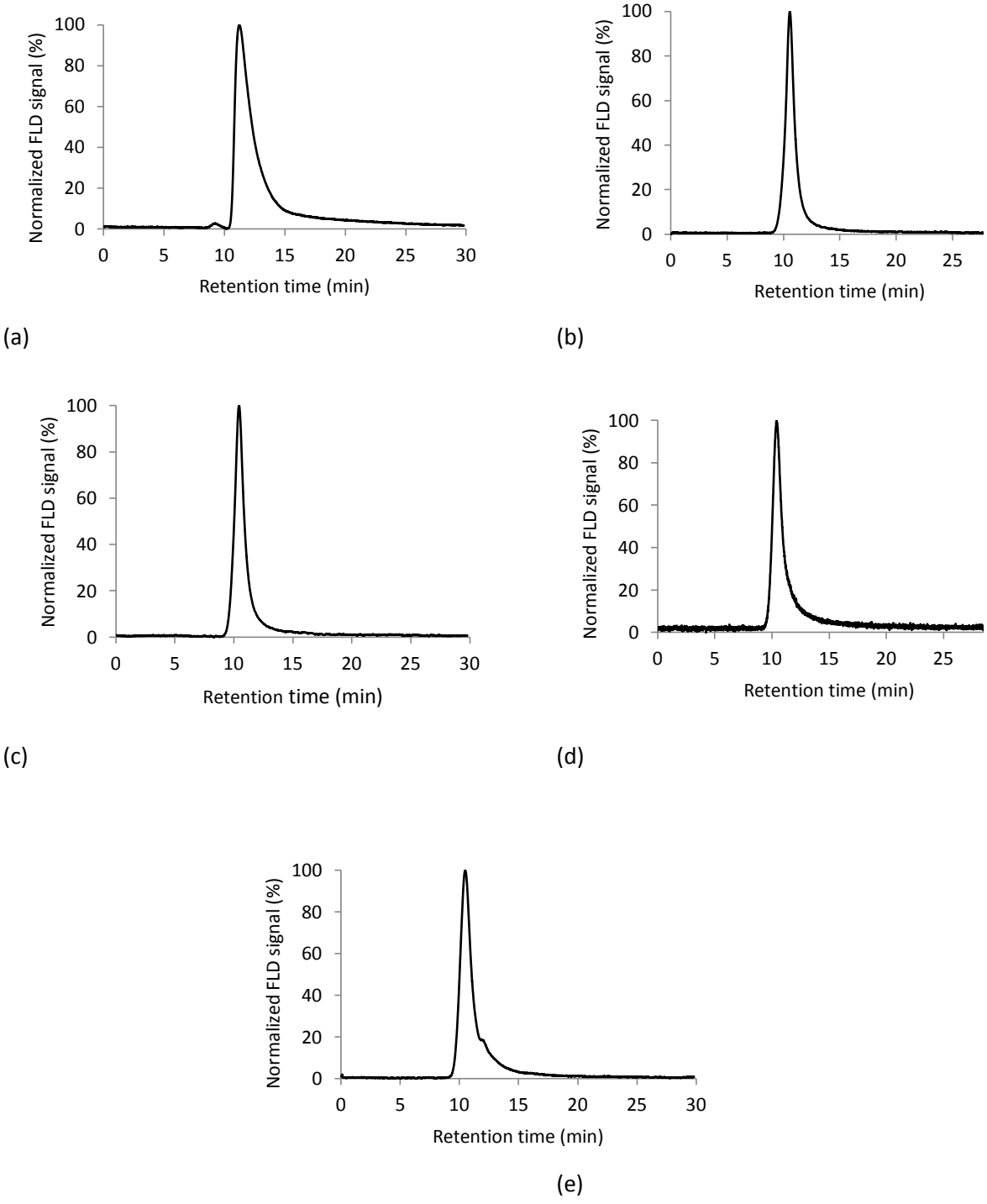

Figure 37. Chromatograms of the SR-FA sample obtained in the RP-C18 column and recorded by FLD at $\lambda_{Exc}/\lambda_{Em}$ = 240/450 nm, using a mobile phase composition consisting of 0% (a), 10% (b), 15% (c), 25% (d), and 30% (e) (v/v) of acetonitrile

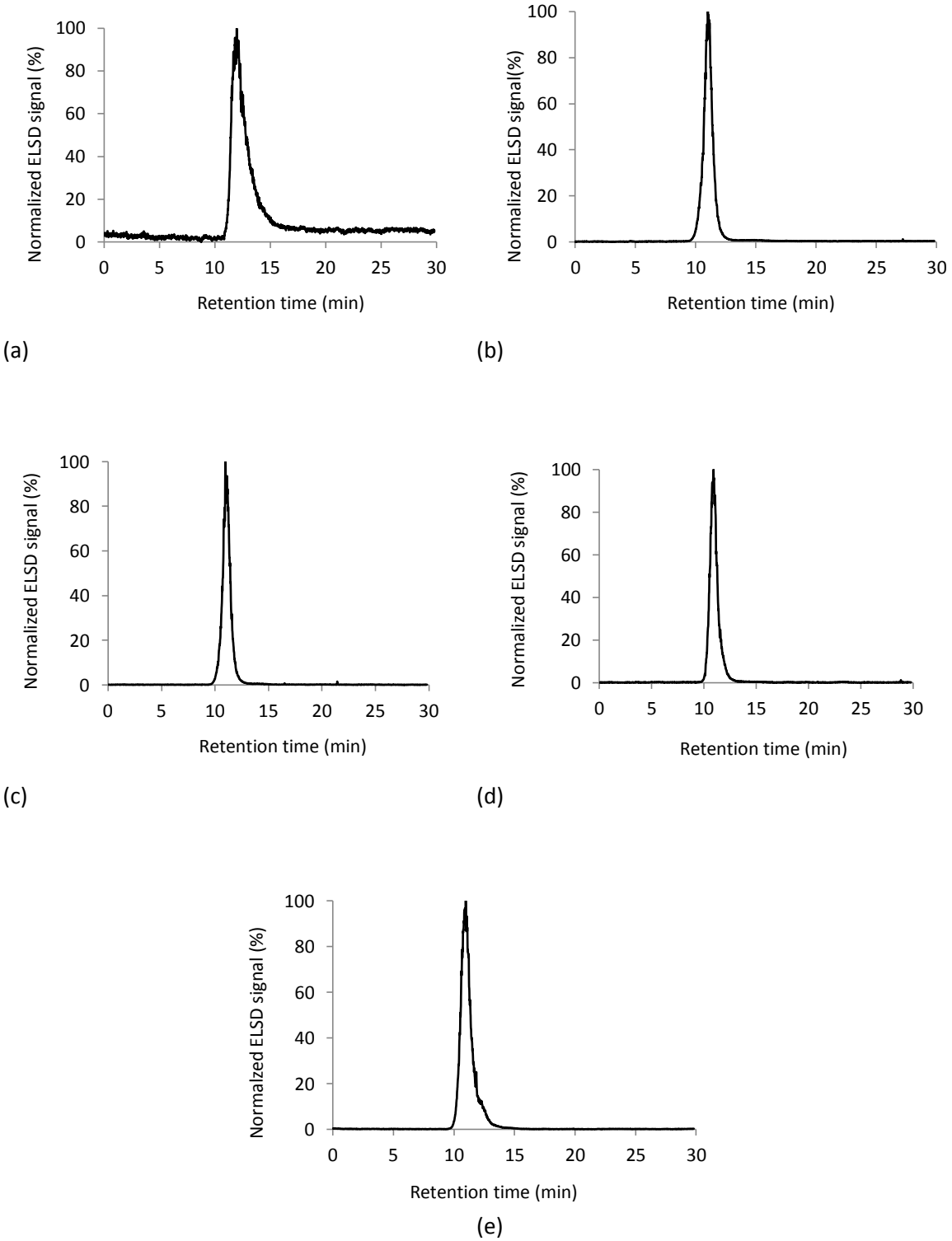

Figure 38. Chromatograms of the SR-FA sample obtained in the RP-C18 column and recorded by ELSD at 60°C and 3.5 bar, using a mobile phase composition consisting of 0% (a), 10% (b), 15% (c), 25% (d), and 30% (e) (v/v) of acetonitrile

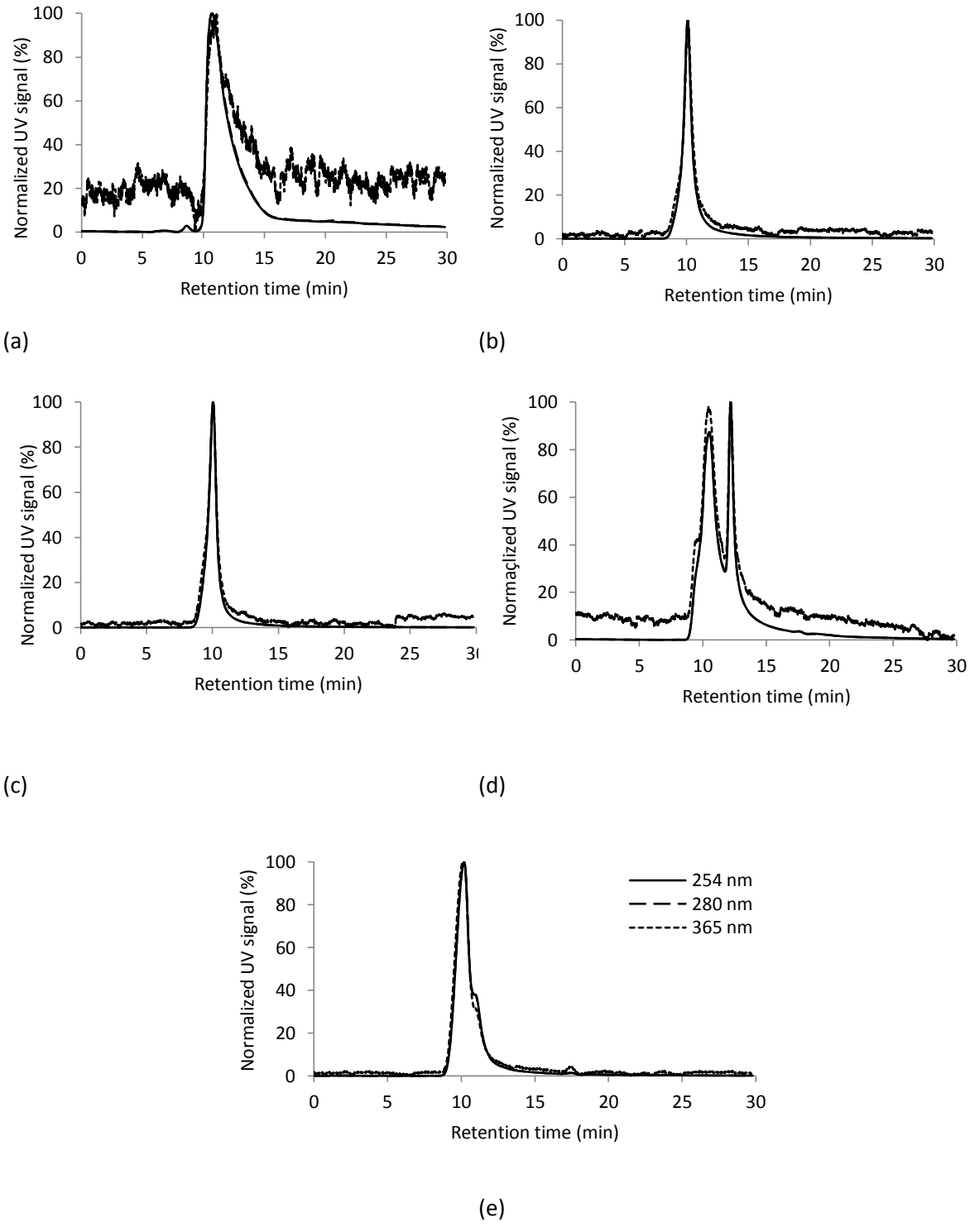

Figure 39. Chromatograms of the PL-FA sample obtained in the RP-C18 column and recorded by UV absorption at 254 nm, 280 nm, and 365 nm, using a mobile phase composition consisting of 0% (a), 10% (b), 15% (c), 25% (de), and 30% (e) (v/v) of acetonitrile

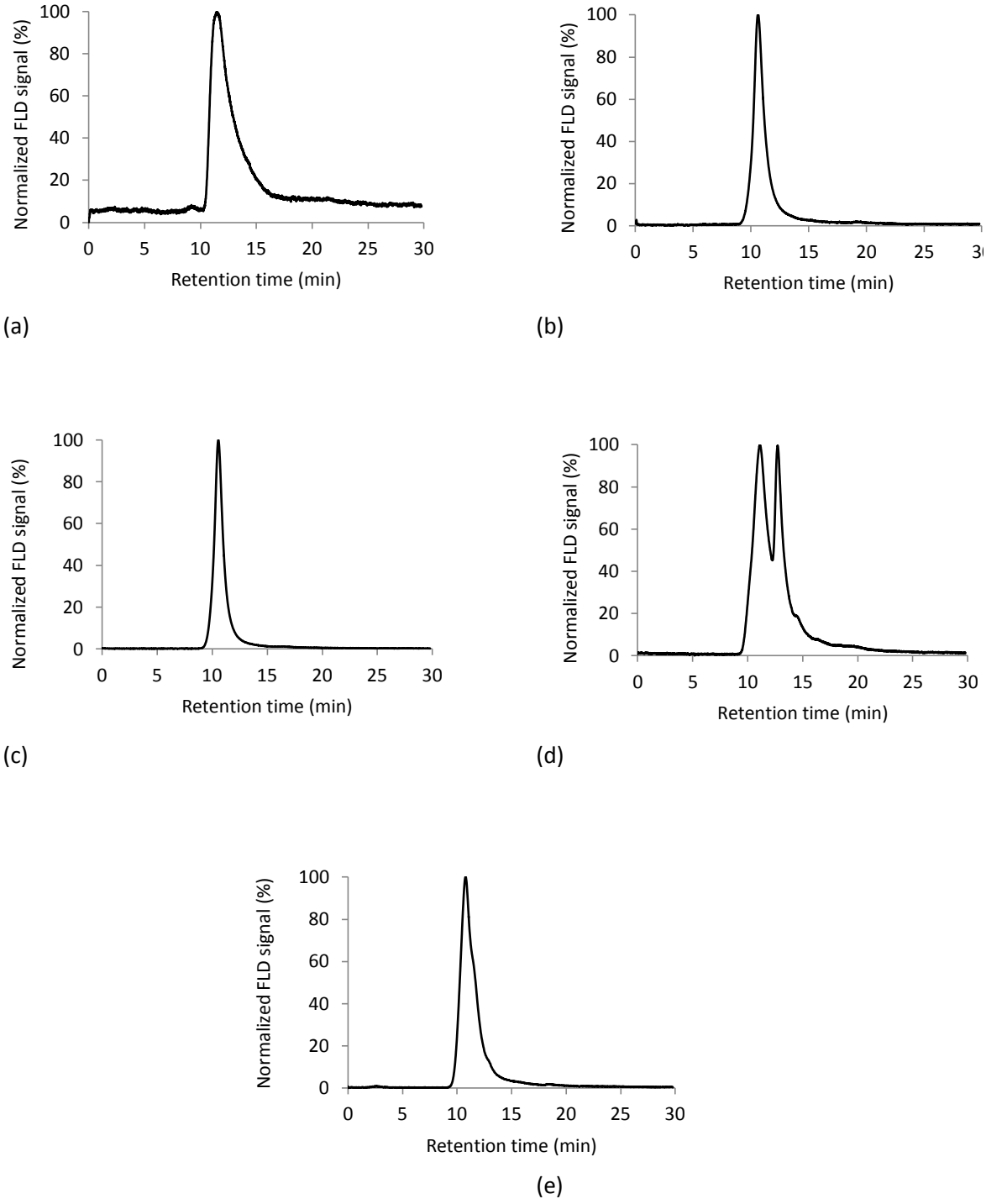

Figure 40. Chromatograms of the PL-FA sample obtained in the RP-C18 column and recorded by FLD at $\lambda_{Exc}/\lambda_{Em}$ = 240/450 nm, using a mobile phase composition consisting of 0% (a), 10% (b), 15% (c), 25% (d), and 30% (e) (v/v) of acetonitrile

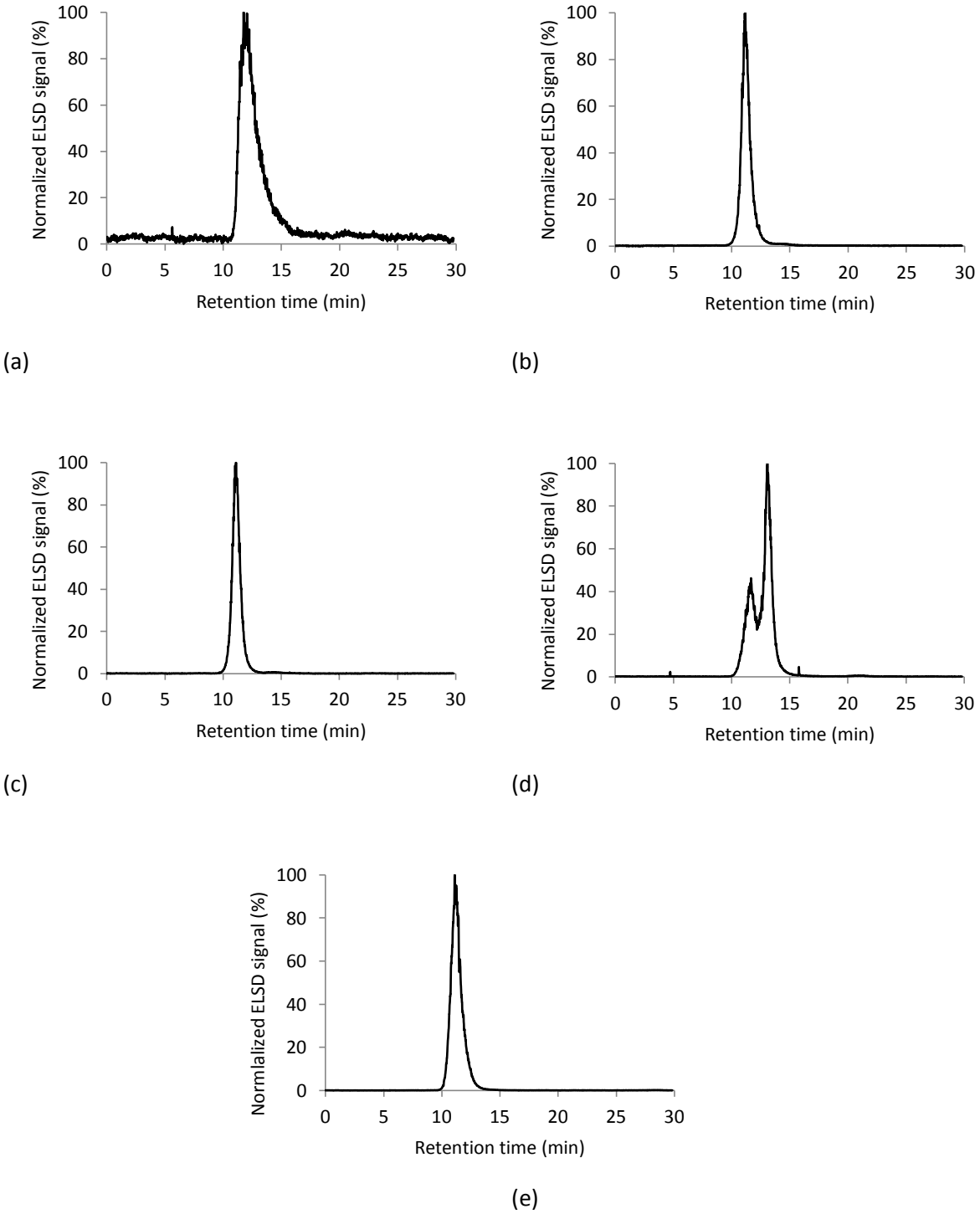

Figure 41. Chromatograms of the PL-FA sample obtained in the RP-C18 column and recorded by ELSD at 60°C and 3.5 bar, using a mobile phase composition consisting of 0% (a), 10% (b), 15% (c), 25% (e), and 30% (f) (v/v) of acetonitrile

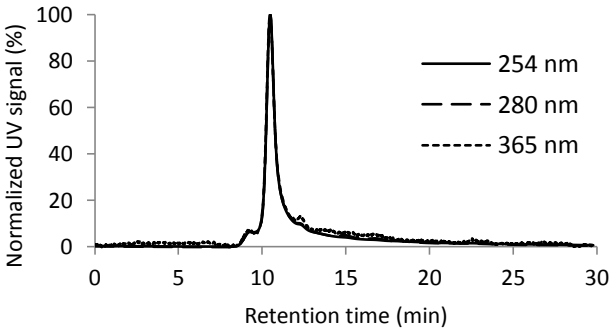

Figure 42. Chromatogram of the aerosol WSOM sample obtained in the RP-C18 column and recorded by UV absorption at 254 nm, 280 nm, and 365 nm, using a mobile phase composition consisting of 25% (v/v) acetonitrile

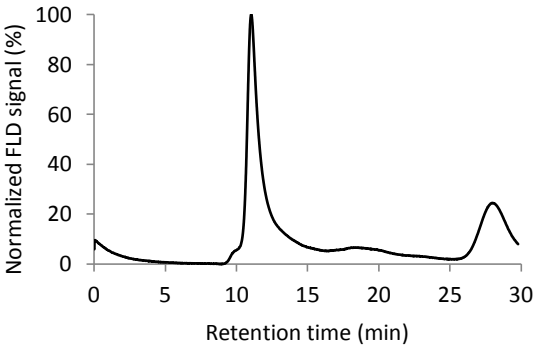

Figure 43. Chromatogram of the aerosol WSOM sample obtained in the RP-C18 column and recorded by FLD at $\lambda_{Exc}/\lambda_{Em}$ = 240/450 nm, using a mobile phase composition consisting of 25% (v/v) acetonitrile

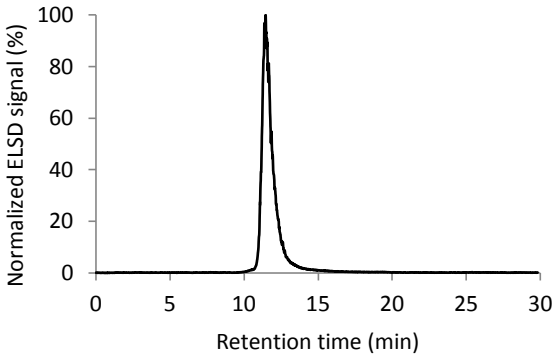

Figure 44. Chromatogram of the aerosol WSOM sample obtained in the RP-C18 column and recorded by ELSD at 60°C and 3.5 bar, using a mobile phase composition consisting of 25% (v/v) acetonitrile

References

Abdulla, H. A. N.;Minor, E. C.;Dias, R. F. and Hatcher, P. G. 2010. Changes in the compound classes of dissolved organic matter along an estuarine transect: A study using FTIR and 13C NMR. *Geochimica et Cosmochimica Acta,* 74**,** 3815-3838.

Ahmad, S. R. and Reynolds, D. M. 1995. Synchronous fluorescence spectroscopy of wastewater and some potential constituents. *Water Research,* 29**,** 1599-1602.

Alberts, J. J. and Takács, M. 2004a. Comparison of the natural fluorescence distribution among size fractions of terrestrial fulvic and humic acids and aquatic natural organic matter. *Organic Geochemistry,* 35**,** 1141-1149.

Alberts, J. J. and Takács, M. 2004b. Total luminescence spectra of IHSS standard and reference fulvic acids, humic acids and natural organic matter: comparison of aquatic and terrestrial source terms. *Organic Geochemistry,* 35**,** 243-256.

Allan, J. D. and Castillo, M. M. 2007. Dissolved organic matter. *Stream Ecology: Structure and Function of Running Waters* Second edition ed. Netherlands Springer. 150-152

Allpike, B. P.;Heitz, A.;Joll, C. A. and Kagi, R. I. 2007. A new organic carbon detector for size exclusion chromatography. *Journal of Chromatography A,* 1157**,** 472-476.

Bagastyo, A. Y.;Keller, J.;Poussade, Y. and Batstone, D. J. 2011. Characterisation and removal of recalcitrants in reverse osmosis concentrates from water reclamation plants. *Water Research,* 45**,** 2415-2427.

Baigorri, R.;Fuentes, M.;González-Gaitano, G. and García-Mina, J. M. 2007. Analysis of molecular aggregation in humic substances in solution. *Colloids and Surfaces A: Physicochemical and Engineering Aspects,* 302**,** 301-306.

Barbaro, E.;Zangrando, R.;Moret, I.;Barbante, C.;Cescon, P. and Gambaro, A. 2011. Free amino acids in atmospheric particulate matter of Venice, Italy. *Atmospheric Environment,* 45**,** 5050-5057.

Bernal, J.;Ares, A. M.;Pól, J. and Wiedmer, S. K. 2011. Hydrophilic interaction liquid chromatography in food analysis. *Journal of Chromatography A,* 1218**,** 7438-7452.

Blahov, E.;Jandera, P.;Cacciola, F. and Mondello, L. 2006. Two-dimensional and serial column reversed-phase separation of phenolic antioxidants on octadecyl-, polyethyleneglycol-, and pentafluorophenylpropylsilica columns. *Journal of Separation Science* 29**,** 555 – 566.

Bot, A. and Benites, J. 2005. Organic matter decomposition and the soil food web. *The importance of soil organic matter: Key to drougth-resistant soil and sustained food production.* Rome, Italy: FAO. 5-10

Brudin, S. S.;Shellie, R. A.;Haddad, P. R. and Schoenmakers, P. J. 2010. Comprehensive two-dimensional liquid chromatography: Ion chromatography×reversed-phase liquid chromatography for separation of low-molar-mass organic acids. *Journal of Chromatography A,* 1217**,** 6742-6746.

Cacciola, F.;Jandera, P.;Blahov, E. and Mondello, L. 2006. Development of different comprehensive two dimensional systems for the separation of phenolic antioxidants. *Journal of Separation Science,* 29**,** 2500 – 2513.

Cacciola, F.;Jandera, P.;Hajdu, Z.;Cêsla, P. and Mondello, L. 2007. Comprehensive two-dimensional liquid chromatography with parallel gradients for separation of phenolic and flavone antioxidants. *Journal of Chromatography A,* 1149**,** 73–87.

Cacciola, F.;Jandera, P. and Mondello, L. 2007. Temperature effects on separation on zirconia columns: Applications to one- and two-dimensional LC separations of phenolic antioxidants. *Journal of Separation Science* 30**,** 462 – 474.

Caravaca, F.;Lax, A. and Albaladejo, J. 1999. Organic matter, nutrient contents and cation exchange capacity in fine fractions from semiarid calcareous soils. *Geoderma,* 93**,** 161-176.

Carletti, P.;Roldán, M. L.;Francioso, O.;Nardi, S. and Sanchez-Cortes, S. 2010. Structural characterization of humic-like substances with conventional and surface-enhanced spectroscopic techniques. *Journal of Molecular Structure,* 982**,** 169-175.

Cavalli, F.;Facchini, M. C.;Decesari, S.;Mircea, M.;Emblico, L.;Fuzzi, S.;Ceburnis, D.;Yoon, Y. J.;O'Dowd, C. D.;Putaud, J. P. and Dell'Acqua, A. 2004. Advances in characterization of size-resolved organic matter in marine aerosol over the North Atlantic. *J. Geophys. Res.,* 109**,** D24215.

Chen, J.;LeBoeuf, E. J.;Dai, S. and Gu, B. 2003. Fluorescence spectroscopic studies of natural organic matter fractions. *Chemosphere,* 50**,** 639-647.

Chen, J. G., Baohua ; Royer, Richard A.; Burgos,William D. 2003. The roles of natural organic matter in chemical and microbial reduction of ferric iron. *The Science of the Total Environment* 307**,** 167-178.

Chen, X.;Kong, L.;Su, X.;Fu, H.;Ni, J. and Zou, R. Z. a. H. 2004. Separation and identification of compounds in Rhizoma chuanxiong by comprehensive two-dimensional liquid chromatography coupled to mass spectrometry. *Journal of Chromatography A,* 1040**,** 169–178.

Chin, Y.-P.;Aiken, G. and O'Loughlin, E. 1994. Molecular Weight, Polydispersity, and Spectroscopic Properties of Aquatic Humic Substances. *Environmental Science & Technology,* 28**,** 1853-1858.

Cohen, S. A. and R.Schure, M. (eds.) 2008. *Multidimensional Liquid Chromatography: Theory ans application in industrial chemestry and the life sciences*.

Conte, P. and Piccolo, A. 1999. Conformational Arrangement of Dissolved Humic Substances. Influence of Solution Composition on Association of Humic Molecules. *Environmental Science & Technology,* 33**,** 1682-1690.

Coulier, L.;Kaal, E. R. and Hankemeier, T. 2005. Comprehensive two-dimensional liquid chromatography and hyphenated liquid chromatography to study the degradation of poly(bisphenol A)carbonate. *Journal of Chromatography A,* 1070**,** 79-87.

Cozzolino, A.;Conte, P. and Piccolo, A. 2001. Conformational changes of humic substances induced by some hydroxy-, keto-, and sulfonic acids. *Soil Biology and Biochemistry,* 33**,** 563-571.

Cruz, C. N. and Pandis, S. N. 2000. Deliquescence and Hygroscopic Growth of Mixed Inorganic−Organic Atmospheric Aerosol. *Environmental Science & Technology,* 34**,** 4313-4319.

Dabek-Zlotorzynska, E.;Aranda-Rodriguez, R. and Graham, L. 2005. Capillary electrophoresis determinative and GC-MS confirmatory method for water-soluble organic acids in airborne particulate matter and vehicle emission. *Journal of Separation Science,* 28**,** 1520-1528.

Davis, J. M. and Giddings, J. C. 1983. Statistical theory of component overlap in multicomponent chromatograms. *Analytical Chemestry,* 55**,** 418-424.

de Villiers, A.;Lestremau, F.;Szucs, R.;Gélébart, S.;David, F. and Sandra, P. 2006. Evaluation of ultra performance liquid chromatography: Part I. Possibilities and limitations. *Journal of Chromatography A,* 1127**,** 60-69.

Decesari, S.;Facchini, M. C.;Fuzzi, S.;McFiggans, G. B.;Coe, H. and Bower, K. N. 2005. The water-soluble organic component of size-segregated aerosol, cloud water and wet depositions from Jeju Island during ACE-Asia. *Atmospheric Environment,* 39**,** 211-222.

Decesari, S.;Facchini, M. C.;Fuzzi, S. and Tagliavini, E. 2000. Characterization of water-soluble organic compounds in atmospheric aerosol: A new approach. *J. Geophys. Res.,* 105**,** 1481-1489.

Dessureault-Rompré, J.;Luster, J.;Schulin, R.;Tercier-Waeber, M.-L. and Nowack, B. 2010. Decrease of labile Zn and Cd in the rhizosphere of hyperaccumulating Thlaspi caerulescens with time. *Environmental Pollution* 158**,** 1955-1962.

Diane M. McKnight;Boyer, E. W.;Wsesterhoff, P. K.;Doran, P. T.;Kulbe, T. and Andersen, D. T. 2001. Spectrofluorometric characterization of dissolved organic matter for indication of precursor organic material and aromaticity. *Limnology and Oceanography* 46**,** 38-48.

Dittmar, T. and Kattner, G. 2003. Recalcitrant dissolved organic matter in the ocean: major contribution of small amphiphilics. *Marine Chemistry,* 82**,** 115-123.

Doig, L. E. L., Karsten 2006. Influence of dissolved organic matter on nickel bioavailability and toxicity to Hyalella azteca in water-only exposures. *Aquatic Toxicology,* 76**,** 203-216.

Duarte, R. M. B. O. and Duarte, A. C. 2010. A new chromatographic response function for use in size-exclusion chromatography optimization strategies: Application to complex organic mixtures. *Journal of Chromatography A,* 1217**,** 7556-7563.

Duarte, R. M. B. O. and Duarte, A. C. 2011. Optimizing size-exclusion chromatographic conditions using a composite objective function and chemometric tools: Application to natural organic matter profiling. *Analytica Chimica Acta,* 688**,** 90-98.

Duarte, R. M. B. O.;M. S. Silva, A. and Duarte, A. C. 2008. Two-Dimensional NMR Studies of Water-Soluble Organic Matter in Atmospheric Aerosols. *Environment Science Technology,* 42**,** 8224-8230.

Duarte, R. M. B. O.;Pio, C. A. and Duarte, A. C. 2004. Synchronous Scan and Excitation-Emission Matrix Fluorescence Spectroscopy of Water-Soluble Organic Compounds in Atmospheric Aerosols. *Journal of Atmospheric Chemistry,* 48**,** 157-171.

Duarte, R. M. B. O.;Pio, C. A. and Duarte, A. C. 2005. Spectroscopic study of the water-soluble organic matter isolated from atmospheric aerosols collected under different atmospheric conditions. *Analytica Chimica Acta,* 530**,** 7-14.

Duarte, R. M. B. O.;Santos, E. B. H. and Duarte, A. C. 2003. Spectroscopic characteristics of ultrafiltration fractions of fulvic and humic acids isolated from an eucalyptus bleached Kraft pulp mill effluent. *Water Research,* 37**,** 4073-4080.

Duarte, R. M. B. O.;Santos, E. B. H.;Pio, C. A. and Duarte, A. C. 2007. Comparison of structural features of water-soluble organic matter from atmospheric aerosols with those of aquatic humic substances. *Atmospheric Environment,* 41**,** 8100-8113.

Dugo, P.;Cacciola, F.;Kumm, T.;Dugo, G. and Mondello, L. 2008. Comprehensive multidimensional liquid chromatography: Theory and applications. *Journal of Chromatography A,* 1884**,** 353-368.

Eom, H. Y.;Park, S.-Y.;Kim, M. K.;Suh, J. H.;Yeom, H.;Min, J. W.;Kim, U.;Lee, J.;Youm, J.-R. and Han, S. B. 2010. Comparison between evaporative light scattering detection and charged aerosol detection for the analysis of saikosaponins. *Journal of Chromatography A,* 1217**,** 4347-4354.

Facchini, M. C.;Decesari, S.;Mircea, M.;Fuzzi, S. and Loglio, G. 2000. Surface tension of atmospheric wet aerosol and cloud/fog droplets in relation to their organic carbon content and chemical composition. *Atmospheric Environment,* 34**,** 4853-4857.

Facchini, M. C.;Fuzzi, S.;Zappoli, S.;Andracchio, A.;Gelencsér, A.;Kiss, G.;Krivácsy, Z.;Mészáros, E.;Hansson, H.-C.;Alsberg, T. and Zebühr, Y. 1999. Partitioning of the organic aerosol component between fog droplets and interstitial air. *J. Geophys. Res.,* 104**,** 26821-26832.

Floyd, T. R. 1988. Use of Two-Dimensional Liquid Chromatography in the Analysis of Additives in Cellulose Acetate Polymer. *Chromatographia* 25**,** 791-796.

François, I.;Sandra, K. and Sandra, P. 2009. Comprehensive liquid chromatography: Fundamental aspects and practical considerations—A review. *Analytica Chimica Acta,* 641**,** 14-31.

Gašparović, B.;Vojvodić, V. and Ćosović, B. 1997. Characterization of organic matter in fractionated seawater samples using o-nitrophenol as an electrochemical probe. *Analytica Chimica Acta,* 338**,** 179-190.

Gelencsér, A.;Hoffer, A.;Krivácsy, Z.;Kiss, G.;Molnár, A. and Mészáros, E. 2002. On the possible origin of humic matter in fine continental aerosol. *Journal of Geophysical Research,* 107**,** 4137.

Gheorghiu, C. S., D.S. ; Al-Reasi, H.A. ; McGeer, J.C. ; Wilkie, M.P. 2010. Influence of natural organic matter (NOM) quality on Cu–gill binding in the rainbow trout (Oncorhynchus mykiss). *Aquatic Toxicology* 97**,** 343-352.

Ghosh, K. and Schnitzer, M. 1980. Macromolecular Structures of Humic Substances. *Soil Science,* 129**,** 266-276.

Ginzburg, A.;Macko, T.;Dolle, V. and Brüll, R. 2011. Characterization of polyolefins by comprehensive high-temperature two-dimensional liquid chromatography (HT 2D-LC). *European Polymer Journal,* 47**,** 319-329.

Gonsior, M.;Peake, B. M.;Cooper, W. T.;Podgorski, D. C.;D'Andrilli, J.;Dittmar, T. and Cooper, W. J. 2011. Characterization of dissolved organic matter across the Subtropical Convergence off the South Island, New Zealand. *Marine Chemistry,* 123**,** 99-110.

Graber, E. R. and Rudich, Y. 2006. Atmospheric HULIS: How humic-like are they? A comprehensive and critical review. *Atmospheric Chemistry and Physics* 6**,** 729-753.

Guéguen, C.;Guo, L. and Tanaka, N. 2005. Distributions and characteristics of colored dissolved organic matter in the Western Arctic Ocean. *Continental Shelf Research,* 25**,** 1195-1207.

Guiochon, G.;Marchetti, N.;Mriziq, K. and Shalliker, R. A. 2008. Implementations of two-dimensional liquid chromatography. *Journal of Chromatography A,* 1189**,** 109-168.

Guo, Y. and Gaiki, S. 2011. Retention and selectivity of stationary phases for hydrophilic interaction chromatography. *Journal of Chromatography A,* 1218**,** 5920-5938.

Haitzer, M.;Höss, S.;Traunspurger, W. and Steinberg, C. 1998. Effects of dissolved organic matter (DOM) on the bioconcentration of organic chemicals in aquatic organisms -- a review. *Chemosphere,* 37**,** 1335-1362.

Hautala, K.;Peuravuori, J. and Pihlaja, K. 2000. Measurement of aquatic humus content by spectroscopic analyses. *Water Research,* 34**,** 246-258.

Havers, N.;Burba, P.;Lambert, J. and Klockow, D. 1998. Spectroscopic Characterization of Humic-Like Substances in Airborne Particulate Matter. *Journal of Atmospheric Chemistry,* 29**,** 45-54.

Henry, F.;Coeur-Tourneur, C.;Ledoux, F.;Tomas, A. and Menu, D. 2008. Secondary organic aerosol formation from the gas phase reaction of hydroxyl radicals with m-, o- and p-cresol. *Atmospheric Environment,* 42**,** 3035-3045.

Her, N.;Amy, G.;McKnight, D.;Sohn, J. and Yoon, Y. 2003. Characterization of DOM as a function of MW by fluorescence EEM and HPLC-SEC using UVA, DOC, and fluorescence detection. *Water Research,* 37**,** 4295-4303.

Hessen, D. O. and Tranvik, L. J. 1998. Sources and age of aquatic humus *In:* KEKNIGHT and AIKEN (eds.) *Aquatic humic substances: ecology and biogeochemistry* Germany: Springer. 9-10

Horst, A. v. d. and Schoenmakers, P. J. 2003. Comprehensive two-dimensional liquid chromatography of polymers. *Journal of Chromatography A,* 1000**,** 693-709.

Hu, L.;Chen, X.;Kong, L.;Su, X. and Zou, M. Y. a. H. 2005. Improved performance of comprehensive two-dimensional HPLC separation of traditional Chinese medicines by using a silica monolithic column and normalization of peak heights. *Journal of Chromatography A,* 1092**,** 191–198.

Huber, S. A.;Balz, A.;Abert, M. and Pronk, W. 2011. Characterisation of aquatic humic and non-humic matter with size-exclusion chromatography - organic carbon detection - organic nitrogen detection (LC-OCD-OND). *Water Research,* 45**,** 879-885.

Hudson, N.;Baker, A. and Reynolds, D. 2007. Fluorescence analysis of dissolved organic matter in natural, waste and polluted waters—a review. *River Research and Applications,* 23**,** 631-649.

Hung, H. M.;Katrib, Y. and S. T, M. 2005. Products and mechanisms of the reaction of the oleic acid with ozone and nitrate radical. *Journal Physical Chemistry A,* 109**,** 4517-4530.

Hur, J. L., Bo-Mi 2011. Characterization of binding site heterogeneity for copper within dissolved organic matter fractions using two-dimensional correlation fluorescence spectroscopy. *Chemosphere,* In Press, Corrected Proof.

Iinuma, Y.;Engling, G.;Puxbaum, H. and Herrmann, H. 2009. A highly resolved anion-exchange chromatographic method for determination of saccharidic tracers for biomass

combustion and primary bio-particles in atmospheric aerosol. *Atmospheric Environment,* 43**,** 1367-1371.

Im, K.;Park, H.-w.;Lee, S. and Chang, T. 2009. Two-dimensional liquid chromatography analysis of synthetic polymers using fast size exclusion chromatography at high column temperature. *Journal of Chromatography A,* 1216**,** 4606-4610.

Jandera, P. 2008. Stationary phases for hydrophilic interaction chromatography, their characterization and implementation into multidimensional chromatography concepts. *Journal of Separation Science,* 31**,** 1421-1437.

Jandera, P. 2011. Stationary and mobile phases in hydrophilic interaction chromatography: a review. *Analytica Chimica Acta,* 692**,** 1-25.

Jandera, P.;Fischer, J.;Lahovská, H.;Novotná, K.;Cesla, P. and Kolárová, L. 2006. Two-dimensional liquid chromatography normal-phase and reversed-phase separation of (co)oligomers. *Journal of Chromatography A,* 1119**,** 3-10.

Jeong, E.-K.;Cha, H.-J.;Ha, Y. W.;Kim, Y. S.;Ha, I. J. and Na, Y.-C. 2010. Development and optimization of a method for the separation of platycosides in Platycodi Radix by comprehensive two-dimensional liquid chromatography with mass spectrometric detection. *Journal of Chromatography A,* 1217**,** 4375-4382.

Kaiser, K. and Benner, R. 2009. Biochemical composition and size distribution of organic matter at the Pacific and Atlantic time-series stations. *Marine Chemistry,* 113**,** 63-77.

Kaiser, K.;Guggenberger, G.;Haumaier, L. and Zech, W. 2002. The composition of dissolved organic matter in forest soil solutions: changes induced by seasons and passage through the mineral soil. *Organic Geochemistry,* 33**,** 307-318.

Kalbitz, K.;Geyer, S. and Geyer, W. 2000. A comparative characterization of dissolved organic matter by means of original aqueous samples and isolated humic substances. *Chemosphere,* 40**,** 1305-1312.

Kazi, T. G.;Jamali, M. K.;Arain, M. B.;Afridi, H. I.;Jalbani, N.;Sarfraz, R. A. and Ansari, R. 2009. Evaluation of an ultrasonic acid digestion procedure for total heavy metals determination in environmental and biological samples. *Journal of Hazardous Materials,* 161**,** 1391-1398.

Kennedy, M. D.;Chun, H. K.;Quintanilla Yangali, V. A.;Heijman, B. G. J. and Schippers, J. C. 2005. Natural organic matter (NOM) fouling of ultrafiltration membranes: fractionation of NOM in surface water and characterisation by LC-OCD. *Desalination,* 178**,** 73-83.

Kimberly A. Prather;Courtney D. Hatch and and Vicki H. Grassian 2008. Analysis of Atmospheric Aerosols. *Annual Review of Analytical Chemistry,* 1**,** 485-514.

Kiss, G.;Tombácz, E.;Varga, B.;Alsberg, T. and Persson, L. 2003. Estimation of the average molecular weight of humic-like substances isolated from fine atmospheric aerosol. *Atmospheric Environment,* 37**,** 3783-3794.

Kiss, G.;Varga, B.;Galambos, I. and Ganszky, I. 2002. Characterization of water-soluble organic matter isolated from atmospheric fine aerosol. *J. Geophys. Res.,* 107**,** 8339.

Kitanovski, Z.;Grgic, I. and Veber, M. 2011. Characterization of carboxylic acids in atmospheric aerosols using hydrophilic interaction liquid chromatography tandem mass spectrometry. *Journal of Chromatography A,* 1218**,** 4417-4425.

Kivilompolo, M. and Hyötyläinen, T. 2007. Comprehensive two-dimensional liquid chromatography in analysis of Lamiaceae herbs: Characterisation and quantification of antioxidant phenolic acids. *Journal of Chromatography A,* 1145**,** 155–164.

Kivilompolo, M.;Obůrka, V. and Hyötyläinen, T. 2008. Comprehensive two-dimensional liquid chromatography in the analysis of antioxidant phenolic compounds in wines and juices. *Analytical and Bioanalytical Chemistry* 391**,** 373-380.

Koch, B. P.;Ludwichowski, K.-U.;Kattner, G.;Dittmar, T. and Witt, M. 2008. Advanced characterization of marine dissolved organic matter by combining reversed-phase liquid chromatography and FT-ICR-MS. *Marine Chemistry,* 111**,** 233-241.

Koprivnjak, J. F.;Pfromm, P. H.;Ingall, E.;Vetter, T. A.;Schmitt-Kopplin, P.;Hertkorn, N.;Frommberger, M.;Knicker, H. and Perdue, E. M. 2009. Chemical and spectroscopic characterization of marine dissolved organic matter isolated using coupled reverse osmosis-electrodialysis. *Geochimica et Cosmochimica Acta,* 73**,** 4215-4231.

Krivácsy, Z.;Gelencsér, A.;Kiss, G.;Mészáros, E.;Molnár, Á.;Hoffer, A.;Mészáros, T.;Sárvári, Z.;Temesi, D.;Varga, B.;Baltensperger, U.;Nyeki, S. and Weingartner, E. 2001. Study on the Chemical Character of Water Soluble Organic Compounds in Fine Atmospheric Aerosol at the Jungfraujoch. *Journal of Atmospheric Chemistry,* 39**,** 235-259.

Krivácsy, Z.;Kiss, G.;Ceburnis, D.;Jennings, G.;Maenhaut, W.;Salma, I. and Shooter, D. 2008. Study of water-soluble atmospheric humic matter in urban and marine environments. *Atmospheric Research,* 87**,** 1-12.

Krivácsy, Z.;Kiss, G.;Varga, B.;Galambos, I.;Sárvári, Z.;Gelencsér, A.;Molnár, Á.;Fuzzi, S.;Facchini, M. C.;Zappoli, S.;Andracchio, A.;Alsberg, T.;Hansson, H. C. and Persson, L. 2000. Study of humic-like substances in fog and interstitial aerosol by size-exclusion chromatography and capillary electrophoresis. *Atmospheric Environment,* 34**,** 4273-4281.

Laitinen, T.;Ehn, M.;Junninen, H.;Ruiz-Jimenez, J.;Parshintsev, J.;Hartonen, K.;Riekkola, M.-L.;Worsnop, D. R. and Kulmala, M. 2011. Characterization of organic compounds in 10- to 50-nm aerosol particles in boreal forest with laser desorption-ionization aerosol mass spectrometer and comparison with other techniques. *Atmospheric Environment,* 45**,** 3711-3719.

Lakowicz, J. R. 2010. Introduction to Fluorescence. *Principles of Fluorescence Spectroscopy.* USA: Springer. 1-25

Lankes, U.;Lüdemann, H.-D. and Frimmel, F. H. 2008. Search for basic relationships between "molecular size" and "chemical structure" of aquatic natural organic matter--Answers from 13C and 15N CPMAS NMR spectroscopy. *Water Research,* 42**,** 1051-1060.

Leenheer, J. A. 1985. Fractionation techniques for aquatic humic substances. *In:* AIKEN (ed.) *Humic substances in soil, sediment, and water: Geochemistry, isolation and characterization.* New York: Wiley-Interscience. 410

Leenheer, J. A. 2007. Progression from model structures to molecular structures of natural organic matter components. *Annals of Environmental Science,* 1**,** 57-58.

Lestremau, F.;Cooper, A.;Szucs, R.;David, F. and Sandra, P. 2006. High-efficiency liquid chromatography on conventional columns and instrumentation by using temperature

as a variable: I. Experiments with 25 cm × 4.6 mm I.D., 5 [mu]m ODS columns. *Journal of Chromatography A,* 1109**,** 191-196.

Li, M.;McDow, S. R.;Tollerud, D. J. and Mazurek, M. A. 2006. Seasonal abundance of organic molecular markers in urban particulate matter from Philadelphia, PA. *Atmospheric Environment,* 40**,** 2260-2273.

Li, Z. Z., Lixiang 2010. Cadmium transport mediated by soil colloid and dissolved organic matter: A field study. *Journal of Environmental Sciences,* 22**,** 106-115.

Lin, P.;Huang, X.-F.;He, L.-Y. and Zhen Yu, J. 2010. Abundance and size distribution of HULIS in ambient aerosols at a rural site in South China. *Journal of Aerosol Science,* 41**,** 74-87.

Lindroos, A.-J. B., Thomas; Derome, John; Derome, Kirsti 2003. The Weathering of Mineral Soil by Natural Soil Solutions. *Water, Air, & Soil Pollution,* 149**,** 269-279.

Lloret, E. D., C.; Gaillardet, J.; Albéric, P.; Crispi, O.; Chaduteau, C.; Benedetti, M. F. 2011. Comparison of dissolved inorganic and organic carbon yields and fluxes in the watersheds of tropical volcanic islands, examples from Guadeloupe (French West Indies). *Chemical Geology,* 280**,** 65-78.

Louchouarn, P.;Amon, R. M. W.;Duan, S.;Pondell, C.;Seward, S. M. and White, N. 2010. Analysis of lignin-derived phenols in standard reference materials and ocean dissolved organic matter by gas chromatography/tandem mass spectrometry. *Marine Chemistry,* 118**,** 85-97.

Lu, Y. A., Herbert E. 2002. Characterization of copper complexation with natural dissolved organic matter (DOM)—link to acidic moieties of DOM andcompetition by Ca andMg. *Water Research* 36**,** 5083-5101.

Ma, H.;Allen, H. E. and Yin, Y. 2001. Characterization of isolated fractions of dissolved organic matter from natural waters and a wastewater effluent. *Water Research,* 35**,** 985-996.

MacCarthy, P. 2001. The principles of humic substances: an introduction to the first principle. *In:* GHABBOUR and DAVIES (eds.) *Humic Substances structures, models and functions.* Cambridge, UK: The Royal Society of Chemistry 19-30

Mancinelli, V.;Rinaldi, M.;Finessi, E.;Emblico, L.;Mircea, M.;Fuzzi, S.;Facchini, M. C. and Decesari, S. 2007. An anion-exchange high-performance liquid chromatography method coupled to total organic carbon determination for the analysis of water-soluble organic aerosols. *Journal of Chromatography A,* 1149**,** 385-389.

Mathur, S. P. and Farnham, R. S. 1985. Geochemistry of humic substances in natural and cultivated peatlands. *In:* AIKEN (ed.) *Humic Substances in Soil, Sediment , and Water: Geochemistry, Isolation, and Characterization.* Wiley-Interscience Publication. 53-86

Matthews, B. J. H.;Jones, A. C.;Theodorou, N. K. and Tudhope, A. W. 1996. Excitation-emission-matrix fluorescence spectroscopy applied to humic acid bands in coral reefs. *Marine Chemistry,* 55**,** 317-332.

Mayol-Bracero, O. L.;Guyon, P.;Graham, B.;Roberts, G.;Andreae, M. O.;Decesari, S.;Facchini, M. C.;Fuzzi, S. and Artaxo, P. 2002. Water-soluble organic compounds in biomass burning aerosols over Amazonia 2. Apportionment of the chemical composition and importance of the polyacidic fraction. *Journal of Geophysical Research,* 107**,** 8091.

McCalley, D. V. 2010. Study of the selectivity, retention mechanisms and performance of alternative silica-based stationary phases for separation of ionised solutes in

hydrophilic interaction chromatography. *Journal of Chromatography A,* 1217**,** 3408-3417.

McFiggans, G.;Alfarra, M. R.;Allan, J.;Bower, K.;Coe, H.;Cubison, M.;Topping, D.;Williams, P.;Decesari, S.;Facchini, C. and Fuzzi, S. 2005. Simplification of the representation of the organic component of atmospheric particulates. *Faraday Discussions,* 130**,** 341-362.

McKnight, D. M.;Wesshaw, R. L. and MacCarthy, P. 1985. An introduction to humic substances in soil, sediment, and water. *In:* AIKEN (ed.) *Humic Substances In Soil, Sediment , and Water: Geochemistry, Isolation, and Characterization.* Wiley-Interscience Publication. 1-12

Micić;, V.;Kruge;, M. A.;Köster;, J. and Hofmann, T. 2011. Natural, anthropogenic and fossil organic matter in river sediments and suspended particulate matter: A multi-molecular marker approach *Science of the Total Environment* 409**,** 905-919.

Minor, E. and Stephens, B. 2008. Dissolved organic matter characteristics within the Lake Superior watershed. *Organic Geochemistry,* 39**,** 1489-1501.

Mudhoo, A. G., V. K. 2011. Sorption, Transport and Transformation of Atrazine in Soils, Minerals and Composts: A Review. *Pedosphere,* 21**,** 11-25.

Murphy, R. E.;Schure, M. R. and Foley, J. P. 1998. Effect of Sampling Rate on Resolution in Comprehensive Two-Dimensional Liquid Chromatography. *Analytical Chemistry* 70**,** 1585-1594.

Nagao, S.;Matsunaga, T.;Suzuki, Y.;Ueno, T. and Amano, H. 2003. Characteristics of humic substances in the Kuji River waters as determined by high-performance size exclusion chromatography with fluorescence detection. *Water Research,* 37**,** 4159-4170.

Nakajima, H.;Okada, K.;Kuroki, Y.;Nakama, Y.;Handa, D.;Arakaki, T. and Tanahara, A. 2008. Photochemical formation of peroxides and fluorescence characteristics of the water-soluble fraction of bulk aerosols collected in Okinawa, Japan. *Atmospheric Environment,* 42**,** 3046-3058.

Northcott, G. L. J., K. C. 2000. Experimental approaches and analytical techniques for determining organic compound bound residues in soil and sediment. *Environmental Pollution,* 108**,** 19-43.

O'Loughlin, E. and Chin, Y.-P. 2001. Effect of detector wavelength on the determination of the molecular weight of humic substances by high-pressure size exclusion chromatography. *Water Research,* 35**,** 333-338.

Oliva, P. V., Jerôme; Dupré, Bernard ; Pôl Fortuné, Jean ; Martin, François ; Braun, Jean Jacques ; Nahon, Daniel ; Robain, Henri 1999. The effect of organic matter on chemical weathering: Study of a small tropical watershed: Nsimi-Zoétélé site, Cameroon. *Geochimica et Cosmochimica Acta,* 63**,** 4013-4035.

Oorts, K. V., B.; Merckx, R. 2003. Cation exchange capacities of soil organic matter fractions in a Ferric Lixisol with different organic matter inputs. *Agriculture, Ecosystems & Environment,* 100**,** 161-171.

Opiteck, G. J.;Ramirez, S. M.;Jorgenson, J. W. and Moseley, M. A. 1998. Comprehensive Two-Dimensional High-Performance Liquid Chromatography for the Isolation of

Overexpressed Proteins and Proteome Mapping. *Analytical Biochemestry* 258**,** 349-361.

Parlanti, E.;Morin, B. and Vacher, L. 2002. Combined 3D-spectrofluorometry, high performance liquid chromatography and capillary electrophoresis for the characterization of dissolved organic matter in natural waters. *Organic Geochemistry,* 33**,** 221-236.

Parlanti, E.;Wörz, K.;Geoffroy, L. and Lamotte, M. 2000. Dissolved organic matter fluorescence spectroscopy as a tool to estimate biological activity in a coastal zone submitted to anthropogenic inputs. *Organic Geochemistry,* 31**,** 1765-1781.

Parshintsev, J.;Hyötyläinen, T.;Hartonen, K.;Kulmala, M. and Riekkola, M.-L. 2010. Solid-phase extraction of organic compounds in atmospheric aerosol particles collected with the particle-into-liquid sampler and analysis by liquid chromatography-mass spectrometry. *Talanta,* 80**,** 1170-1176.

Paula G, C. 1996. Characterization of marine and terrestrial DOM in seawater using excitation-emission matrix spectroscopy. *Marine Chemistry,* 51**,** 325-346.

Peng, C.;Chan, M. N. and Chan, C. K. 2001. The Hygroscopic Properties of Dicarboxylic and Multifunctional Acids: Measurements and UNIFAC Predictions. *Environmental Science & Technology,* 35**,** 4495-4501.

Perminova, I. V.;Frimmel, F. H.;Kovalevskii, D. V.;Abbt-Braun, G.;Kudryavtsev, A. V. and Hesse, S. 1998. Development of a perdictive model for calculation of molecular weight of humic substances. *Water Research,* 32**,** 872-881.

Pernet-Coudrier, B.;Companys, E.;Galceran, J.;Morey, M.;Mouchel, J.-M.;Puy, J.;Ruiz, N. and Varrault, G. 2011. Pb-binding to various dissolved organic matter in urban aquatic systems: Key role of the most hydrophilic fraction. *Geochimica et Cosmochimica Acta,* 75**,** 4005-4019.

Persson, L.;Alsberg, T.;Ledin, A. and Odham, G. 2006. Transformations of dissolved organic matter in a landfill leachate--A size exclusion chromatography/mass spectrometric approach. *Chemosphere,* 64**,** 1093-1099.

Peuravuori, J.;Koivikko, R. and Pihlaja, K. 2002. Characterization, differentiation and classification of aquatic humic matter separated with different sorbents: synchronous scanning fluorescence spectroscopy. *Water Research,* 36**,** 4552-4562.

Peuravuori, J.;Lehtonen, T.;Lepane, V. and Pihlaja, K. 2005. Comparative study for differentiation of aquatic humic-type organic constituents by capillary zone electrophoresis using polyvinyl alcohol-coated capillary. *Talanta,* 67**,** 103-111.

Piccolo, A. 2002. The supramolecular structure of humic substances: A novel understanding of humus chemistry and implications in soil science. *Advances in Agronomy.* Academic Press. 57-134

Pól, J.;Hohnová, B. and Hyötyläinen, T. 2007. Characterisation of *Stevia Rebaudiana* by comprehensive two-dimensional liquid chromatography time-of-flight mass spectrometry. *Journal of Chromatography A,* 1150**,** 85–92.

Pól, J.;Hohnová, B.;Jussila, M. and Hyötyläinen, T. 2006. Comprehensive two-dimensional liquid chromatography–time-of-flight mass spectrometry in the analysis of acidic compounds in atmospheric aerosols. *Journal of Chromatography A,,* 1130**,** 64–71.

Popovici, S. T.;Horst, A. v. d. and Schoenmakers, P. J. 2005. Two-dimensional chromatography as a tool for studying band broadening in size-exclusion chromatography. *Journal of Separtion Science,* 28**,** 1457-1466.

Rao, R. N. and Shinde, D. D. 2009. Two-dimensional LC–MS/MS determination of antiretroviral drugs in rat serum and urine. *Journal of Pharmaceutical and Biomedical Analysis* 50**,** 994-999.

Raust, J.-A.;Bruell, A.;Sinha, P.;Hiller, W. and Pasch, H. 2010. Two-dimensional chromatography of complex polymers, 8. Separation of fattyalcohol ethoxylates simultaneously by end group and chain length. *Journal of Separation Science,* 33**,** 1375-1381.

Reemtsma, T. 2009a. Determination of molecular formulas of natural organic matter molecules by (ultra-) high-resolution mass spectrometry Status and needs. *Journal of Chromatography A,* 1216**,** 3687-3701.

Reemtsma, T. 2009b. Determination of molecular formulas of natural organic matter
molecules by (ultra-) high-resolution mass spectrometry
Status and needs. *Journal of Chromatography A,* 1216**,** 3687–3701.

Relan, P.;Girdhar, K. and Khanna, S. 1984. Molecular configuration of compost's humic acid by viscometric studies. *Plant and Soil,* 81**,** 203-208.

Rosario-Ortiz, F. L.;Snyder, S. A. and Suffet, I. H. 2007. Characterization of dissolved organic matter in drinking water sources impacted by multiple tributaries. *Water Research,* 41**,** 4115-4128.

Samy, S.;Mazzoleni, L. R.;Mishra, S.;Zielinska, B. and Hallar, A. G. 2010. Water-soluble organic compounds at a mountain-top site in Colorado, USA. *Atmospheric Environment,* 44**,** 1663-1671.

Sannigrahi, P.;Sullivan, A. P.;Weber, R. J. and Ingall, E. D. 2005. Characterization of Water-Soluble Organic Carbon in Urban Atmospheric Aerosols Using Solid-State 13C NMR Spectroscopy. *Environmental Science & Technology,* 40**,** 666-672.

Santos, E. B. H.;Filipe, O. M. S.;Duarte, R. M. B. O.;Pinto, H. and Duarte, A. C. 2001. Fluorescence as a Tool for Tracing the Organic Contamination from Pulp Mill Effluents in Surface Waters. *Acta hydrochimica et hydrobiologica,* 28**,** 364-371.

Saxena, P. and Hildemann, L. M. 1996. Water-soluble organics in atmospheric particles: A critical review of the literature and application of thermodynamics to identify candidate compounds. *Journal of Atmospheric Chemistry,* 24**,** 57-109.

Saxena, P.;Hildemann, L. M.;McMurry, P. H. and Seinfeld, J. H. 1995. Organics alter hygroscopic behavior of atmospheric particles. *Journal of Geophysical Research,* 100**,** 18755-18770.

Selberg, A.;Viik, M.;Ehapalu, K. and Tenno, T. 2011. Content and composition of natural organic matter in water of Lake Pitkjärv and mire feeding KuKe River (Estonia). *Journal of Hydrology,* 400**,** 274-280.

Sepúlveda, J. P., Silvio; Hughen, Konrad A. 2011. Sources and distribution of organic matter in northern Patagonia fjords, Chile (~44-47°S): A multi-tracer approach for carbon cycling assessment. *Continental Shelf Research,* 31**,** 315-329.

Sharp, E. L.;Parsons, S. A. and Jefferson, B. 2006. Seasonal variations in natural organic matter and its impact on coagulation in water treatment. *Science of the Total Environment,* 363**,** 183-194.

Shellie, R. A. and Haddad, P. R. 2006. Comprehensive two-dimensional liquid chromatography. *Analytical and Bioanalytical Chemistry,* 386**,** 405-415.

Shulman, M. L.;Jacobson, M. C.;Carlson, R. J.;Synovec, R. E. and Young, T. E. 1996. Dissolution behavior and surface tension effects of organic compounds in nucleating cloud droplets. *Geophysical Research Letters,* 23**,** 277-280.

Sierra, M. M. D.;Giovanela, M.;Parlanti, E. and Soriano-Sierra, E. J. 2005. Fluorescence fingerprint of fulvic and humic acids from varied origins as viewed by single-scan and excitation/emission matrix techniques. *Chemosphere,* 58**,** 715-733.

Snyder, L. R.;Kirkland, J. J. and Dolan, J. W. 2010. Reversed-phase chromatography for neutral samples. *Introduction to modern liquid chromatography.* third edition ed. New Jersey: John Wiley & Sons, Inc. . 253-301

Steinberg, C. 2003. Introduction. *Ecology of humic substances in freshwaters.* Springer. 9-19

Stenson, A. C. 2008. Reversed-Phase Chromatography Fractionation Tailored to Mass Spectral Characterization of Humic Substances. *Environmental Science & Technology,* 42**,** 2060-2065.

Stevenson, F. J. 1985. Geochemistry of soil humic substances. *In:* AIKEN (ed.) *Humic Substances in Soil, Sediment , and Water: Geochemistry, Isolation, and Characterization.* Wiley-Interscience Publication. 13-52

Stevenson, F. J. 1994a. Biochemestry of the formation of humic substances. *Humus Chemistry: Genesis, Composition, Reactions* Second Edition ed. Canada: John Wiley & Sons, Inc. . 188-211

Stevenson, F. J. 1994b. Extraction, fractionation, and general chemical composition of soil organic matter *Humus Chemestry Genesis, Compositions, Reactions.* 2nd Edition ed. New York: Wiley: John Wiley and Sons. 24-58

Stevenson, F. J. 1994c. Organic matter in soils: Pools, distribution, transformation, and function. *Humus Chemestry Genesis, Compositions, Reactions.* 2nd Edition ed. New York: John Wiley and Sons. 14-18

Stoll, D. R. and Carr, P. W. 2005. Fast, Comprehensive Two-Dimensional HPLC Separation of Tryptic Peptides Based on High-Temperature HPLC. *Journal American Chemical Society 9* 127**,** 5034-5035.

Stone, E. A.;Hedman, C. J.;Sheesley, R. J.;Shafer, M. M. and Schauer, J. J. 2009. Investigating the chemical nature of humic-like substances (HULIS) in North American atmospheric aerosols by liquid chromatography tandem mass spectrometry. *Atmospheric Environment,* 43**,** 4205-4213.

Swietlik, J.;Dabrowska, A.;Raczyk-Stanislawiak, U. and Nawrocki, J. 2004. Reactivity of natural organic matter fractions with chlorine dioxide and ozone. *Water Research,* 38**,** 547-558.

Swift, R. S. 1999. Macromolecular properties of soil humic substances: fact, fiction, and opinion. *Soil science,* 164**,** 790-802.

Tanaka, N.;Kimura, H.;Tokuda, D.;Hosoya, K.;Ikegami, T.;Ishizuka, N.;Minakuchi, H.;Nakanishi, K.;Shintani, Y.;Furuno, M. and Cabrera, K. 2004. Simple and Comprehensive Two-Dimensional Reversed-Phase HPLC Using Monolithic Silica Columns. *Anal. Chem.,* 76**,** 1273-1281.

Tercero Espinoza, L. A.;ter Haseborg, E.;Weber, M. and Frimmel, F. H. 2009. Investigation of the photocatalytic degradation of brown water natural organic matter by size exclusion chromatography. *Applied Catalysis B: Environmental,* 87**,** 56-62.

Tercero Espinoza, L. A.;ter Haseborg, E.;Weber, M.;Karle, E.;Peschke, R. and Frimmel, F. H. 2011. Effect of selected metal ions on the photocatalytic degradation of bog lake water natural organic matter. *Water Research,* 45**,** 1039-1048.

Thurman, E. M. 1985. Classification of dissolved organic carbon. *Organic Geochemstry of Natural Waters.* Kluwer Academic Publishers 103-109

Tremblay, L. and Gagné, J.-P. 2009. Organic matter distribution and reactivity in the waters of a large estuarine system. *Marine Chemistry,* 116**,** 1-12.

Tsukasaki, A. and Tanoue, E. 2010. Chemical qualification of electrophoretically detectable peptides and sugar chains in oceanic surface particulate organic matter. *Marine Chemistry,* 119**,** 33-43.

Tuckermann, R. and Cammenga, H. K. 2004. The surface tension of aqueous solutions of some atmospheric water-soluble organic compounds. *Atmospheric Environment,* 38**,** 6135-6138.

Turtoi, A.;Mazzucchelli, G. D. and Pauw, E. D. 2010. Isotope coded protein label quantification of serum proteins—Comparison with the label-free LC–MS and validation using the MRM approach. *Talanta* 80**,** 1487-1495.

Twardowska, I. K., Joanna 2003. Sorption of metals onto natural organic matter as a function of complexation and adsorbent–adsorbate contact mode. *Environment International* 28**,** 783- 791.

Uchimiya, M. C., SeChin ; Klasson,K.Thomas 2011. Screening biochars for heavy metal retention in soil: Role of oxygen functional groups. *Journal of Hazardous Materials*

Ulrich Pöschl 2005. Atmospheric Aerosols: Composition, Transformation, Climate and Health Effects. *Atmospheric Chemistry,* 44**,** 7520-7540.

Valsecchi, S. M. and Polesello, S. 1999. Analysis of inorganic species in environmental samples by capillary electrophoresis. *Journal of Chromatography A,* 834**,** 363-385.

Vancampenhout, K.;Wouters, K.;De Vos, B.;Buurman, P.;Swennen, R. and Deckers, J. 2009. Differences in chemical composition of soil organic matter in natural ecosystems from different climatic regions - A pyrolysis-GC/MS study. *Soil Biology and Biochemistry,* 41**,** 568-579.

Varga, B.;Kiss, G.;Ganszky, I.;Gelencsér, A. and Krivácsy, Z. 2001. Isolation of water-soluble organic matter from atmospheric aerosol. *Talanta,* 55**,** 561-572.

Vergnoux, A.;Di Rocco, R.;Domeizel, M.;Guiliano, M.;Doumenq, P. and Théraulaz, F. 2011. Effects of forest fires on water extractable organic matter and humic substances from Mediterranean soils: UV-vis and fluorescence spectroscopy approaches. *Geoderma,* 160**,** 434-443.

Vervoort, N.;Daemen, D. and Török, G. 2008. Performance evaluation of evaporative light scattering detection and charged aerosol detection in reversed phase liquid chromatography. *Journal of Chromatography A,* 1189**,** 92-100.

Vivó-Truyols, G. and Schoenmakers, P. J. 2006. Chemical variance, a useful tool for the interpretation and analysis of two-dimensional chromatograms. *Journal of Chromatography A,* 1120**,** 273-281.

Wang, L.;Wu, F.;Zhang, R.;Li, W. and Liao, H. 2009. Characterization of dissolved organic matter fractions from Lake Hongfeng, Southwestern China Plateau. *Journal of Environmental Sciences,* 21**,** 581-588.

Wang, M.;Wang, X.;Ching, C. B. and Chen, W. N. 2010. Proteomic profiling of cellular responses to Carvedilol enantiomers in vascular smooth muscle cells by iTRAQ-coupled 2-D LC–MS/MS. *Journal of proteomics* 73**,** 1601 - 1611.

Wang, X.;Barber, W. E. and Carr, P. W. 2006. A practical approach to maximizing peak capacity by using long columns packed with pellicular stationary phases for proteomic research. *Journal of Chromatography A,* 1107**,** 139-151.

Wang, Y.;Kong, L.;Hub, L.;Lei, X.;Yang, L.;Chou, G.;Zou, H.;Wang, C.;Bligh, S. W. A. and Wang, Z. 2007a. Biological fingerprinting analysis of the traditional Chinese prescription Longdan Xiegan Decoction by on/off-line comprehensive two-dimensional biochromatography. *Journal of Chromatography B,* 860**,** 185-194.

Wang, Y.;Kong, L.;Hub, L.;Lei, X.;Yang, L.;Chou, G.;Zou, H.;Wang, C. and Bligh, S. W. A. a. Z. W. 2007b. Biological fingerprinting analysis of the traditional Chinese prescription Longdan Xiegan Decoction by on/off-line comprehensive two-dimensional biochromatography. *Journal of Chromatography B.*

Wei, Q.-s.;Feng, C.-h.;Wang, D.-s.;Shi, B.-y.;Zhang, L.-t.;Wei, Q. and Tang, H.-x. 2008. Seasonal variations of chemical and physical characteristics of dissolved organic matter and trihalomethane precursors in a reservoir: a case study. *Journal of Hazardous Materials,* 150**,** 257-264.

Went, F. W. 1960. Blue Hazes in the Atmosphere. *Nature,* 187**,** 641-643.

Woods, G. C.;Simpson, M. J.;Koerner, P. J.;Napoli, A. and Simpson, A. J. 2011. HILIC-NMR: Toward the Identification of Individual Molecular Components in Dissolved Organic Matter. *Environmental Science & Technology,* 45**,** 3880-3886.

Wu, F. C.;Evans, R. D. and Dillon, P. J. 2003. Separation and Characterization of NOM by High-Performance Liquid Chromatography and On-Line Three-Dimensional Excitation Emission Matrix Fluorescence Detection. *Environmental Science & Technology,* 37**,** 3687-3693.

Xia, L. and Gao, Y. 2010. Chemical composition and size distributions of coastal aerosols observed on the US East Coast. *Marine Chemistry,* 119**,** 77-90.

Xu, H. A., B. ; Grimvall, A. 1988. Influence of pH and organic substances on the adsorption of As(V) on geological materials *Water, Air, and Soil Pollution* 40**,** 293-305.

Yamashita, Y.;Cory, R. M.;Nishioka, J.;Kuma, K.;Tanoue, E. and Jaffé, R. 2010. Fluorescence characteristics of dissolved organic matter in the deep waters of the Okhotsk Sea and the northwestern North Pacific Ocean. *Deep Sea Research Part II: Topical Studies in Oceanography,* 57**,** 1478-1485.

Yamashita, Y. and Tanoue, E. 2003. Chemical characterization of protein-like fluorophores in DOM in relation to aromatic amino acids. *Marine Chemistry,* 82**,** 255-271.

Yves Dudal and Frédéric Gérard 2004. Accounting for natural organic matter in aqueous chemical equilibrium models: a review of the theories and applications. *Earth-Science Reviews* 66**,** 199-216.

Zappoli, S.;Andracchio, A.;Fuzzi, S.;Facchini, M. C.;Gelencsér, A.;Kiss, G.;Krivácsy, Z.;Molnár, Á.;Mészáros, E.;Hansson, H. C.;Rosman, K. and Zebühr, Y. 1999. Inorganic, organic and macromolecular components of fine aerosol in different areas of Europe in relation to their water solubility. *Atmospheric Environment,* 33**,** 2733-2743.

Zech, W. S., Nicola; Guggenberger, Georg; Kaiser, Klaus; Lehmann, Johannes; Miano, Teodoro M.; Miltner, Anja; Schroth, Götz 1997. Factors controlling humification and mineralization of soil organic matter in the tropics. *Geoderma,* 79**,** 117-161.

Zelenyuk, A.;Ezell, M. J.;Perraud, V.;Johnson, S. N.;Bruns, E. A.;Yu, Y.;Imre, D.;Alexander, M. L. and Finlayson-Pitts, B. J. 2010. Characterization of organic coatings on hygroscopic salt particles and their atmospheric impacts. *Atmospheric Environment,* 44**,** 1209-1218.

Zhang, B.;Mathewson, S. and Chenb, H. 2009. Two-dimensional liquid chromatographic methods to examine phenylboronate interactions with recombinant antibodies. *Journal of Chromatography A,* 1216**,** 5676-5686.

Zhang, L.;Li, A.;Lu, Y.;Yan, L.;Zhong, S. and Deng, C. 2009. Characterization and removal of dissolved organic matter (DOM) from landfill leachate rejected by nanofiltration. *Waste Management,* 29**,** 1035-1040.

Zhou, Q.;Cabaniss, S. E. and Maurice, P. A. 2000. Considerations in the use of high-pressure size exclusion chromatography (HPSEC) for determining molecular weights of aquatic humic substances. *Water Research,* 34**,** 3505-3514.